

**SPIE
Poland Chapter**

**Research & Development
Treatises
Volume 7**

**NON-CONTACT THERMOMETRY
Measurement Errors**

Krzysztof Chrzanowski

RDT Series

SPIE Polish Chapter, Warsaw 2001

Copyright @ 2001 by SPIE-PL. All rights reserved. Printed in Poland. No parts of this publication may be reproduced or distributed in any form or by any means, or stored in a data base or retrieval system, without the prior written permission of the publisher.

Cover by M. Pluta, SPIE PL Chapter's Editor

ISBN 83-904273-5-5

Published by:

Polish Chapter of SPIE
18 Kamionkowska Street
03-805 Warsaw, Poland
Telephone: (48-22) 8102589, (48-22) 8703874
Fax: (48-22) 8133265, (48-22) 810-68-97
Email: iosto@atos.warman.com.pl

Distributor:

Institute of Applied Optics
18 Kamionkowska Str.
03-305 Warsaw
Poland
Telephone: (48-22) 8132051, (48-22) 8703874
Fax: (48-22) 8133265, (48-22) 810-68-97
Email: iosto@atos.warman.com.pl

Reviewers:

Prof. Antoni Rogalski, Military University of Technology, Poland
Prof. Józef Piotrowski, VIGO Ltd., Poland

Table of contents

1. Introduction	1
1.1 Concept of temperature.....	1
1.2 Units of temperature.....	1
1.3 Types of systems used for non-contact temperature measurement.....	1
1.3.1 Human role in measurement	3
1.3.2 Location of system spectral bands	4
1.3.3 Presence of an additional source	4
1.3.4 Number of system spectral bands	5
1.3.5 Number of measurement points	7
1.3.6 Width of system spectral band	8
1.3.7 Transmission media	9
1.3.8 Non-classified systems.....	9
1.4 Accuracy of measurements	9
1.5 Division of errors of non-contact temperature measurement.....	12
1.6 Terminology	14
1.7 Structure of the book.....	15
1.8 References.....	16
2. Thermal radiation	18
2.1 Nomenclature	18
2.2 Quantities and units.....	20
2.3 Basic laws	22
2.3.1 Planck law	22
2.3.2 Wien law	24
2.3.3 Stefan-Boltzmann law.....	25
2.3.4 Wien displacement law	26
2.3.5 Lambert (cosine) law	27
2.3.6 Calculations.....	28
2.3.7 Emission into imperfect vacuum.....	31
2.4 Radiant properties of materials.....	31
2.4.1 Emission properties.....	33
2.4.2 Relationships between radiative properties of materials	35
2.4.3 Emissivity of common materials.....	37
2.5 Transmission of optical radiation in atmosphere.....	38
2.5.1 Optical properties of atmosphere	39
2.5.2 Numerical calculations.....	40
2.6 Source/receiver flux calculations	42
2.6.1 Geometry without optics	43
2.6.2 Geometry with optics	44
2.7 References.....	49

3. Methods of non-contact temperature measurement.....	50
3.1 Passive methods.....	54
3.1.1 Singleband method.....	54
3.1.2 Dualband method.....	63
3.1.3 Multiband method.....	69
3.2 Active methods.....	73
3.2.1 Singleband method.....	73
3.3 References.....	75
4. Errors of passive singleband thermometers.....	77
4.1 Mathematical model.....	77
4.2 Calculations.....	85
4.2.1 Electronic errors.....	89
4.2.2 Radiometric errors.....	94
4.2.3 Calibration errors.....	101
4.3 Conclusions.....	102
4.4 References.....	103
5. Errors of passive dualband thermometers.....	104
5.1 Mathematical model.....	104
5.2 Calculations.....	108
5.2.1 Relative disturbance resistance function.....	109
5.2.2 Detector noise.....	111
5.2.3 Emissivity.....	112
5.2.4 Reflected radiation.....	113
5.2.5 Atmosphere.....	114
5.3 Conclusions.....	115
5.4 References.....	116
6. Errors of passive multiband thermometers.....	117
6.1 Sources of errors.....	117
6.2 Model of errors.....	118
6.3 Calculations.....	121
6.3.1 Electronic errors.....	123
6.3.2 Radiometric errors.....	126
6.3.3 Calibration errors.....	129
6.4 Conclusions.....	130
6.5 References.....	132
7. Errors of active singleband thermometers.....	133
Appendix: Relative disturbance resistance function <i>RDRF</i>.....	135
Subject index.....	137
About Author.....	140

Introduction to the Series

This SPIE-PL series referred to as Research and Development Treatises (RDT) is a substitute for reading the original papers on a single and well focused scientific/technical problem in the field of applied optics and optical engineering. It is supposed that the selected problem is discussed by a single author (or a group of co-authors) as completely as possible, starting from its formulation, motivation, theoretical analysis, through experiments (if applicable), engineering development, implementation in applied sciences and/or practice.

Scientific, research and engineering papers that were published in scientific or technical journals or even conference proceedings are in general the basis for the RDT series. The monotypical papers can simply be reprinted in a logical way to render clearly the selected problem starting from its initial formulation and ending at its potential applications.

An alternative is a selection of an original book or its most important chapter from a large text that was published before in Polish language. After translation into English the original material can be included in the RDT series. Another possibility is to select a number of journal papers published in or even unpublished previously and to construct of them a uniform monograph of a reasonable size. This is just a case of Dr Chrzanowski work on non-contact thermometry with special emphasis on measurement errors.

I thank Dr Chrzanowski for his Volume 7 in the series and believe that it will be a useful publication for a large community of applied scientists/researches, engineers, practitioners, and students in the field of optics, optoelectronics and other related areas of applied sciences and engineering.

Maksymilian Pluta
SPIE-PL Editor, RDT Series

Author's Preface

There are significant advantages of non-contact thermometers in comparison to contact thermometers due to their easiness of operation, non-destructive character of measurement, speed of measurement, and possibilities to measure temperature of moving objects. Therefore, there are nowadays hundreds of thousands or more of pyrometers, thermal scanners and thermal cameras that are used over the world for non contact temperature measurements. One of disadvantages of non-contact thermometers is significant and difficult to predict variations of accuracy of temperature measurement. Users of non-contact thermometers are often confronted with a problem of estimation of accuracy of these instruments.

In spite of wide range of applications of non-contact thermometers, the problem of accuracy of these instruments received little attention. Manuals of different non-contact thermometers provide only basic knowledge about errors of these systems. Books about non-contact thermometry or infrared technology avoid problems of accuracy of non-contact thermometers concentrating on their design. A few scientific papers devoted to the problem of accuracy of the systems discussed here provide inconsistent results, particularly in the area of measuring thermal cameras. This situation has prompted the author to undertake the writing of this monograph and to bridge, at least partly, the existing gap in non-contact thermometry. I hope that this monograph can be useful for both the users and designers of non-contact thermometers enabling them to understand mechanism of error generation during measurement with these instruments and to estimate influence of measurement conditions and system design on measurement accuracy.

I would like to acknowledge the support from the State Committee for Scientific Research (KBN) Poland in my research in the area of non-contact thermometry; 3 grants received from KBN enabled writing this monograph.

Krzysztof Chrzanowski

1. Introduction

1.1 *Concept of temperature*

If two objects are in thermal equilibrium with a third object, then they are in thermal equilibrium with each other. From this it follows that there exists a certain attribute or state property that describes the thermodynamic states of objects which are in thermal equilibrium with each other, and this is termed *temperature* [1]. Any system can be used as thermometer if it has one or more physical properties (e.g. electrical resistance or voltage) which varies reproducibly and monotonically with temperature. Such a property can be used to indicate temperature on an arbitrary empirical scale.

1.2 *Units of temperature*

Due to historical reasons four units of measurement of temperature are used: degrees of Fahrenheit, degrees of Celsius, degrees of Rankine, and kelvins. The International Bureau of Weights and Measures CIPM recommends only two units: kelvin K or degree of Celsius °C [2]. Relationships between these four units of temperature measurement are presented below.

The Celsius scale is defined in terms of Kelvin scale as

$$^{\circ}\text{C} = \text{K} - 273.15$$

where °C means degree Celsius (or centigrade), and K means kelvin.

The Fahrenheit scale is defined in terms of Celsius scale as

$$^{\circ}\text{F} = 9/5 \text{ }^{\circ}\text{C} + 32$$

where °F means degrees of Fahrenheit. Fahrenheit scale is commonly used in USA and Great Britain.

The Rankine scale is a scale for which the zero is intended to be approximately the absolute zero and can be calculated as

$$^{\circ}\text{R} = ^{\circ}\text{F} + 459.67$$

where °R means Rankine degree. This scale is sometimes used in USA and Great Britain when calculations are to be performed in terms of absolute temperatures.

The kelvin K will be used as a unit of temperature in almost all cases in this book. Only exceptionally there will be used the degree of Celsius °C.

1.3 *Classification of systems for non-contact thermometry*

There are many systems -thermometers- that enable temperature measurement. However, all these systems can be divided into two basic groups: systems for contact measurement, when there exists physical contact between the tested object and the thermometer (or its sensing element), and systems for non-contact temperature measurement, when there is no such a contact. The non-contact thermometers are especially suited for measurements of temperature of moving or contact sensitive objects, objects inside vacuum, vessels or in hazardous locations are nowadays widely used in industry, science, medicine and environmental protection.

Non-contact thermometers employ different physical phenomena to determine temperature of the tested object: radiation phenomenon, refraction or phase Doppler phenomenon [3], luminescence phenomenon, Schlieren phenomenon etc. However, almost all systems used in practice for non-contact temperature measurement employ the phenomenon of thermal radiation that carries information about object temperature and are termed the radiation thermometers. Therefore, further discussion will be limited only to radiation thermometers, although we must remember that other types of non-radiation thermometers can find wider areas of applications in the near future. Next, the systems using a newly developed technique of great theoretical potentials called Laser Absorption Radiation Thermometry [4, 5] can be also classified as radiation thermometers as they still employ the radiation phenomenon. However, the LART is usually treated as a new separate technique and the LART systems will not be discussed in this book.

Non-contact radiation thermometers can be divided into a few groups according to different criteria: human role in the measurement, location of system spectral bands, presence of an additional cooperating source, number of system spectral bands, number of measurement points, width of system spectral bands and transmission media [Fig. 1.1].

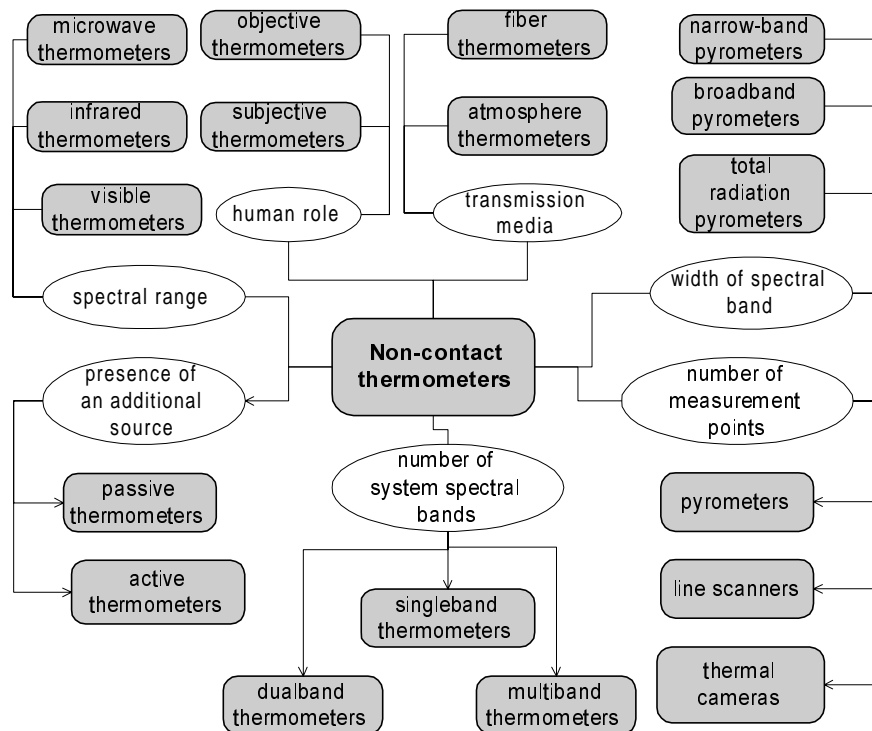


Fig. 1.1. Classifications of non-contact thermometers

1.3.1 Human role in measurement

On the basis of human role in measurement process the non-contact thermometers can be divided into subjective thermometers and objective thermometers. Humans take active part in measurement process using subjective systems. In case of objective pyrometers the role of a man is limited only to reading thermometer indications or human role is completely eliminated for automated measurement processes.

History of development non-contact thermometers started with manually operated subjective thermometers called optical pyrometers that used radiation emitted by the tested object in the visible range of optical radiation to determine object temperature.

An optical pyrometer measures the radiation from the target in a narrow band of visible range, centered usually in the red/yellow portion of spectrum. The operator sights the pyrometer on the target. At the same time he can see in the eyepiece the image of an internal tungsten lamp filament. Next, he matches the filament color to the target color by varying the current through the filament with a rheostat. When the target image and the tungsten filament are of the same color, then the target temperature can be read from the scale rheostat knob. If the target color and filament color are the same, then the filament image apparently vanishes, so these pyrometers have also been called disappearing filament pyrometers.

Because of subjective character of measurement process the optical pyrometers are slow, they do not offer immediate readout of measurement results, and results cannot be also stored in electronic form. Because of these disadvantages optical pyrometers cannot be used in many technological processes. Nowadays, optical pyrometers are very rarely used in industry; they are almost exclusively used in laboratories for control of other types of non-contact thermometers. Objective thermometers measure temperature indirectly in two stages. Power of optical radiation that comes to the system detector (or detectors) in one or more spectral bands is measured in the first stage. Object temperature is determined on the basis of the measured radiometric signals in the second stage by carrying out a certain calculation algorithm.

Because of this principle of measurement, the objective pyrometers always consist of at least two basic blocks: the detection block and temperature determination block. We can theoretically imagine such a thermometer, for example, as an infrared detector directly connected to a microprocessor calculating object temperature on the basis of a signal at the detector output. However, such two-block systems are not met in practice. Even simple objective thermometers usually consists of five or more blocks.

An optical objective is usually used before the detection system to increase the amount of radiation emitted by the tested object that comes to the detector and to limit thermometer field of view. The signal at the output of the detector is typically amplified, converted into more convenient electronic form and finally

digitized. A separate visualization block is typically used for presentation of measurement results.

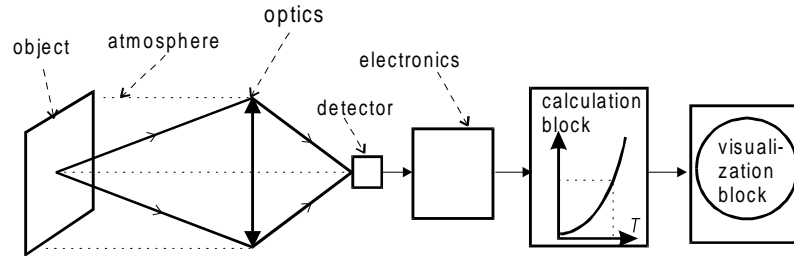


Fig. 1.2. A general diagram of a typical simple objective thermometer

1.3.2 Location of system spectral bands

Non-contact thermometers can be divided basing on criterion of location of a thermometer spectral band (or bands) into visible thermometers, infrared thermometers and microwave thermometers. Theoretically, it is also possible to design systems of spectral band (or bands) located in ultraviolet range or even X range for measurement of very high temperatures. However, the author has not heard so far about any practical thermometers of spectral bands located in these spectral ranges.

Temperatures measured in almost all practical applications vary from about 200K to about to 3000K. Objects of such temperatures emit most thermal radiation in infrared range, little in visible range, and very little in microwave range. History of non-contact thermometers started from discussed earlier visible thermometers called the optical pyrometers. However, nowadays, probably more than 99% of all non-contact thermometers are infrared thermometers. Visible (optical) thermometers are rarely met in practical applications, and microwave thermometers are still at laboratory stage of development. However, in future the number of microwave thermometers can rise significantly because of one very useful in some applications feature. Visible and infrared thermometers can typically measure temperature only on the surface of the tested objects as most materials are opaque in visible and infrared range. Microwave thermometers can measure temperature under the surface of most objects opaque in visible and infrared range but transparent in microwave range. The latter thermometers enable, for example, temperature measurement of tissues under human skin.

1.3.3 Presence of an additional source

It is possible to measure passively object temperature only on the basis of power of radiation emitted by the object in one or more spectral bands. The systems using this measurement methods will be termed “the passive systems”.

By using an additional cooperating source that emits radiation directed to the tested object and measuring the reflected radiation we can get some information about emissive properties of the tested object. Such information can at least theoretically

improve accuracy of non-contact temperature measurements. The systems that consist of a cooperating source emitting radiation directed to the tested object and a classical passive thermometer measuring both the radiation emitted by the source and reflected by the object and the radiation emitted by the object will be called the active systems.

Active thermometers are more sophisticated, more expensive and so far only in few applications they can really offer better accuracy than passive systems. Therefore, nowadays, almost all practical non-contact thermometers are passive ones.

To prevent any possible misunderstanding we must add that many modern systems use an artificial source of radiation -a laser- but only for indication of the measurement point, not as the additional radiation source really needed in measurement process and they are typical passive thermometers.

1.3.4 Number of system spectral bands

Both passive and active non-contact thermometers, according to criterion of number of system spectral bands, can be divided into three basic groups: single-, dual- and multiband systems. Singleband systems determine object temperature on the basis of the power of optical radiation measured in one spectral band; dualband systems - in two spectral bands, and multiband systems - in at least three spectral bands.

Passive singleband systems measure directly the power from the tested object within a single spectral band of the measuring instrument. Radiation emitted by the object that comes to detector produces an electrical signal at the detector output. The value of this signal carries information about the object temperature, which is determined using system calibration chart derived from radiometric calculation of the output signal as a function of blackbody temperature. The temperature measured in this way can be corrected for case of real objects (non-blackbodies) if only their emissivity over the spectral band is known. Incomplete knowledge of the object emissivity is the most common source of bias errors in temperature measurement using passive singleband systems. These systems are additionally vulnerable to such error sources as reflected radiation, limited atmospheric transmittance, variations of radiation emitted by optical components, detector noise and other system internal electronic sources [6,7]. However, their overriding advantage is simplicity, as they require only one spectral band and these systems dominate in industrial and science applications.

The ratio of the power emitted by a graybody at two different wavelengths does not depend on the object emissivity but only on the object temperature. Passive dualband systems use this property of Planck function, measuring received power in two separate spectral bands. The object temperature is usually determined using a calibration chart that represents a ratio of the emitted power in these two bands as a function of the object temperature. However, a dual-band temperature measurement is unbiased only in the case of gray-body objects, or when the ratio

At present, at least 95% of systems available commercially on market are passive singleband systems; passive dualband systems are rather rarely used; passive multiband systems are still at a laboratory stage of development. Similarly to the passive systems it is theoretically possible to design active single- and multiband thermometers.

Active singleband systems determine temperature of the tested object in three stages. First, the power of the radiation emitted by the co-operating source and reflected by the object is measured. Second, the power of the radiation emitted by the tested object within the system spectral band is measured. Third, the object temperature is calculated on the basis of the values of the measured power of the reflected radiation and the emitted radiation. Similar measurement procedures can be used for active dual- and multiband systems.

So far the author of this book has met only one commercially available active singleband thermometer [17] and knows only one report about development of a active multiband system used in practice [18].

1.3.5 Number of measurement points

Non-contact thermometers according to number and location of measurement points, can be divided into pyrometers, line scanners and thermal cameras. Pyrometers enable temperature measurement of only a single point or rather of a single sector (usually a circle or a square) of the surface of the tested object. Line scanners enable temperature measurement of many points located along a line. Thermal cameras enable temperature measurement of thousands of points located within a rectangle, square or circle and create a two-dimensional image of temperature distribution on this area.

Most commercially available non-contact thermometers are pyrometers. They are small, light and low-cost systems that found numerous applications in industry, science etc. enabling easy point temperature measurement. Line scanners are specially suitable for temperature measurement of moving objects and found applications in automotive industry, welding, robotics etc. Thermal cameras offer the greatest capabilities of all discussed types of non-contact thermometers. Modern cameras enable creation of two-dimensional image of resolution close to resolution of typical television image. As they enable presentation of measurement results in form of electronic image they are very convenient for users. Therefore, in spite of their high price, thermal cameras found numerous applications such as control of electrical supply lines, heat supply lines, civil engineering, environmental protection, non-destructive testing and so on, and their number is rising quickly.

Almost all pyrometers, line scanners and thermal cameras are passive singleband systems that use the passive singleband method of temperature measurement. This means, they measure the signal generated at the detector output by the radiation emitted by the tested object within the system spectral band and the

object temperature is determined on the basis of the value of this signal. However, in spite of the same method of temperature measurement there are great differences in construction of pyrometers, line scanners and thermal cameras; particularly when we compare pyrometers and thermal cameras.

Basically, all these groups of systems are built using the same blocks: optics, detector, electronics, calculation block, visualization block. However, the mentioned above blocks are simple in case of pyrometers but can be very sophisticated in case of thermal cameras because of a few reasons. First, the pyrometers use usually a single or two lens (or mirrors) optical objective while thermal cameras typically employ multi-lens systems. Additionally, sophisticated scanning systems are used in thermal cameras with single or linear detectors to create two-dimensional thermal image. Second, the pyrometers usually use low cost thermal detectors or non-cooled photoelectric detectors in situation when much more expensive cooled photoelectric detectors are employed in thermal cameras. Next, typical singleband pyrometers are always built using single detector when many thermal cameras are built using linear or two-dimensional matrix of detectors. Third, the electronic block of pyrometers is needed to amplify and convert into more convenient form low-speed signal at the output of the detector, when in case of thermal cameras it is a high-speed signal that must be determined with much greater accuracy. Fourth, the visualization block of pyrometers is needed only to present measurement results in form of a row of digits in situation when the visualization block of thermal cameras is needed to present high quality thermal image.

1.3.6 Width of system spectral band

Non-contact thermometers can be divided on the basis of width of system spectral band onto three basic groups.

The first group are total radiation (broadband) thermometers that measure radiation in theoretically unlimited, practically broadband, spectral band. These systems typically use thermal detectors. The width of their spectral band is limited by spectral region of transmission of the optics or windows. Their spectral band usually varies from about 0.3-1 μm to about 12-20 μm . They have been termed "total radiation thermometers" because they measure almost all of the radiation emitted by the tested objects. They are usually simple, low cost systems of wide temperature spans susceptible to measurement errors caused by limited transmittance of the atmosphere.

The second group are band-pass thermometers. They were initially derived from total radiation (broadband) thermometers. Lenses, windows and filters were selected to transmit only a selected portion of spectrum. The 8-14 μm band is a typical choice for general-purpose band-pass thermometers because of very good atmospheric transmission in this band.

The third group are narrow-band thermometers that operate over a narrow range of wavelengths. The spectral range of most narrow band thermometers is typically determined by the optical filter. Filters are used to restrict response to

selected wavelengths to meet the need of a particular application. For example, the $5\pm 0.2\mu\text{m}$ band is used to measure glass surface temperature because glass surface emits strongly in this region, but poorly below or immediately above this band. Next, the $3.43\pm 0.2\mu\text{m}$ band is often used for temperature measurement of thin films or polyethylene-type plastics etc.

1.3.7 Transmission media

As is shown in Fig. 1.2 that presents a diagram of a measurement process with a typical non-contact thermometer, the radiation emitted by the tested object comes through atmosphere, next through optics (lenses, windows, filters) before it reaches the detector. The distance between the object and the optics is usually over 0.5 m, and the distance between the optics and the detector is typically below 0.1m. The optics, the detector and other blocks of the thermometer are mechanically mounted in the same housing. This fixed, inflexible configuration is not a good solution in situations when direct sighting due to obstructions is impossible, significant RF and EMI interference is present and electronics must be placed in safe distance, or very high temperatures exist. It is better in such situations to use flexible fiber thermometers.

Fiber non-contact thermometers can be generally defined as systems in which an optical fiber is used for transmission of radiation emitted by the object to the detector. There are a few different designs of such systems.

It is possible to design a fiber thermometer without the optics block. One end of optical fiber is located close to the surface of the tested object and the other end is adjacent to the surface of detector. However, in order to have small measurement area, the fiber end must be located very close to the surface of the object. As it is not always possible or convenient, fiber thermometers with a small optical objective at the end close to the tested object are more popular.

1.3.8 Non-classified systems

There are nowadays carried out many projects on development of new types of non-contact thermometers. It is possible to find in literature reports about new types of systems that are not included to the discussed above classification scheme. One of these new systems is for example laser absorption pyrometer [19] that uses laser to modulate temperature of the tested object. However, it seems that probably over 99% of commercially available systems can be classified using the scheme shown in Fig. 1.1.

1.4 Accuracy of measurements

Measurement is a non-accurate operation. Result of measurement generally always differs from the true value of the measured quantity. Equality of the measurement result and the true value of the measured quantity is an exceptional incident and we do not know when such an incident occurs.

Accuracy of measurement result can be only estimated. It can be done using classical error theory or modern uncertainty theory. Classical error theory proposes so called limit error as a measure of measurement accuracy. Models that can be used for determination of limit errors can be found in many books dealing with metrology.

Uncertainty theory proposes the uncertainty as such a measure. Rules for evaluation of uncertainty in measurement are presented in the "Guide to the expression of uncertainty in measurement" published in 1993 by four main international metrological organizations: the International Organization for Standardization (ISO), the International Electrotechnical Commission (IEC), the International Organization of Legal Metrology (OIML), and the International Bureau of Weights and Measures (BIPM).

The terms "accuracy", "error", "systematic error", "random error", "uncertainty" and "limit error" apparently seem to be easily understood intuitively. However, in practice these terms are often a source of confusion as it is possible to find radically different definitions in different literature sources. Therefore, let us define them clearly now to prevent any possible misunderstanding.

The *International Vocabulary of Basic and General Terms in Metrology* commonly abbreviated VIM, published jointly by the mentioned above seven international metrological organizations, can be considered as the present day most important international standard [20]. Definitions of five mentioned above terms according to the VIM are presented below.

Accuracy of measurement [VIM3.5] - closeness of the agreement between the result of a measurement and true value of the measurand,

where the "measurand" is a specific quantity subject to measurement¹.

Error (of measurement) [VIM 3.10] - result of a measurement minus the value of the measurand.

Random error [VIM 3.13] - result of a measurement minus the mean that would result from an infinite number of measurements of the same measurand carried out under repeatability conditions.

Comment: By means of statistical analysis it is possible to estimate the random error.

Systematic error [VIM 3.14] mean that would result from an infinite number of measurements of the same measurand carried out under repeatability conditions minus the value of the measurand.

Comment: The systematic error equals to error minus random error. Similarly to earlier defined terms "measurand" and "error" it cannot be fully known; it can be only estimated.

Uncertainty (of measurement) [VIM 3.9] - a parameter, associated with the result of a measurement, that characterizes the dispersion of the values that could be re-

¹ Because the term "measurand" is relatively new and still not accepted widely in literature, the term "measured quantity" will be used in the rest of this book.

sonably attributed to the measurand (the parameter mentioned above is usually a standard deviation or a given multiple of it).

The term "limit error" is not included into the VIM. However, on the basis of analysis of the Ref. [21] it can be defined as presented below

Limit error - a range around the result of the measurement in which the true value of the measured quantity is located with high value of probability.

From analysis of the presented above definitions we can make three basic conclusions.

First, that "accuracy" is only a qualitative concept that should not be associated with numbers. This means that we should not specify instrument accuracy as equal to a certain number as it is unfortunately a common practice so far. We are allowed according to the VIM to say only that accuracy is good, bad etc.

Second, the defined according to the VIM term "error" is a perfect measure of measurement accuracy. However, this true error of measurement is always unknown because the true value of the measured quantity is unknown. The same can be said about its component: the systematic error. Let us temporarily call the term "error" as the "true error" to make a better distinction with the term "limit error".

Third, two other measures of measurement accuracy: the uncertainty and limit error of the result of a measurement may be evaluated. These two measures of measurement accuracy are useful for users of measuring instruments who know only the instrument indication and want to estimate accuracy of the measurement result. Guidelines on evaluation of uncertainty of measurement results are presented in the mentioned earlier "Guide to the expression of uncertainty in measurement", guidelines on evaluation of limit error – in numerous metrology handbooks.

Although the true errors of measurement cannot be practically exactly determined, mathematical model of true errors of measurement process are useful for both designers and the users of measuring instruments.

It is always possible to assume that the measured quantity is exactly known, simulate certain measurement conditions, and then to model mathematically the measuring instrument and calculate its indications for the assumed conditions. The true error of measurement equals the instrument indication minus the assumed value of the measured quantity. Simulations carried out for different measurement conditions and different instrument designs enable to find optimal instrument design and to create software or hardware blocks that can improve accuracy of measurement.

Mathematical models of true errors that arise during measurement process can also be experimentally verified in most cases. It is typically possible to use a standard object of exactly known measured quantity as a tested object. Testing of measuring instruments by their manufacturers in order to determine instrument accuracy are typically carried out in this way.

Mathematical models of true errors are not so vital for users of measuring instruments as they are for the manufacturers. Nevertheless, the models can help them significantly as they enable analysis of sources of measurement errors

and show mechanism of error generation. Therefore, the models can be used to predict influence of measurement conditions on instrument indications.

The main aim of this book is to present mathematical models of true errors of temperature measurement with modern non-contact thermometers. Models of limit errors and uncertainties will not be presented here.

1.5 Division of errors of non-contact temperature measurement

All methods of non-contact temperature measurement employed by the radiation thermometers are indirect methods. Output temperature is determined on the basis of the power of thermal radiation emitted by the tested object and measured in one or more spectral bands using different mathematical models [Fig. 1.3]. These models in modern radiation thermometers can be implemented in microprocessors of stand-alone devices or in software programs for thermometers cooperating with a microcomputer.

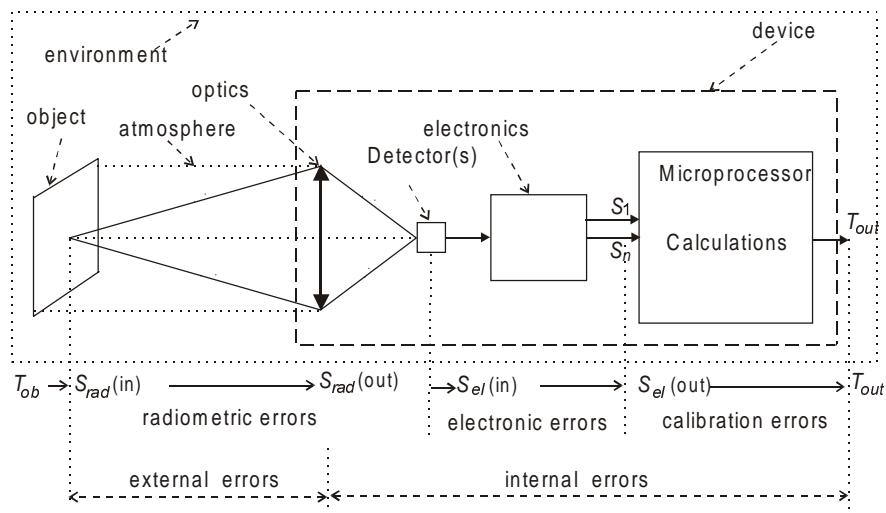


Fig. 1.3. Graphical presentation of the measurement process with radiation thermometers

The mathematical models used to determine thermometer indications are always based on certain assumptions about measurement process made to enable to predict radiation coming to the thermometer detector (or detectors). These assumptions depend mostly on method of measurement, although they can also be different in case of two systems using the same measurement method but manufactured by different companies. Now, let us mention only a few assumptions. In case of passive singleband systems it is typically assumed that the user can determine accurately the object effective emissivity. Measurement methods of some passive singleband systems are also based on assumption that atmospheric transmittance equals one. Next, the method used by most dualband systems assumes that the object emissivity is the same in both spectral bands of the system. Further on, the pas-

sive multiband method of temperature measurement assumes that the function of object emissivity versus wavelength can be interpolated by a certain type of mathematical functions.

There are always some differences between the measurement conditions assumed by the mathematical model used for calculation of the output temperature and the real conditions due to many reasons. The example assumption used in passive singleband method is not fulfilled when the user will estimate the object effective emissivity with limited accuracy. This and many other sources of differences between the measurement conditions assumed by the mathematical models used in radiation thermometers for calculation of output temperature will be discussed in details in Chapters 4-7. Now, let us conclude that due to the discussed differences the radiometric signal coming to the detector in one or more spectral bands differs from the expected values and the output temperature is calculated with an error. As the discussed errors of determination of output temperature are caused by sources within the radiometric channel between the tested object and the detector of the thermometer let us call them the radiometric errors.

The output temperature can be determined with significant errors even when the radiometric errors are negligible due to existence of the electronic errors and the calibration errors.

Electronic errors are the errors of output temperature determination due to non-perfect transformation of the radiometric signal(s) into output electrical signal(s). As most important sources of the electronic errors we can mention noise, non-linearity, non-uniformity of the detector, limited stability of the detector cooling system, variation of the preamplifier gain and offset, limited resolution and limited linearity of the analogue/digital converter.

Calibration errors are the errors of output temperature determination caused by limited accuracy of standard sources of radiation used during calibration of the thermometer. They are typically generated mostly due to limited accuracy of the blackbodies used during calibration process. As the accuracy of presently used blackbodies is relatively high the calibration errors are almost always smaller than the radiometric errors or the electronic errors.

As it was presented above, the errors of temperature measurement with radiation thermometers, according to their source, can be generally divided into three basic groups: radiometric errors, electronic errors and calibration errors. However, these errors can be divided into external errors and internal (device) errors, too. This new division of temperature measurement errors is more convenient when it is necessary to treat the whole thermometer as a single block. As can be seen in Fig. 1.3, group of internal errors consists of earlier defined calibration errors, electronic errors and partially of radiometric errors caused by sources within the thermometer. As a consequence, external errors are radiometric errors caused by factors outside the thermometer.

1.6 Terminology

In spite of relatively long traditions of systems for non-contact temperature measurement there are still no internationally accepted terminology standards in most areas of this technology. At present, only terminology related to quantities of optical radiation and detectors of this radiation is relatively well standardized [22]. However, there are vast areas of this technology where terminology is not standardized. It results in situation when different authors use different terminology describing non-contact thermometers in scientific papers, manuals and catalogues making them difficult to understand. Such a situation is particularly difficult for newcomers to this technology and non-native English speakers. Some examples will be discussed next.

We will start with the terms used in literature instead of earlier defined the term "thermal camera" because of a particular confusion in this area. If we make a review of literature dealing with infrared technology then we would find that there are at least eleven different terms used as synonyms of the term thermal camera: thermograph [23], thermovision [24,25], FLIR (forward looking infrared) [27], thermal imaging camera [29], infrared imaging system IIS [28], thermal viewer [29], infrared viewer [29], infrared imaging radiometer [30], thermal viewer, thermal data viewer, thermal video system [31]

Second, measurement thermal cameras and thermal scanners are considered in this book as types of non-contact thermometers as they are mostly used for temperature measurement. However, only devices for point measurement –pyrometers– are often treated as thermometers in literature [32].

Third, the non-contact thermometers according to number of spectral bands were divided in Section 1.3 into three basic groups: single-, dual- and multiband systems. However, the terms "single-wavelength", "single-spectral", "monocolor", "singlecolor" are frequently used in literature instead of the term "singleband". The term "singleband" was chosen instead of the terms "singlewavelength" or "singlespectral" because there is no practical possibility to measure radiation for exactly one wavelength; measurements are made always for a finite band. The terms "mono-color", "single-color" were not used because the term "color" has its meaning for visible systems in situation when most non-contact thermometers are infrared systems.

Fourth, the term "fiber thermometer" is used in this book to define a non-contact thermometer in which an optical fiber is used to transmit the radiation emitted by the object to the detector. However, one should be careful as the term "fiber thermometer" is sometimes used to describe contact thermometers in which a fiber is used as a sensor for temperature measurement. Such a contact measurement can be done, for example, using temperature–dependent fluorescence behavior of optically excited phosphors that are applied at the end of the fiber [33]. Temperature of this fiber end is determined by measurement of the decay time of luminescence signals generated by pulses of xenon light.

1.7 Structure of the book

As it was emphasized in Section 1.4, this book is limited to the dominant group of non-contact thermometers: the radiation thermometers that employ the phenomenon of thermal radiation to determine object temperature. Therefore, the whole Chapter 2 “*Thermal radiation*” is devoted to discussion about properties of thermal radiation. Quantities and units of this kind of radiation are presented in Section 2.1 and basic laws – in Section 2.2. The laws describe only phenomenon of thermal radiation emitted by an ideal type of objects: the blackbodies. Radiant properties of real materials are discussed in Section 2.3 to enable analysis radiation emitted by real materials. Next, the influence of the atmosphere on propagating radiation is discussed in Section 2.4. Finally, rules of source/receiver flux calculations are presented in Section 2.5.

It was presented in Section 1.4 that there are many different types of non-contact thermometers. However, there are only a few different methods of non-contact temperature measurement because many different types of non-contact thermometers use the same measurement method. There is, for example, no significant differences between measurement methods used by singleband pyrometers, thermal scanners or thermal cameras. Four most important methods of non-contact temperature measurement are discussed in Chapter 3 “*Methods of non-contact temperature measurement*”: passive singleband method, passive dualband method, passive multiband method and active singleband method. Single and dualband passive methods were included to the analyzed group because almost all available on the market radiation thermometers use one of these methods. Active singleband method was also included because a few such thermometers are commercially available and their number may increase in future. Systems using the passive multiband methods are so far not commercially available. However, there is a significant interest in these systems and there are quite a few reports in literature about development of such systems.

Chapters 4-7 are devoted to presentation of mathematical models and calculation results of errors of temperature measurement with four analyzed systems: passive singleband thermometers, passive dualband thermometers, passive multiband thermometers and active singleband thermometers. All these chapters have the same structure. First, a mathematical model is developed. Next, calculations of errors of temperature measurement are carried out and the results are discussed. Special care was taken to make calculations for systems of parameters similar to the systems practically used and for typical measurement conditions. The calculation results are always graphically illustrated to show clearly connections between the measurement results, thermometer parameters and measurement conditions. Conclusions about accuracy of the analyzed systems in typical measurement conditions and recommendations for optimal system design are presented at the end of each chapter.

Values of the disturbance resistance function DRF can be useful for a quick determination of errors of instrument indications due to an estimated error of determination of effective emissivity, effective background temperature or effective atmospheric transmittance. Therefore, the values of this function for typical single-band passive thermometers are presented in the Appendix.

1.8 References

1. Hudson R. P., Measurement of temperature, *Rev. Sci. Instrum.* 51(7), 871-880 (1980)
2. Preston-Thomas P., The International Temperature Scale of 1990 (ITS-90), *Metrologia* 27, 3-10 (1990).
3. Mendonsa Ruth A., Laser-Based Systems Measures Fuel Droplet Temperatures, *Photonics Spectra*, April 1998, p. 131.
4. Schreiber E., Neuer G., The laser absorption pyrometer for simultaneous measurement of surface temperature and emissivity, *Proceedings of TEMPEKO'96, Torino*, 365-370 (1997).
5. Edwards G., Lewick A., Xie Z., Laser emissivity free thermometry, *Proceedings of TEMPEKO'96, Torino*, 383-388 (1997).
6. Chrzanowski K. Comparison of shortwave and longwave measuring thermal imaging systems, *Applied Optics*, 34, 2888-2897(1995).
7. Chrzanowski K., Experimental verification of theory of influence from measurement conditions and system parameters on temperature measurement accuracy with IR systems, *Applied Optics*, 35, 3540-3547 (1996).
8. Chrzanowski K., Influence of measurement conditions and system parameters on accuracy of remote temperature measurement with dualspectral IR systems, *Infrared Physics and Technology*, 37, 295-306 (1996).
9. Coates P. B. , Wavelength specification in optical and photoelectric pyrometry, *Metrologia*, 13,1-5 (1977).
10. Hahn J.W., Rhee C., Reference wavelength method for a two-color pyrometer, *App. Opt.*, 26, 5276-5278 (1987)
11. Barani G., Tofani A., Comparison of some algorithms commonly used in infrared pyrometry: computer simulation, in *Thermosense XIII, ed.George S. Baird*, Proc. SPIE 1467, 458-468 (1991).
12. Andreic Z., Numerical evaluation of the multiple-pair method of calculating temperature from a measured continuous spectrum, *App. Opt.*, 27,4073-4075 (1988).
13. Andreic Z., Distribution temperature calculations by fitting the Planck curve to a measured spectrum, *App. Opt.*, 31, 126-130 (1992).
14. Tank V., Infrared temperature measurement with automatic correction of the influence of emissivity, *Infrared Phys.* 29, 211-212 (1989).
15. Tank V, Dietl H. Multispectral Infrared Pyrometer For Temperature Measurement With Automatic Correction Of The Influence Of Emissivity, *Infrared Phys.* 30, 331, (1990).
16. Hunter G. B., Alleman C.D., Eagar T.W., Multiwavelength pyrometry : an improved method, *Opt. Eng.*, 24, 1081-1085 (1985).
17. Laser pyrometer, Pyrometer Inc., 1994.
18. Daniel N., Wiliams D., Full spectrum multiwavelength pyrometry for non-grey surfaces, *SPIE*, Vol. 1682, p. 260-270, 1992
19. Schreiber E., Neuer G., The laser absorption pyrometer for simultaneous measurement of surface temperature and emissivity, *TEMPEKO 1997*, p. 365-370.

20. *International Vocabulary of Basic and General Terms in Metrology*, International Organisation for Standardisation, 1993.
21. Sydenham P. H., *Handbook of measurement science*, Vol.1: Theoretical fundamentals, p.263, John Wiley & Sons Ltd., (1992).
22. *International Lighting Vocabulary*, CIE Publ. No. 1 7.4, IEC Publ. No. 50(845), (1987).
23. *Thermographic Terminology - Supplement 2 to Acta Thermographica*, 1978.
24. *Spatial resolution determination*, AGA Publication 556.110, 1975.
25. *Thermal resolution determination*, AGA Publication 556.110, 1975.
26. Ratches J. A., *Static Performance Model for Thermal Imaging Systems*, Opt.Eng.15,6, 525-530 (1976).
27. Lloyd J.M., *Thermal imaging systems*, Plenum Press, New York (1975).
28. SPIE '88 Technical Symposium on Optics, Electro-Optics & Sensors-Technical Program
29. *Thermal Imaging Camera Argus – Manual*, EEV Ltd., 1996.
30. *Radiometer 760BB Manual*, Inframetrics Inc. 1994.
31. www.fsi.com/glossary.html
32. *IR Answers and Solutions Handbook*, IRCON Inc., 1997.
33. *Temperature measurement in industry: Radiation Thermometry*, VDI/VDE 3511 Part 4, Verein Deutscher Ingenieure, Dusseldorf, p.97, 1995.

2. Thermal radiation

2.1 Nomenclature

The term "thermal radiation" defines radiation that is radiated by bodies due to thermal motion of the atoms and the molecules they are built. However, it must be emphasized that the term "thermal radiation" does not specify wavelengths of the emitted radiation.

According to the International Lighting Vocabulary published by International Lighting Commission CIE and the International Electrotechnical Commission IEC [1] considered nowadays as an international primary authority on terminology in radiometry, electromagnetic radiation between radio radiation and X radiation is termed the optical radiation. Thus, the optical radiation can be defined as radiation of wavelengths higher than about 1 nm and lower than about 1 mm.

The range of optical radiation is divided into 3 sub-ranges: infrared radiation, visible radiation and ultraviolet radiation. Thermal radiation can be emitted in all three sub-ranges of optical radiation. In fact it is also emitted and can be detected in one of sub-ranges of radio radiation: the microwave radiation. However, for typical temperatures met on the Earth almost all thermal radiation is emitted within the infrared range. Therefore, thermal radiation is often called infrared radiation and vice versa. Such a situation commonly met in literature can be sometimes very misleading.

There have not been presented so far precise limits of optical radiation or limits of its sub-ranges in international standards. There was presented in the International Lighting Vocabulary of CIE a proposal of division of optical radiation but not as compulsory division but only as a recommended division [Tab. 2.1]. Additionally, in case of visible radiation, due to human diversity, only approximate limits were given. Next, what is even more important, the CIE recommendations are not accepted in many communities working in the field of optical radiation due to many, mostly historical reasons.

Tab. 2.1. Division of optical radiation recommended by the CIE

Name	Wavelength range
UV-C	0.1 μm - 0.28 μm
UV-B	0.28 μm - 0.315 μm
UV-A	0.315 μm - 0.4 μm
VIS	approximately 0.36-0.4 μm to 0.76 -0.8 μm
IR-A	0.78 μm - 1.4 μm
IR-B	1.4 μm - 3 μm
IR-C	3 μm - 1000 μm

Confusion in area of limits and further division of sub-ranges of optical radiation is particularly clear in case of infrared radiation range. There are many proposals of division of infrared range published in literature, only a few chosen ones are shown in Tab. 2.2.

Tab. 2.2. Different divisions of infrared range proposed in literature

Nr	Source	Proposal
1	International Lighting Vocabulary of CIE	IR-A 0.78 μm - 1.4 μm IR-B 1.4 μm - 3 μm , IR-C 3 μm - 1000 μm
3	Guide for Spectroscopy-Catalog, Jobin Yvon, 1993	Near IR 0.65 μm - 1.5 μm Middle IR 1.5- 5 μm , Far IR >5 μm
4	The Photonics Spectrum Reference Wall Chart, Photonics Spectra, 1995	Near IR 0.68 μm -3 μm Middle IR 3- 30 μm , Far IR 30-1000 μm
5	Hudson R.D., Infrared System Engineering, John Wiley&Sons, 1969.	Near IR 0.76 μm -3 μm Middle IR 3- 6 μm , Far IR 6-15 μm Extremely Far IR >15 μm
6	Mc Graw-Hill Encyclopedia of Physics, ed. Sybil P. Parker, 1993. P. 570	IR radiation: 1 μm -1000 μm
7	ed. Robert M. Besancon, The Encyclopedia of Physics, Van Nostrand Reinhold Company, 1974	IR radiation: 0.7 μm -1000 μm Near IR 0.7-1.5 μm - Intermediate IR 1.5-20 μm Far IR 20-1000 μm
8	www.FSI.com\meas.html	The infrared band 0.7 -100 μm is often further subdivided into four smaller bands, the boundaries of which are also arbitrarily chosen. They include: the "near infrared" (0.75-3 μm), the "middle infrared" (3-6 μm), the "far infrared" (6-15 μm) and the "extreme infrared" (15-100 μm).
9	www.FSI.com\glossary.html	SWIR band from about 0.7 μm to 1.1 μm (sentence from the definition of infrared film) MWIR -the middle infrared spectrum, usually from 2.4 to 7.0 μm . Near Infrared(SWIR) - The shortest wavelength infrared radiation band - 0.7 to 1.4 μm . Thermal Radiation - Electromagnetic energy whose natural wavelength fall between 0.7 and 100 μm .

Existing terminology of modern thermal cameras increases confusion in area of division of infrared range. So far, almost all thermal cameras have their

spectral bands optimized for 3-5 μm or 8-12 μm atmospheric windows. The cameras of 8-12 μm spectral band are usually called long-wavelength LW cameras. The 3-5 μm cameras should be more properly called mid-wave MW cameras. However, they are often termed “short-wave SW thermal cameras” as the real short-wave cameras almost do not exist.

Precise division of infrared radiation is particularly important for any book on subject of radiation thermometers as they are usually systems of spectral bands located within infrared range. Therefore for the purpose of analysis carried out in this book a precise division of infrared radiation shown in Tab. 2.4 will be used. The division shown in Tab. 2.4 is based on limits of spectral bands of infrared detectors commonly used in most non-contact thermometers. Wavelength 1.1 μm is a sensitivity limit of popular Si detectors. Similarly wavelength of 3 μm is a long-wave sensitivity limit of PbS detectors; wavelength 6 μm is a sensitivity limit of InSb, PbSe detectors and HgCdTe detectors optimized for 3-5 μm atmospheric window; and finally wavelength 15 μm is a long-wave sensitivity limit of HgCdTe detectors optimized for 8-12 μm atmospheric window.

Tab. 2.4. Division of optical radiation used in this book

Name	Wavelength range
very near infrared VNIR	0.78 μm - 1.1 μm
near infrared NIR	1.1 μm - 3 μm
middle infrared MIR	3 μm - 6 μm
far infrared FIR	6 -15 μm
very far infrared VFIR	15 μm - 1000 μm

If we compare the division accepted in this book with the division proposed by Hudson in Ref.[3] (number 5 in Tab. 2.2) then we will see that the division used in this book is a modified division proposed by Hudson in Ref.[3]. An additional range “very near infrared” was added due to significant importance of silicon Si detectors in radiation thermometry.

2.2 Quantities and units

It is possible to find in different books different symbols, units and other nomenclature used to describe properties of optical radiation as there is still no a single standard recognized by all people working in field of technology. The symbols, units and other nomenclature used in this book generally conform to the mentioned earlier Lighting Vocabulary published by the International Lighting Commission CIE. The terminology used in this standard is entering common practice in a number of fields dealing with optical radiation. If the symbols or units used in this book are not in agreement with the Vocabulary, there is an additional information in a footnote.

There are three types of quantities of optical radiation: radiant quantities, luminous quantities and photon quantities. Radiant quantities are measures of opti-

cal radiation properties such as radiated power and its spatial and angular distribution in SI units. Photon quantities are measures of the same properties when number of photons is a unit of radiant energy. A photon quantity can be calculated by dividing the radiant quantity by energy of a single photon. Finally, luminous quantities are modified radiant quantities to indicate human response to them.

Basic symbols are the same for all three types of quantities. However, different indexes are used to identify type of quantity (e-radiant, p-photon, v-luminous). For example ϕ_e , ϕ_p , ϕ_v symbols are used to indicate radiant flux, photon flux and luminous flux.

Photon and luminous quantities are only exceptionally used in literature on subject of non-contact temperature measurement; radiant quantities are typically used. Therefore only radiant quantities will be employed in this book and symbols of radiant quantities will be used without any additional index as presented next.

Radiant flux (power) Φ is the time flow of radiant energy emitted, transferred or received by a surface or region of space (unit: watt, where $1 \text{ W} = 1 \text{ J s}^{-1}$).

Flux can be considered as the fundamental quantity; the other quantities defined next are geometric or spectral distributions of flux.

Radiant exitance M^2 is the radiant flux per unit area in a specified surface that is leaving the specified surface (unit: W m^{-2}).

Radiant intensity I is the solid angle density of radiant flux, the radiant flux per unit solid angle incident on, passing through, or emerging from a point in space and propagating in a specified direction (unit: W sr^{-1}). The defining equation can be written as

$$I = \frac{d\Phi}{d\omega},$$

where $d\Phi$ is the element of flux incident on or emerging from a point within the element $d\omega$ of solid angle in a specified direction.

Radiance L is the area and solid angle density of radiant flux, the radiant flux per unit projected area and per unit solid angle incident on, passing through, or emerging in a specified direction from specified point in a specified surface (unit: $\text{W m}^{-2} \text{ sr}^{-1}$). The defining equation can be written as

$$L = \frac{d^2\Phi}{dA d\omega} = \frac{d^2\Phi}{d\omega dA_0 \cos\theta},$$

where $dA = dA_0 \cos\theta$ is the quantity called the projected area, $d\omega$ is the element of solid angle in the specified direction and θ is the angle between this direction and the normal to the surface at the specified point.

Irradiance E is the area density of radiant flux, the radiant flux per unit area in a specified surface that is incident on or passing through the specified surface (unit: W m^{-2}).

² The exitance M has been called *emittance* in the past but nowadays this term is generally reserved as a replacement term for *emissivity*, a property of a material surface.

All the presented earlier quantities can be defined also as spectral quantities. For example the spectral radiance L_λ is the spectral concentration of the radiance L (typical unit: $\text{W m}^{-2} \text{sr}^{-1} \mu\text{m}^{-1}$) defined as

$$L_\lambda = \frac{dL}{d\lambda}.$$

L_λ for wavelength λ can be interpreted as radiant flux emitted from the area of area 1 m^2 within the solid angle of 1 steradian in the specified direction and within the spectral band $[\lambda-0.5\mu\text{m}, \lambda+0.5\mu\text{m}]$ if the μm was chosen as a unit of the wavelength λ .

2.3 Basic laws

2.3.1 Planck law

All objects above the temperature of absolute zero emit thermal radiation due to thermal motion of the atoms and the molecules. The hotter they are, the more they emit. Spectral distribution of thermal radiation emitted by an ideal radiator – a blackbody - is described by the Planck law

$$M_\lambda(T) = \frac{2\pi hc^2}{\lambda^5 \left(e^{hc/\lambda kT} - 1 \right)} \quad (2.1)$$

where M_λ is the spectral radiant exitance in $\text{W m}^{-2} \mu\text{m}^{-1}$, T is the blackbody temperature in Kelvins, λ is the wavelength in μm , $h=6.626176 \times 10^{-34} \text{ J s}$ is the Planck constant, $c = 2.9979246 \times 10^8 \text{ m/s}$ is the speed of the light in the vacuum, $k=1.380662 \times 10^{-23} \text{ J K}^{-1}$ is the Boltzmann's constant.

It is common to express the Eq. (2.1) in the form

$$M_\lambda(T) = \frac{c_1}{\lambda^5 \left(e^{c_2/\lambda T} - 1 \right)} \quad (2.2)$$

where c_1 and c_2 are the constants of values $c_1=3.741832 \times 10^4 \text{ [W cm}^2 \mu\text{m}^4]$ and $c_2 = 14387.86 \mu\text{m K}$. However, it must be noted that it is possible to find in literature different values of the constants c_1 and c_2 because as values of many others physical constants they are continually refined when improved measurement techniques become available. Additionally, we must remember that the constants c_1 and c_2 can be presented using other units, too.

The spectral radiant exitance M_λ in the form shown in Eq. (2.2) expresses the power of radiation within a spectral interval of $1 \mu\text{m}$ around the wavelength λ emitted into a hemisphere by a blackbody having an area of 1 cm^2 .

It is customary to refer all radiometric measurements and calculations to a spectral interval equal to the unit in which wavelength is measured. As wavelength in optical radiometry is usually expressed in μm therefore the spectral interval is ex-

pressed in μm , too. However, we must remember that in practical measurements the spectral interval of the measuring device usually differ from $1\mu\text{m}$.

The term *blackbody* used above describes a body that allows all incident radiation to pass into it and absorbs internally all of the incident radiant energy. This must be true for all wavelengths and for all angles of incidence. Blackbody is also the most efficient radiator. A perfect blackbody at room temperatures would appear totally black to the eye, hence the origin of the name. The spectral radiant exitance of a blackbody at temperatures ranging from room temperature up to temperature of the Sun is shown in Fig. 2.1.

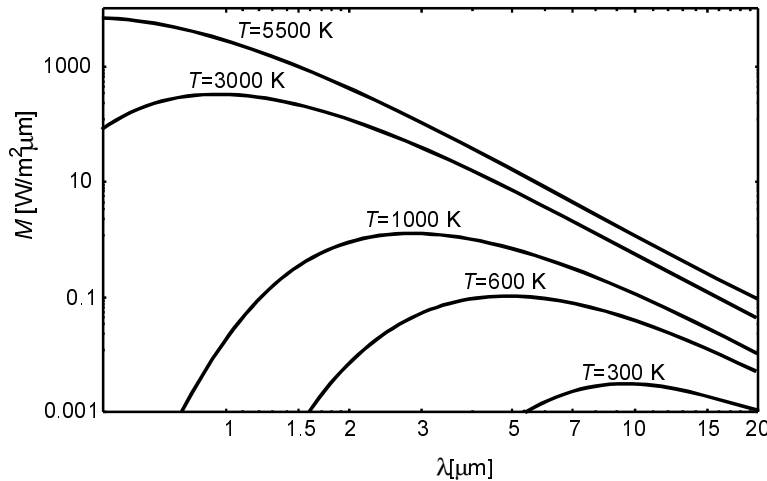


Fig. 2.1. Spectral radiant exitance of a blackbody at different temperatures

The Planck law enables calculation of the spectral radiant exitance M_λ at and is very useful in many radiometric calculations. However, sometimes it can be also interesting to determine the blackbody temperature T when its radiant exitance M_λ is known. It can be done using a following formula that can be treated as an inverse Planck law

$$T = \frac{c_2}{\ln \left[\frac{(c_1 + \lambda^5 M_\lambda)^\lambda}{(\lambda^5 M_\lambda)^\lambda} \right]} \quad (2.3)$$

The relationship between the temperature T and the spectral exitance M_λ for different wavelengths λ calculated using the Eq. (2.3) is presented in Fig. 2.2. The Eq.(2.3) can be used for calculation of object temperature when its radiant spectral exitance M_λ for a narrow spectral band is measured.

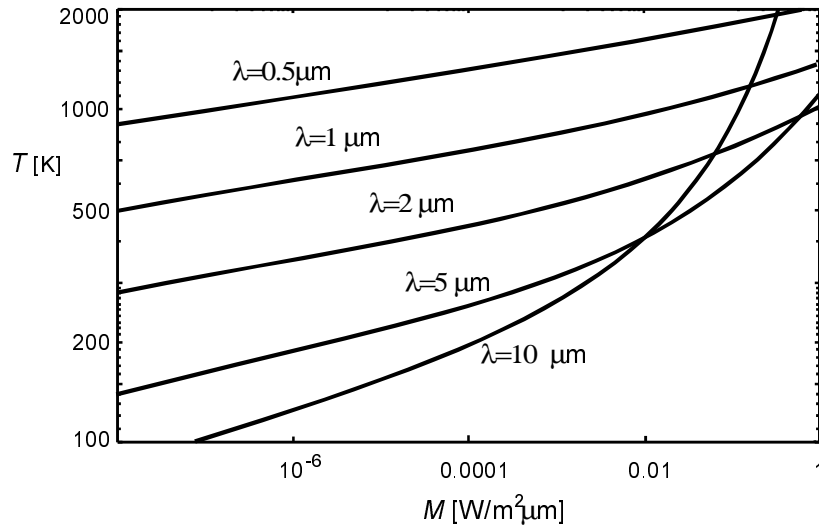


Fig. 2.2. Relationship between the temperature T and the radiant spectral exitance M_λ for the different wavelengths λ

2.3.2 Wien law

The Wien law represents a simplified version of the Planck law on assumption that $\exp[(c_2/\lambda T) - 1] \approx [(c_2/\lambda T)]$

$$M_\lambda(T) = \frac{c_1}{\lambda^5 \exp(c_2 / \lambda T)}. \quad (2.4)$$

The relative error of exitance calculation using the Wien law can be defined as ratio of the difference of exitance calculated using the Wien law $M(Wien)$ and exitance calculated using the Planck law $M(Planck)$ to exitance calculated using the Planck law $M(Planck)$

$$rel_error = \frac{M_\lambda(Wien) - M_\lambda(Planck)}{M_\lambda(Planck)} \quad (2.5)$$

The values of relative error rel_error for different wavelengths and temperatures using the Eq. (2.5) are shown in Fig. 2.3. As it can be seen the rel_error rises with temperature and wavelength. If we make some calculations using Eq. (2.5) then we can come to two more details rules. First, that the error caused by using Wien law is about 1.5% for wavelength of maximum radiation and decreases rapidly for shorter wavelengths. Second, when $\lambda T \leq 3000 \mu\text{m K}$ then the $rel_error \leq 1\%$.

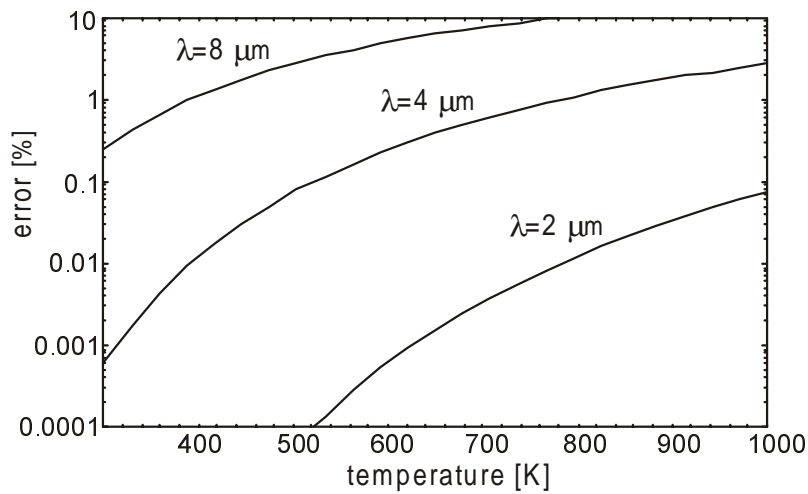


Fig. 2.3. Relative error of exitance calculation using the Wien law

Application of the Wien law causes decrease in calculations accuracy but it also significantly simplifies calculation of many equations with integrals, etc. Therefore, the Wien law was often used instead of the Planck law in the past before introduction of personal computers. Nowadays, commonly available personal computers can solve analytically or numerically many sophisticated formulas within seconds and the Planck law is typically used.

2.3.3 Stefan-Boltzmann law

Integrating Plack's law over wavelength from zero to infinity gives an expression for radiant exitance, the flux radiated into a hemisphere by a blackbody of a unit area. This total radiant flux emitted from the surface of an object at the temperature T is expressed by Stefan-Boltzman law, in the form

$$M = \sigma T^4, \quad (2.6)$$

where M is the radiant exitance of a blackbody in unit W/m^2 and σ is the Stefan-Boltzman constant and the currently recommended value for σ is $5.67032 \cdot 10^{-8} \text{Wm}^{-2} \text{K}^{-4}$.

Results of calculations of dependence of the radiant exitance M on the blackbody temperature T are shown in Fig. 2.4. Using this figure it is possible quickly to estimate radiant power emitted by a blackbody of area equal to 1 m^2 and temperature T .

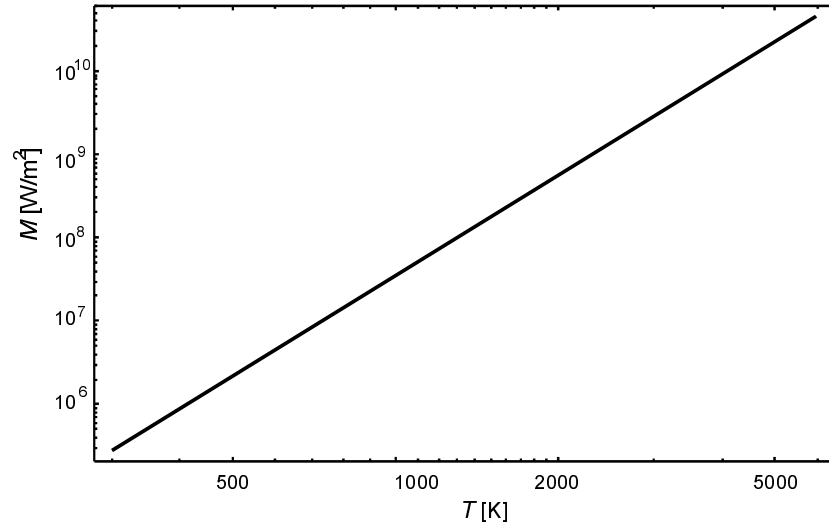


Fig. 2.4. Dependence of radiant exitance M on blackbody temperature T

2.3.4 Wien displacement law

If one differentiates the Planck formula and solves for the maximum yields a simple relationship between the wavelength λ_{max} where the Planck formula has its maximum value of radiant exitance $M_{\lambda_{max}}$ and the temperature T of the blackbody. The resulting relationship is called Wien's displacement law and is given by

$$\lambda_{max}T = A \quad (2.7)$$

where $A=2897.8$ in $\mu\text{m K}$.

Dependence of wavelength at which the maximum spectral exitance occurs on temperature is shown in graphical form in Fig. 2.5. As we can see in this figure, the λ_{max} varies inversely with absolute temperature and for typical temperatures met in industry, science, environment etc. is located within range of infrared radiation. It is the main reason why most of non-contact system for temperature measurement are infrared systems. Next, the λ_{max} for typical Earth scenery is located within the range 8-12 μm and therefore most surveillance thermal cameras use this spectral bands.

Using the Wien displacement law (2.7) and the Planck law (2.2) we can calculate the radiant exitance M_{λ} at wavelength λ_{max} at which the maximum spectral exitance occurs for any temperature. The dependence of $M(\lambda=\lambda_{max})$ on temperature T is presented in Fig. 2.6.

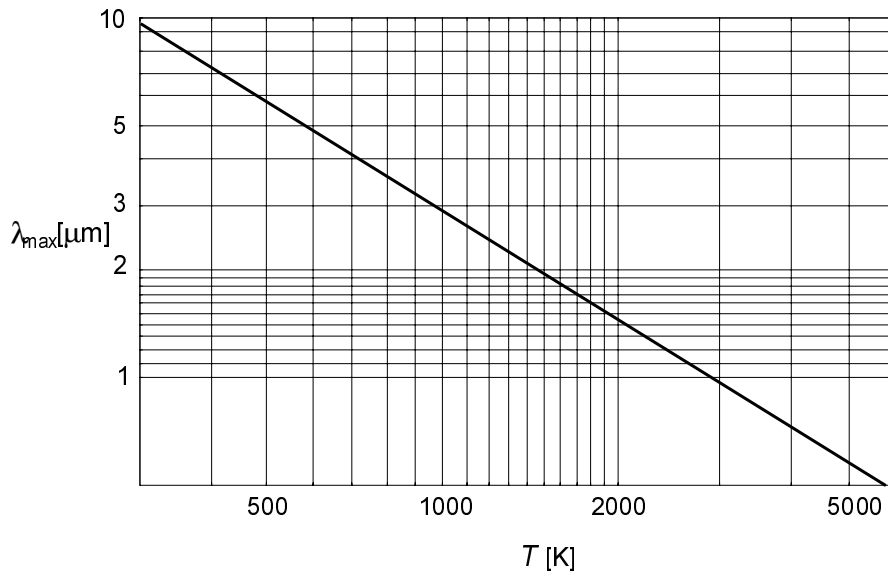


Fig. 2.5. Dependence of wavelength λ_{max} at which the maximum spectral exitance occurs on temperature T

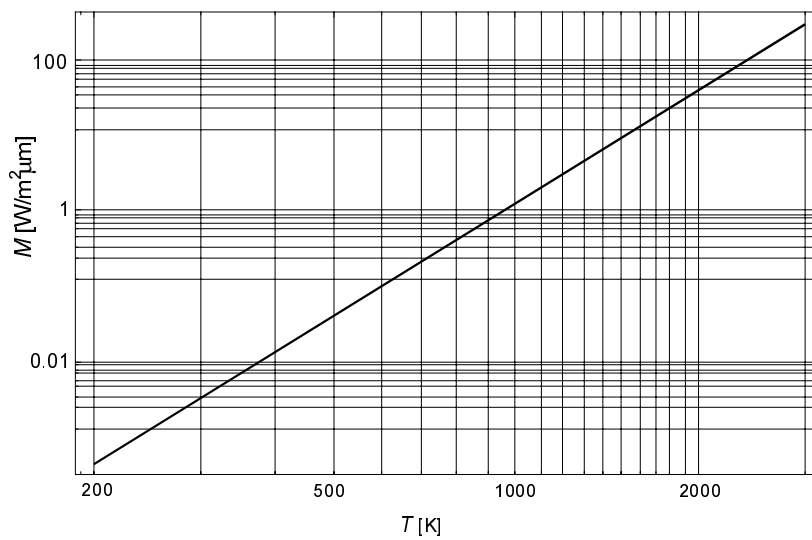


Fig. 2.6. Function of radiant exitance M_λ at wavelengths λ_{max} at which the maximum spectral exitance occurs on temperature T

2.3.5 Lambert (cosine) law

When radiance of an element of a surface is the same in all direction within the hemisphere over this element then the following relationship is fulfilled

$$I(\theta) = I_n \cos \theta , \quad (2.8)$$

where $I(\theta)$ is the radiant intensity in direction of the angle θ to the direction normal to the surface, I_n is the radiant intensity in the direction normal to the surface.

An ideal surface that fulfils the Lambert cosine law is called the Lambertian surface. For the Lambertian surface there exists a following relationship between the radiant exitance M and the radiant radiance L

$$M = \pi L . \quad (2.9)$$

The relationship (2.9) is sometimes called the Lambert law instead of the earlier presented law.

2.3.6 Calculations

It is possible to calculate object exitance in any spectral band $\Delta\lambda$ by integrating the Planck formula (2.2) within this spectral band

$$M_{\Delta\lambda} = \int_{\Delta\lambda} \frac{c_1}{\lambda^5 (e^{c_2/\lambda T} - 1)} d\lambda , \quad (2.10)$$

where $M_{\Delta\lambda}$ is the object exitance in the spectral band $\Delta\lambda$.

Formula (2.10) is of great importance as it is the basis for any calculations of radiant power emitted by objects and received by a detector. There have been developed many tables and simplified formulas to enable calculation of the integral (2.10) with a help of a simple calculator or without it. However, nowadays, commonly met personal computers can be easily used to carry out even much more sophisticated calculations within seconds. Therefore, such tables and formulas lost its usefulness for a present day scientist, engineer or technician. However, it seems that easy to memorize charts enabling very quick calculations of spectral radiant power in any spectral band still can be useful.

Let us define the relative exitance M_{rel} as a ratio of the exitance M_λ for the wavelength λ to the exitance $M_{\lambda_{max}}$ for wavelength λ_{max} at which exitance has its maximum. Next, let us define the relative wavelength λ_{rel} as a fraction of the wavelength λ_{max}

$$M_{rel}(\lambda_{rel}) = \frac{M_\lambda}{M_{\lambda_{max}}} \quad \lambda_{rel} = \frac{\lambda}{\lambda_{max}} . \quad (2.11)$$

On the basis of the Planck law and the Wien displacement law the formula (2.11) can be presented in the following form

$$M_{rel} = \frac{e^{c_2/A} - 1}{\lambda_{rel}^5 (e^{c_2/A\lambda_{rel}} - 1)} . \quad (2.12)$$

As we can see in Eq. (2.12) the relative spectral radiant exitance M_{rel} does not depend on the object temperature T . Therefore $M_{rel}(\lambda_{max})$ represents a single, easy to memorize, function that is shown in graphical form in Fig. 2.7.

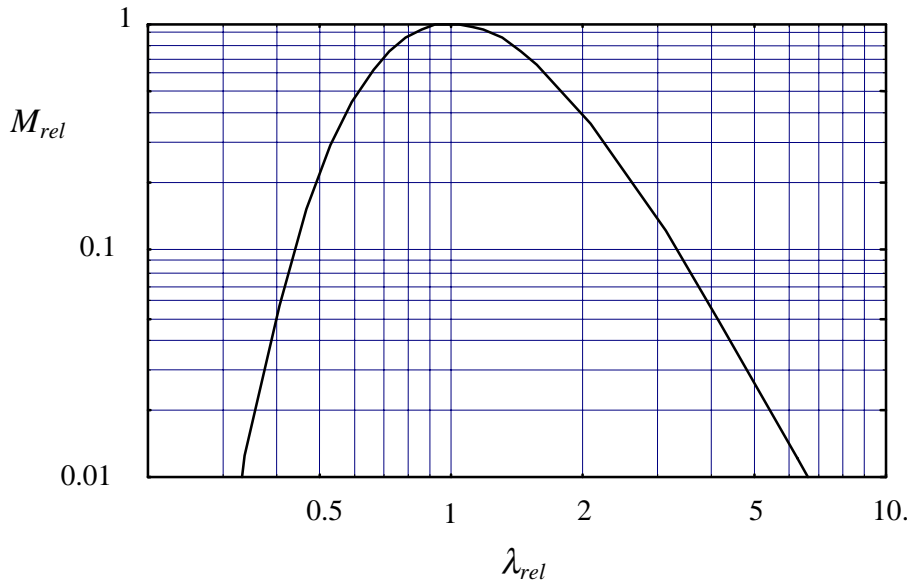


Fig. 2.7. Relative spectral radiant exitance M_{rel}

Fraction $Y(\lambda_{rel})$ of total radiant power emitted at wavelengths of values below the relative wavelength λ_{rel} can be calculated from a formula

$$Y(\lambda_{rel}) = \frac{\int_0^{\lambda_{rel}} M_{\lambda} d\lambda}{\int_0^{\infty} M_{\lambda} d\lambda}, \tag{2.13}$$

and presented in graphical form in Fig. 2.8.

We can see in Fig. 2.8 that exactly one fourth of the total flux of a black-body is emitted at the wavelengths below the emission peak λ_{max} . It means that we can generally expect to register more radiation at longer wavelengths than at shorter ones.

It is possible to determine the spectral radiant exitance M_{λ} for any the wavelength λ or any the spectral bands $\Delta\lambda$ without help of a calculator or a computer using the earlier presented charts when relative modest precision will suffice.

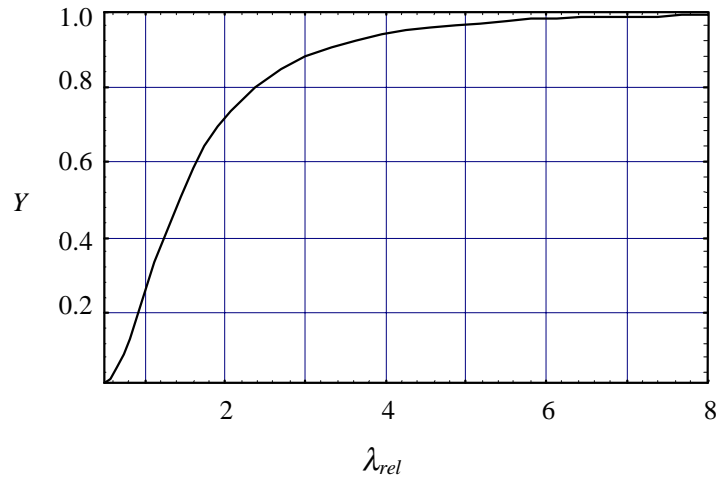


Fig. 2.8. Fraction $Y(\lambda_{rel})$ of total radiant power emitted below relative wavelength λ_{rel}

The spectral exitance M_λ for any wavelength λ and any the temperature T can be calculated using the following algorithm.

1. Determine λ_{max} for the assumed temperature T using Fig. 2.5.
2. Determine value of the spectral exitance M_λ ($\lambda=\lambda_{max}$) for the assumed temperature T using Fig. 2.6.
3. Calculate the relative wavelength λ_{rel} as the ratio of λ and λ_{max} .
4. Determine the relative spectral exitance M_{rel} for the relative wavelength λ_{rel} calculated in the previous step using Fig. 2.7.
5. Calculate the spectral exitance M for the wavelength λ and the temperature T as the product of M_{rel} and M_λ ($\lambda=\lambda_{max}$).

The spectral exitance M_λ for any the spectral bands $\Delta\lambda = \lambda_2 - \lambda_1$ and any temperature T can be calculated using another algorithm.

1. Determine λ_{max} for the assumed temperature T using the Fig. 2.5.
2. Determine the radiant exitance M_x for the assumed temperature T using the Fig. 2.4.
3. Calculate the relative wavelengths λ_{rel2} as the ratio of λ_2 and λ_{max} , and λ_{rel1} as the ratio of λ_1 and λ_{max} .
4. Determine difference $Y(\lambda_{rel1})$ and $Y(\lambda_{rel2})$ using Fig. 2.8.
5. Calculate the spectral exitance M for the spectral band $\Delta\lambda=\lambda_2 - \lambda_1$ and the temperature T as product of the exitance M calculated in the second step and the difference $Y(\lambda_{rel1})$ and $Y(\lambda_{rel2})$ determined in the previous step.

2.3.7 Emission into imperfect vacuum

The presented earlier laws of thermal radiation are strictly valid for blackbodies emitting into perfect vacuum of refractive index equal to one, where the refractive index is defined as ratio of the speed of light in a perfect vacuum to its speed in the medium. When a blackbody emits radiation into a gas, liquid, or solid having the refractive index $n > 1$, then the equations for Stefan-Boltzman law, Wien displacement law and Planck law have to be modified. It is necessary to replace the wavelength and speed of light in vacuum with their values in the medium.

The Stefan-Boltzman law then becomes

$$M = n^2 \sigma T^4, \quad (2.14)$$

where n is the refractive index of the medium.

The Wien displacement law is modified to a new form

$$n\lambda_m T = 2897.8 \text{ } \mu\text{m K}. \quad (2.15)$$

2.4 Radiant properties of materials

Radiant properties of a material describe its ability to emit, absorb, reflect and transmit optical radiation.

Terminology of radiant properties of materials is probably one the most confusing areas of technical terminology. Authors of different publications use different and sometimes inconsistent definitions. The situation is so complicated that some parameters used in literature, to describe material ability to emit, absorb, reflect and transmit radiation, were not included in the well known terminology standard of optical radiation - the International Lighting Vocabulary [1] - as the CIE decided that further work was needed to establish proper names and definitions of some parameters; particularly describing material ability to reflect and transmit radiation. Next, although the ILV can be considered as the most important terminology standard, there are other standards or books [4,5,6] that propose solutions that differ from the ones found in the ILV. Further on, even the authors [7] that generally accepted the terminology proposed in the IVL add their own exceptions. And finally there are publications that use terminology that is inconsistent with both with the ILV or the works [4,5,6].

According to a school of terminology proposed in work [2] the words used to describe the various radiometric properties of materials should have very specific meaning; especially their endings. In this way, any word that ends in *ion* describes a process: emission, absorption, reflection, transmission. Any words that ends in *ance* represents a property of a specific sample. Finally, any words that ends in *ivity* represents a property of the generic material.

The International Lighting Vocabulary of the CIE generally follows this school of thought and proposes following parameters: reflectance and reflectivity,

absorptance and absorptivity, transmittance and transmissivity to describe property of a specific sample or a property of the generic material.

Reflectance (for incident radiation of a given spectral composition, polarization and geometrical distribution) (ρ) is defined in the ILV as a ratio of the reflected flux to the incident flux in the given conditions. Reflectivity (of a material) (ρ_∞) is reflectance of a layer of the material of such a thickness that there is no change of reflectance with increase in thickness.

Absorptance (α) is defined as ratio of the flux absorbed by the material to flux incident on it under specified conditions. Spectral absorptivity (of an absorbing material) $\alpha_{i,o}(\lambda)$ is spectral internal absorptance of a layer of the material such that the path of the radiation is of unit length, and under the conditions in which the boundary of the material has no influence.

Transmittance (for incident radiation of a given spectral composition, polarization and geometrical distribution) (τ) is ratio of the transmitted flux to the incident flux in the given conditions. Spectral transmissivity (of an absorbing material) $\tau_{i,o}(\lambda)$ is spectral internal transmittance of a layer of the material such that the path of the radiation is of unit length, and under the conditions in which the boundary of the material has no influence.

As pointed by Siegel and Howell [4] for substances opaque at the wavelengths of emission, the intrinsic and the extrinsic parameters describing material ability to emit radiation would be the same as the emission of radiant flux from a opaque material is a surface phenomenon. Probably because of this reason the ILV uses only one term "the emissivity" and symbol ε to describe emissive properties of non-blackbodies surfaces. However, the *1993 Handbook of Fundamentals of the American Society of Heating, Refrigerating, and Air-Conditioning Engineers* [5] uses term "emittance" and the symbol ε to describe emissive properties of actual pieces of materials and points that the term emissivity refers to the property of materials that are optically smooth and thick enough to be opaque. A relatively new American Society for Testing of Materials (ASTM) standard [6] follows this terminology but uses the Roman letter e for emittance and the Greek letter ε for emissivity. Next, there are publications [3] that use the terms "emittance" to mean flux density (an equivalent of earlier defined exitance), not as a mean of radiation efficiency. Further on, there exist publications [8,11] where the terms "absorptivity", "reflectivity" and "transmissivity" have meanings of the terms "absorptance", "reflectance" and "transmittance" defined according to earlier presented scheme. Finally, the term "transmission" is used in the *Handbook of Infrared & Electro-Optical Systems of SPIE* [9] as a quantity describing material property in situation when according to the mentioned earlier standards [1,5,6] this terms is restricted to describe the process.

We will keep to the recommendation of the ILV through the remainder of this book and use the terms "emissivity", "absorptance", "reflectance" and "transmittance" to describe properties of a specific sample. However, a reader must be aware that this school of terminology is not universally accepted.

For people carrying out not-contact temperature measurements material ability to emit radiation is the most important material property. Therefore, in this subchapter we will concentrate on different kinds of the term “emissivity³” used in literature to describe material ability to emit radiation and relationships between emissivity, absorptance, reflectance and transmittance. Because of the mentioned earlier confusion in terminology only these types of emissivity, absorptance, reflectance and transmittance really needed to explain principles of non-contact temperature measurement will be defined next. This limitation is really important as at least eight types of emissivity, four types of absorptance, eight types of reflectance and eight types of transmittance are used in literature to describe material ability to absorb, reflect and transmit radiation.

2.4.1 Emission properties

A blackbody is an ideal radiator which emits as much radiant energy as possible. Such emission can occur only inside an isothermal closed cavity. It is not possible to observe emission of this completely closed cavity. However, it is possible to manufacture a technical blackbody made as a cavity with a small hole in one of the cavity walls. Emission of such a technical blackbody is very close to that of an ideal blackbody.

Emission of real materials is lower than that of an ideal blackbody and we need parameters to characterize the emissive properties of such real materials. The properties are defined by comparison with that of blackbodies at the same temperature and can be described by four parameters: spectral directional emissivity, spectral (hemispherical) emissivity, directional (total) emissivity and total (hemispherical)⁴ emissivity [8,11].

The spectral directional emissivity $\varepsilon_{\lambda,\varphi}$ depends on the wavelength λ and the angle φ and is defined as in the formula

$$\varepsilon_{\lambda,\varphi} = \frac{L_{\lambda,\varphi}}{L_{bb,\lambda,\varphi}} \quad (2.16)$$

where $L_{\lambda,\varphi}$ is the spectral radiance of the material for the wavelength λ in the direction φ and $L_{bb,\lambda,\varphi}$ is the spectral radiance of the blackbody for the wavelength λ in the direction φ .

A particular kind of the spectral emissivity in the direction φ occurs for $\varphi=0$; in the direction normal to the radiating surface as the value of the spectral emissivity is the greatest in this direction. The spectral emissivity in the normal direction $\varepsilon_{\lambda,n}$ can be expressed by the formula

³ Only two kinds of emissivity (directional emissivity and hemispherical emissivity) are defined in the ILV.

⁴ The adjectives in brackets are usually not mentioned.

$$\varepsilon_{\lambda,\varphi} = \frac{L_{\lambda,n}}{L_{bb,\lambda,n}} \quad (2.17)$$

where $L_{\lambda,n}$ is the spectral radiance of material in the normal direction, and $L_{bb,\lambda,n}$ is the spectral radiance of the blackbody in normal direction.

On account of the needs of visual pyrometry, values of normal spectral emissivity for red light are often presented in many emissivity tables [11]. This quantity is expressed by $\varepsilon_{\lambda=0.65,n}$, where 0.65 is the wavelength in μm .

The spectral (hemispherical) emissivity ε_{λ} is defined as ratio of the material spectral exitance M_{λ} to the blackbody spectral exitance $M_{bb,\lambda}$

$$\varepsilon_{\lambda} = \frac{M_{\lambda,n}}{M_{bb,\lambda,n}} \quad (2.18)$$

Directional (total) emissivity in the direction φ is expressed as ratio of the material radiance $L_{T,\varphi}$ in the direction φ to the blackbody radiance $L_{T,\varphi}$ in the direction φ

$$\varepsilon_{T,\varphi} = \frac{L_{T,\varphi}}{L_{bb,T,\varphi}} \quad (2.19)$$

Directional total emissivity in the normal direction $\varepsilon_{T,n}$ is a particularly privileged kind of directional total emissivity $\varepsilon_{T,\varphi}$ for the same reasons as the spectral emissivity in normal direction $\varepsilon_{\lambda,n}$. It can be expressed by the formula

$$\varepsilon_{T,n} = \frac{L_{T,n}}{L_{bb,T,n}} \quad (2.20)$$

where $L_{T,n}$ is the material radiance in the normal direction, and $L_{bb,T,n}$ is the blackbody radiance in normal direction. This type of emissivity is most frequently measured and quoted in literature. It is often confused with the spectral (hemispherical) emissivity ε_{λ} .

Finally, the total hemispherical emissivity ε_T is defined as ratio of the material exitance M_T to the blackbody exitance $M_{bb,T}$

$$\varepsilon_T = \frac{M_T}{M_{bb,T}} \quad (2.21)$$

The spectral directional emissivity $\varepsilon_{\lambda,\varphi}$ gives information about material emissive properties for any the wavelength λ and the angle φ . On the basis of the known spectral directional emissivity $\varepsilon_{\lambda,\varphi}$ it is possible to calculate other types of emissivity: the spectral (hemispherical) emissivity ε_{λ} , the directional total emissivity $\varepsilon_{T,n}$ and the total hemispherical emissivity ε_T . However, as the spectral directional emissivity $\varepsilon_{\lambda,\varphi}$ is often a complex function of the wavelength λ

and the angle φ it is difficult to determine it experimentally. Therefore, functions of the spectral directional emissivity $\varepsilon_{\lambda,\varphi}$ are very rarely published in literature.

There are four types of emissivity that are usually presented in emissivity tables found in literature: the total hemispherical emissivity ε_T , the directional total emissivity in normal direction $\varepsilon_{T,n}$, the spectral directional emissivity in normal direction $\varepsilon_{\lambda,n}$ and spectral directional emissivity in the normal direction $\varepsilon_{\lambda=0.65,n}$ for wavelength $\lambda=0.65\mu\text{m}$. However, their usefulness for user of modern non-contact radiation thermometers is usually limited because of a few reasons.

First, the total emissivity ε_T gives information about material emission into whole hemisphere and in whole optical range. Therefore, values of the ε_T are useful only in case of diffusive gray-body types objects, emissive properties of which do not depend on the angle φ and the wavelength λ .

Second, directional total emissivity in the normal direction $\varepsilon_{T,n}$ presents information about material ability to emit radiation only into one direction ($\varphi = 0$) and in whole range of optical radiation. The angle φ often differs from 0 during real measurements. As emissive properties of most material depend on the angle of observation φ the value of the $\varepsilon_{T,n}$ can be misleading. There is also other reason for limited usefulness of the directional total emissivity in the normal direction $\varepsilon_{T,n}$. Most real materials are selective materials, emissive properties of which depend on wavelength in situation when sensitivity of most non-contact thermometers depend on wavelength, too.

Third, the spectral directional emissivity in the normal direction $\varepsilon_{\lambda,n}$ presents information about material ability to emit radiation into only one direction ($\varphi = 0$). Therefore, the values of $\varepsilon_{\lambda,n}$ can be misleading when measurements are done for other angles. In spite of this, the published functions $\varepsilon_{\lambda,n}(\lambda)$ are usually quite useful as they enable estimation of object emissivity in the thermometer spectral band. However, there is often a problem to find suitable data of $\varepsilon_{\lambda,n}$ in the required spectral band.

Fourth, values of spectral directional emissivity in the normal direction $\varepsilon_{\lambda=0.65,n}$ for the wavelength $\lambda=0.65\mu\text{m}$ are often useless in case of typical infrared systems as the spectral emissivity $\varepsilon_{\lambda,n}$ in infrared range can differ quite significantly from $\varepsilon_{\lambda=0.65,n}$.

2.4.2 Relationships between radiative properties of materials

There are two most important relationships between radiative properties of materials. The first is the radiative energy balance that connects absorptance, reflectance and transmittance. The second is Kirchhoff's law that relates absorptance and emissivity.

Applying energy balance on the surface element, we get that that the sum of hemispherical total absorptance α_T , the hemispherical total reflectance ρ_T and the hemispherical total transmittance τ_T equals 1

$$\alpha_T + \rho_T + \tau_T = 1 \quad (2.22)$$

Next, assuming elementary spectral interval and that some phenomena (luminescence, Raman scattering) are negligible we can write

$$\alpha_{\lambda} + \rho_{\lambda} + \tau_{\lambda} = 1 \quad (2.23)$$

where α_{λ} is the hemispherical spectral absorptance of radiation from the hemisphere, ρ_{λ} is the hemispherical spectral reflectance of radiation from hemisphere into hemisphere, and τ_{λ} is hemispherical spectral transmittance of radiation from hemisphere into hemisphere.

Radiation that reaches material surface comes often not from the whole hemisphere but only from a certain direction. For such a situation the relationships between directional quantities that can be treated as directional spectral energy balance can be written as

$$\alpha_{\lambda, \varphi} + \rho_{\lambda, \varphi} + \tau_{\lambda, \varphi} = 1 \quad (2.24)$$

where $\alpha_{\lambda, \varphi}$ is the directional spectral absorptance of radiation from the direction φ , $\rho_{\lambda, \varphi}$ is directional-hemispherical spectral reflectance of radiation from the direction φ into hemisphere, and $\tau_{\lambda, \varphi}$ is the directional-hemispherical spectral transmittance.

The Kirchhoff's law states that at local thermodynamic equilibrium of an element of material surface, that the directional spectral emissivity $\varepsilon_{\lambda, \varphi}$ is equal to the directional spectral absorptance $\alpha_{\lambda, \varphi}$

$$\varepsilon_{\lambda, \varphi} = \alpha_{\lambda, \varphi} \quad (2.25)$$

It means that material ability to emit radiation into the direction φ is directly connected with its ability to absorb radiation from the direction φ .

Formulas (2.24, 2.25) enable indirect determination of the directional spectral emissivity $\varepsilon_{\lambda, \varphi}$ when the directional-hemispherical spectral reflectance $\rho_{\lambda, \varphi}$ and the directional-hemispherical spectral transmittance $\tau_{\lambda, \varphi}$ are known

$$\varepsilon_{\lambda, \varphi} = 1 - \rho_{\lambda, \varphi} - \tau_{\lambda, \varphi} \quad (2.26)$$

For opaque materials the above presented relationship can be transformed to a new form

$$\varepsilon_{\lambda, \varphi} = 1 - \rho_{\lambda, \varphi} \quad (2.27)$$

Principle of temperature measurement with active systems is based on equations (2.26, 2.27) as they enable indirect way of emissivity determination by measuring relations between the incident flux, the reflected flux and the transmitted flux. However, it must be emphasized that to determine $\varepsilon_{\lambda, \varphi}$ accurately it is necessary to measure not the radiation reflected into the direction φ but into the hemisphere. This misconception brought significant errors in great number of measurements.

2.4.3 Emissivity of common materials

Tables or graphs with data about the four types of emissivity (the total hemispherical emissivity ε_T , directional total emissivity in the normal direction $\varepsilon_{T,n}$, the spectral directional emissivity in normal direction $\varepsilon_{\lambda,n}$ and spectral directional emissivity in the normal direction $\varepsilon_{\lambda=0.65,n}$ for wavelength $\lambda=0.65\mu\text{m}$) can be found in great number of books, papers, reports etc. However, in addition to the discussed in Section 2.4.1 limitations of these parameters there are additional problem with interpretation of typical emissivity data found in literature. First, different sources present sometimes completely inconsistent values. Second, emissivity values are often unclearly defined or they are not defined at all. Parameters in many tables are termed only “emissivity” without any additional explanation whether it is the total hemispherical emissivity ε_T , directional total emissivity in the normal direction $\varepsilon_{T,n}$ or spectral directional emissivity in the normal direction $\varepsilon_{\lambda=0.65,n}$ for the wavelength $\lambda=0.65\mu\text{m}$. As an example can be treated Tab. 2.5 and Tab. 2.6 with emissivities of common materials published by one of leading manufacturers of thermal cameras [12]. The manufacturer, however, honestly emphasizes that the presented values are meant to be used only as a guide and can vary depending on many different factors. To summarize, we can say that in spite of numerous sources with emissivity data it is often difficult to find in literature information about value of object emissivity in real measurement conditions.

Tab. 2.5. Typical emissivities of common metals

Material	State of surface	Temperature [°C]	Emissivity
Aluminum:	foil (bright)	20	0.04
	weathered	20	0.83 - 0.94
Iron	cast, oxidized	100	0.64
	sheet, heavily rusted	20	0.69 - 0.96
Copper:	polished	100	0.05
	heavily oxidized	0.78	0.78
Nickel:	electroplated, polished	20	0.05
Stainless Steel (type 18-8)	polished	20	0.16
	oxidized	60	0.85
Steel	polished	100	0.07
	oxidized	200	0.79

Tab. 2.6. Typical emissivities of other materials

Materials	State of surface	Temperature [°C]	Emissivity
Brick	common red	20	0.93
Carbon candle soot		20	0.95
Concrete	dry	35	0.95
Glass	chemical ware	35	0.95
Oil	lubricating	17	0.87
	film thickness 0.03 mm	20	0.27
	film thickness 0.13 mm	20	0.72
	thick coating	20	0.82
Paint, oil	average of 16 colors	20	0.94
Paper	white	20	0.7 - 0.90
Plaster		20	0.86 - 0.90
Rubber	black 5	20	0.95
Skin	human	32	0.98
Soil	dry	20	0.92
	saturated with water	20	0.95
Water	distilled	20	0.96
	frost crystals	-10	0.98
	snow	-10	0.85
Wood	planed oak	20	0.90

2.5 Transmission of optical radiation in atmosphere

The interaction of emitted optical radiation with atmosphere is a complex process. This subchapter discusses only the essential theories and experimental data needed to explain the influence of the atmosphere on thermal radiation on its way from the source to the detector. Earth's atmosphere is a mixture of many gases. The gaseous contents in atmosphere vary with altitude, time and space. However, the gaseous contents shown in Tab. 2.7 can be considered as typical for clear atmosphere [13]. The major components of the atmosphere are molecules of N_2 and O_2 . Next is argon of much less concentration. Other constituents have very low concentration in atmosphere. However, two of them are important as they mostly decide about atmosphere transmittance.

Water vapor have concentration of about 10^{-5} % to about 10^{-2} % of the volume. The concentration of the water vapor depends significantly on altitude, season, geographic location, time of day, meteorological conditions and is subject to large fluctuations.

Carbon dioxide is more uniformly distributed, with concentration of approximately about $3 \cdot 10^{-2}$ % of the volume. There is higher concentration of carbon dioxide over industrial centers and vegetation areas than over oceans and deserts.

Tab. 2.7. Composition of atmospheric constituent gases

Constituent gas	Content (% by volume)
N ₂	78.084
O ₂	20.9476
Ar	0.934
CO ₂	$3 \cdot 10^{-2}$
H ₂ O	$10^{-5} - 10^{-2}$
Ne	$1.81 \cdot 10^{-3}$
He	$5.2 \cdot 10^{-4}$
CH ₄	$2 \cdot 10^{-4}$
Kr	$1.14 \cdot 10^{-4}$
H ₂	$5 \cdot 10^{-5}$
N ₂ O	$\approx 5 \cdot 10^{-5}$
CO	$\approx 7 \cdot 10^{-6}$
O ₃	0 to $7 \cdot 10^{-6}$
NO	0 to $2 \cdot 10^{-6}$

2.5.1 Optical properties of atmosphere

Thermal radiation emitted by objects carries information about radiance distribution on the surfaces of these objects. Atmosphere can significantly distort this information because of four phenomena: absorption, scattering, emission and turbulence.

The first two phenomena cause attenuation of propagating optical radiation; the third one adds additional radiation, and the fourth one causes distortion of the image of the emitting objects.

There are distinguished two kinds of absorption: molecular absorption and aerosol absorption. However, because of several minor components of the atmosphere, the molecular absorption is a much more significant source of attenuation of propagating radiation than the aerosol absorption is.

Scattering phenomenon causes redistribution of the incident flux into all direction of propagation and diminishes the flux propagation in the original direction. There are distinguished two kinds of atmospheric scattering: molecular (Rayleigh) scattering and aerosol (Mie) scattering. The aerosol scattering affects atmospheric transmittance much more stronger than the molecular scattering does. Generally,

the scattering effect diminishes when wavelength of the propagating radiation increases. Therefore, transmittance of haze is much higher in the infrared than in the visible.

It was shown in Section 2.4.2 that the directional spectral emissivity $\varepsilon_{\lambda, \varphi}$ is equal to the directional spectral absorptance $\alpha_{\lambda, \varphi}$. It means that atmospheric absorptance equals its emissivity. As atmospheric absorptance is always higher than null and atmosphere temperature is also always higher than absolute null it means that the atmosphere must emit its own radiation. However, for short-distance conditions during typical non-contact temperature measurements the atmosphere emissivity is usually very low. Temperature of the atmosphere during most measurement is also lower than the temperature of the tested object. Therefore, the phenomenon of atmosphere emission can be treated as negligible in most temperature measurement applications.

Atmospheric turbulence phenomenon is caused by random irregular air movements. It arises when air molecules of slightly different temperatures are mixed by wind and convection. From optical point of view such random irregular air movements means random fluctuation of refractive index of the atmosphere. When optical radiation propagate through atmosphere, the refractive index varies through the medium and that smears the image generated by the optical system. This effect is evident for distances object-system of at least a few hundredth meters and only for thermal cameras of high quality of the image. Therefore, this phenomenon can significantly degrade performance of military thermal or TV cameras. However, non-contact temperature measurements are rarely made at the distances over 50 m and image quality of typical measurement thermal cameras is not very good. Therefore, the influence of atmospheric turbulence on results of temperature measurement with non-contact thermometers can be almost always treated as negligible.

2.5.2 Numerical calculations

Because of large number of parameters the atmospheric transmittance depends on, it is necessary to employ numerical models to predict with a high degree of accuracy the transmittance through atmosphere for a given path, meteorological conditions and wavelength.

It seems, that there are three most popular numerical models that enable calculation of atmospheric transmittance: LOWTRAN, MODTRAN and HITRAN. All three models were developed in the Air Force Geophysics Laboratory (AFGL). LOWTRAN is a computer code that calculates atmospheric transmittance with low spectral resolution over a wide spectral range. It enables calculation of atmospheric transmittance within spectral range from 0.25 μm to 28.5 μm with a spectral resolution of 0.002 λ that is sufficient for most applications.

MODTRAN is a higher resolution version of LOWTRAN.

HITRAN is actually not a transmission model but a molecular data compilation to be used with line-by-line transmittance codes. Its spectral resolution is about 0.00005λ that makes it especially suitable for laser transmittance calculations.

All three models are continuously updated as new measurements become available and better understanding of transmission process are reached. Currently, LOWTRAN 7 version is available.

Almost all non-contact thermometers are relatively broadband systems in comparison to spectral resolution offered by the LOWTRAN. Therefore, this model or other low-resolution models are used to calculate and correct the influence of the atmosphere on propagating thermal radiation on its way to non-contact thermometers. It happens also, as for typical short-distance measurements the influence of the atmosphere on temperature measurement is often small, that some manufactures of relatively modern systems do not use any transmittance models to correct effect of attenuation of propagating radiation by the atmosphere. As spectral bands of non-contact thermometers are usually located within so called "atmospheric transmittance windows" this practice is quite justified for a short distance measurements [Fig. 2.9-Fig. 2.11], especially when the thermometer spectral band is located within the 8-14 μm window.

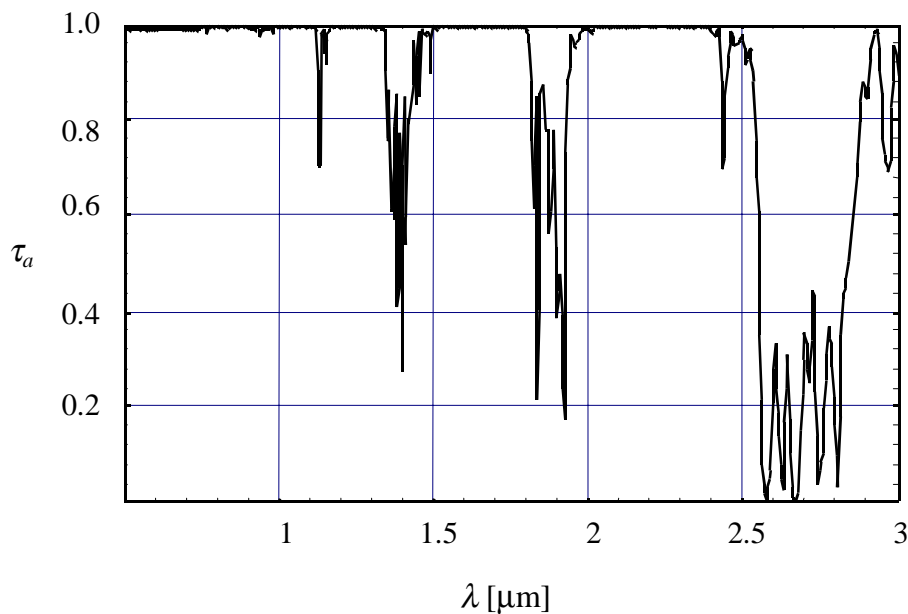


Fig. 2.9. Atmospheric transmittance for 10 m distance in spectral range 1-3 μm

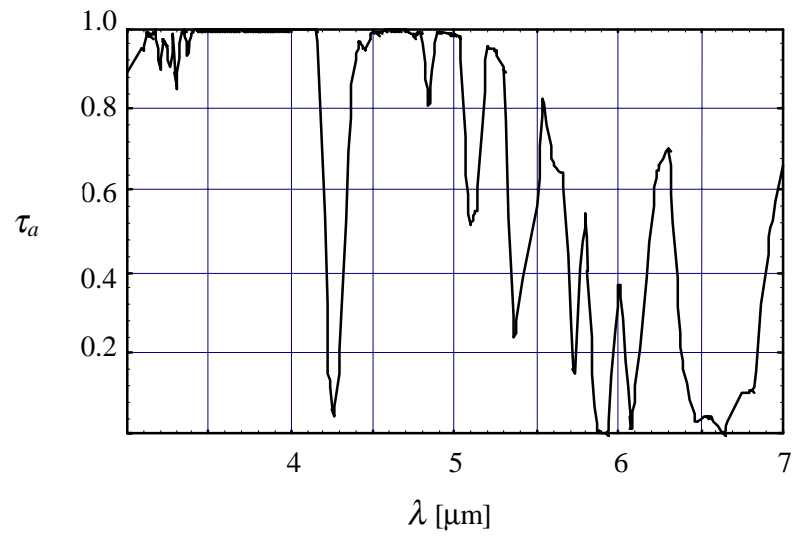


Fig. 2.10. Atmospheric transmittance τ_a for 10 m distance in the spectral range 3-7 μm

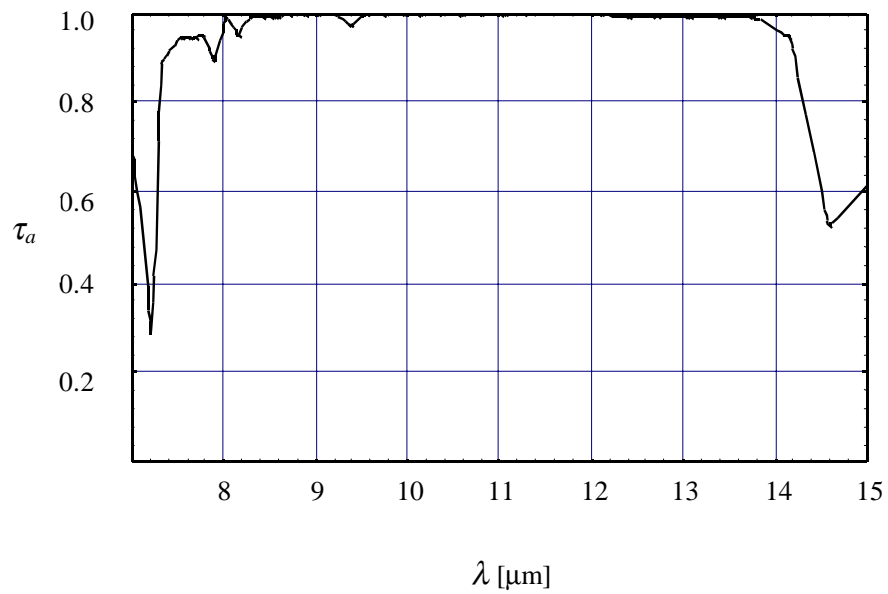


Fig. 2.11. Atmospheric transmittance τ_a for 10 m distance in the spectral range 7-15 μm

2.6 Source/receiver flux calculations

The most general configuration of source/receiver geometry is presented in Fig. 2.12. For this situation the total flux received by the area A_o from the source area S_o can be determined using the formula [1]

$$\Phi = \int_{S_o} \int_{A_o} L \frac{ds_o \cos\theta da_o \cos\psi}{R^2} \quad (2.28)$$

where Φ is the total flux received by the area A_o from the source area S_o , θ is the angle made by the direction of emerging flux with respect to the surface of the source, ds_o is an infinitesimally small element of area at the point of definition in the source, da_o is an infinitesimally small elements of area at the point of definition in the receiver, ψ is the angle made by the direction of coming flux with respect to the surface of the receiver, R is the distance between the emitting point of the source and the receiving point of the receiver.

Formula (2.28) is the fundamental equation describing the transfer of radiation from source to receiver. Many flux transfer problems involve this integration over finite areas of the source and the receiver. The problem can be quite complex analytically because in general L , θ , ψ , and R will be the functions of position in both the source and the receiver surfaces. There exists also general dependency of L on direction embodied in this equation, since the direction from a point in the source to a point in the receiver generally changes as the point in the receiver moves over the receiving surface.

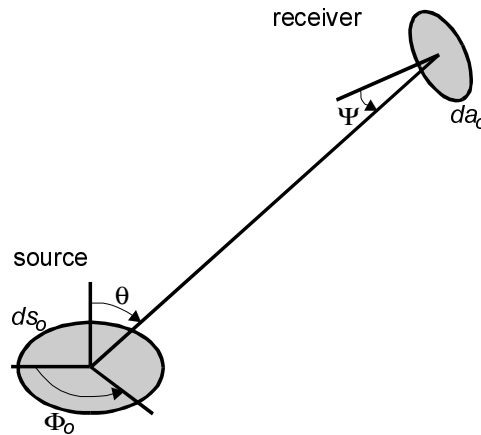


Fig. 2.12. General source/receiver geometry

We can distinguish two general cases of transfer of radiation from source to receiver useful for analysis of non-contact thermometers. First, when the radiation

from the source comes directly to the detector. Second, when the radiation from the source comes to the detector through optical elements.

2.6.1 Geometry without optics

The equation (2.28) can be significantly simplified in three cases that are often met in practical radiation measurement.

For all three cases the angular dimension of detector is assumed to be small. This assumption is fulfilled in most practical cases. The differences between the mentioned above three cases are connected with size of source.

For the first case we have a large circular or quasi-circular source irradiating a small area detector as shown in Fig. 2.13.

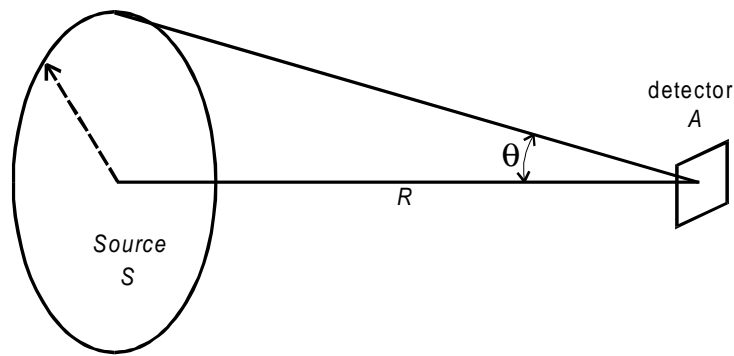


Fig. 2.13. Geometry of a circular source irradiating a small detector

For this case the flux received by the detector can be calculated from this formula

$$\Phi = \pi \cdot L \cdot A \cdot \sin^2 \theta \quad (2.29)$$

where Φ is the flux received by the detector, L is radiance of the source, θ is half of the angle that source subtends from the center of the detector, and A is the detector area.

For the second case a source of infinite size irradiates the detector. Then the angle $\theta = 90^\circ$, $\sin \theta = 1$ and the flux received by the detector can be calculated from this formula

$$\Phi = \pi \cdot L \cdot A. \quad (2.30)$$

For the third case, a small area source of dimensions much smaller than the distance R irradiates the detector. In this case the flux Φ can be calculated using another formula

$$\Phi = \frac{S \cdot L \cdot A}{R^2} \quad (2.31)$$

The presented above formulas (2.29 –2.31) are simple. Nevertheless they enable estimation of the flux obtained by a detector irradiated by many sources used in practice.

2.6.2 Geometry with optics

A block of optics before the detector is used in almost all non-contact thermometers. This block is used to limit the field of view of the detector and to increase the radiation that comes to the detector. Typical optical configuration during measurements with such thermometers is shown in Fig. 2.14.

Let us assume a typical situation when the detector is put exactly into the image plane of the tested object, and it can see, due to the cold shield, only the optics. Next, we assume that a well-corrected imaging aplanatic optics, that fulfils the sinus condition, is used.

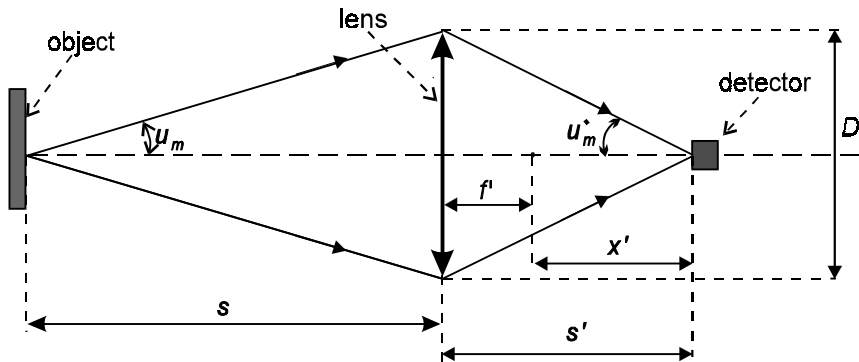


Fig. 2.14. Typical optical configuration during measurements with systems using an optical block before the detector

The radiation emitted by the surface determined by the detector angular dimensions with the solid angle determined by the area of the optical objective and distance optics-object reaches the detector. Derivation of formulas that enable calculation of the flux received by the detector, for the case shown in Fig. 2.14, on the basis of the fundamental equation (2.28) are complicated. Therefore, there will start the final formula that expresses the irradiation in the detector plane

$$E = \pi \tau_o L \sin^2 u_m' \quad (2.32),$$

where π is pi, τ_o is the optical transmittance, L is the object radiance, u_m' is the angle between the optical axis and the maximal aperture ray in the image space, $\sin u_m'$ is numerical aperture of the optical system in the image space.

Formula (2.32) is not too convenient as it requires knowledge about the parameter rarely known: the angle between the optical axis and the maximal aperture ray in image space u_m' . Therefore it is desirable to replace this angle with

typical parameters describing optical system like its focal length f' , aperture diameter D and distance between the optics and the tested object s .

For situations presented in Fig. 2.14, using classical geometrical relationships and the well-known Newton formula we have

$$\sin u'_m = \frac{\frac{D}{2}}{\sqrt{\left(f' + \frac{f'^2}{s - f'}\right)^2 + \left(\frac{D}{2}\right)^2}}. \quad (2.33)$$

After inserting Eq. (2.33) into Eq. (2.32) we obtain

$$E = \frac{\pi\tau_o L D^2}{4 \left[\left(f' + \frac{f'^2}{s - f'}\right)^2 + \left(\frac{D}{2}\right)^2 \right]}. \quad (2.34)$$

Formula (2.34) is equally general as formula (2.32) as it enables calculation of the radiant irradiance E for any distance s but it requires knowledge about only typical parameters of any imaging optics: D and f' .

Now let us consider a case that quite often occur in many applications when the distance s is many times longer than the focal length f' ($s \gg f'$). For such a situation the formula (2.34) simplifies to a new form

$$E = \frac{\pi\tau_o L}{4[F^2 + 1]}, \quad (2.35)$$

where F is the optics F-number that equal the ratio of the focal length f' and the aperture diameter D .

Many optical objectives used in non-contact thermometers, especially in thermal cameras, are systems of F-number higher or close to 2. For such systems $F^2 \gg 1$ and the formula enabling determination of the irradiance in the focal plane simplifies even further

$$E = \frac{\pi\tau_o L}{4F^2}. \quad (2.36)$$

Eq. (2.36) is used in derivation of many theoretical models of parameters of systems used to register optical radiation like *NETD*, *MRTD* or *MDTD* of infrared imaging systems. However, it is necessary to emphasize that Eq. (2.36) and the models derived from it are based on two important assumptions: the object is located in optical infinity ($s \gg \gg f'$) and that optics of high F -number is used. When these two assumptions are not fulfilled the application of Eq. (2.36) can bring significant er-

rors of estimation of the irradiance E . These assumptions are not fulfilled, for example, in optical microscopy where the distance s is short and F is low. Let us determine the irradiance E for such a case.

For a well designed optics that fulfils the sinus condition the lateral magnification of the optical system β equals

$$\beta = \frac{\sin u}{\sin u'} . \quad (2.37)$$

On the basis of geometry rules and the Newton formula we can derive a relationship between numerical aperture in imaging space $\sin u'_m$ and the lateral magnification β in the form

$$\sin^2 u'_m = \frac{1}{4F^2(1+\beta)^2 + 1} , \quad (2.38)$$

that gives a new formula enabling determination of the irradiance E

$$E = \frac{\pi\tau_o L}{4F^2(1+\beta)^2 + 1} . \quad (2.39)$$

Eq. (2.39) shows that that the irradiance E decreases when the lateral magnification β of the optical system increases. Similarly, formula (2.34) suggests that the irradiance E decreases when the distance s decreases. Generally, both Eq. (2.34) and Eq. (2.39) show that the maximum irradiance E occurs when the measured object is in infinity and lateral magnification equals null ($s=\infty$, $\beta=0$). For any other value of the distance s or lateral magnification β , the irradiance E will be lower. Let us define as magnification factor MF the ratio of the maximum irradiance E for the conditions $s=\infty$, $\beta=0$ to the irradiance E for any other value of the s or β . The magnification factor MF can be determined using the following formulas

$$MF = \frac{E(s=\infty)}{E(s)} = \frac{4 \left[\left(f' + \frac{f'^2}{s-f'} \right)^2 + \left(\frac{D}{2} \right)^2 \right]}{D^2(4F^2 + 1)} , \quad (2.40)$$

$$MF = \frac{E(s=\infty, \beta=0)}{E(\beta)} = \frac{4F^2(1+\beta)^2 + 1}{4F^2 + 1} . \quad (2.41)$$

Graphical presentation of Eqs. (2.40-2.41) is shown in Fig. 2.15 - Fig. 2.16.

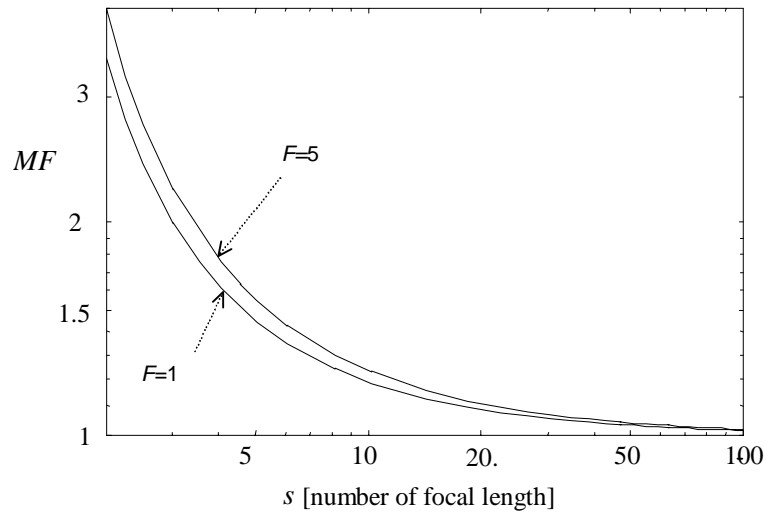


Fig. 2.15. Relationship between the magnification factor MF and the distance object-optics s

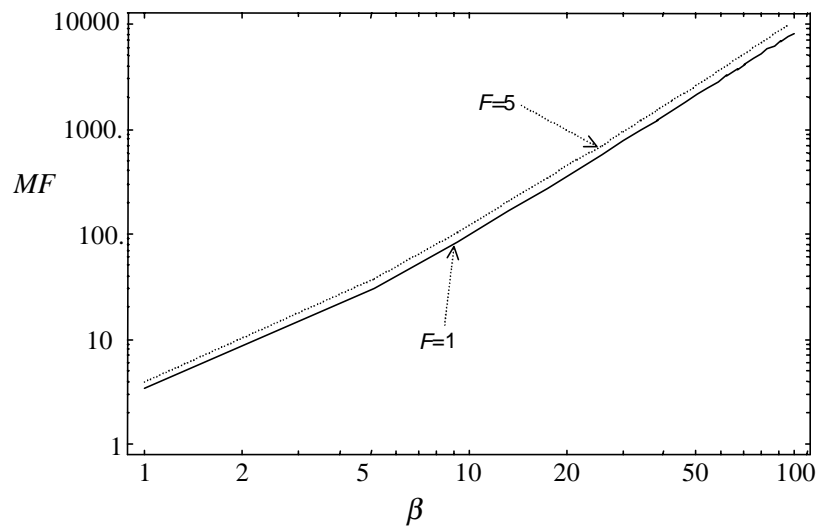


Fig. 2.16. Dependence of the magnification factor MF on the optical lateral magnification β

The magnification factor MF carries information how many times the irradiance E at optics focal plane is lower than for the ideal situation when the distance s equals infinity and the lateral magnification β equals null. From formulas (2.40) and (2.41) we can conclude that the factor MF varies from 1 to infinity and that it decreases with the distance s and increases with the lateral magnification β . As shown in Fig. 2.15 the dependence of MF on the distance s is significant for

the distances s below about $20f$. In case of infrared microscopy (Fig. 2.16), when the lateral magnification $\beta > 1$, the values of MF are even higher. Consequences of these conclusions are significant as many projects to design thermal microscopes of high temperature resolution failed because of the presented dependence of the irradiance E on the magnification β .

2.7 References

1. International Lighting Vocabulary, CIE Publ. No. 1 7.4, IEC Publ. No. 50(845) (1987).
2. Richmond J. C., Rationale for emittance and reflectivity, *Applied Optics* 21,1, 1982.
3. Hudson R. D., *Infrared Systems Engineering*, Wiley-Interscience, 1969.
4. Siegel R., Howell J. R., *Thermal radiation heat transfer*, 2nd ed., Hemisphere Publishing/McGraw-Hill Book Co.; New York, NY, 1981.
5. ASHRAE, 1993 ASHRAE Handbook fundamentals, Amer. Soc. Heat., Refrig., and Air-Cond. Eng., Atlanta, 1993.
6. ASTM, Standard test method for emittance of specular surfaces using spectrometric methods, Standard E-1585, Amer. Soc. Test. Materials, 1916 Race St., Philadelphia, PA 19103, 1994.
7. McCluney William Ross, *Introduction to radiometry and photometry*, Artech House 1994, p.4.
8. Maldague X. P., *Infrared Methodology and Technology*, Gordon and Breach Science Publishers, 1992.
9. Zissis George J. ed., *The Infrared & Electro-Optical Systems Handbook*, Vol.1: Sources of radiation, Chapt. 1 Radiation Theory, p.199, SPIE (1993).
10. Wolfe W.L., Proclivity for emissivity, *Applied Optics*, 1 (1982).
11. Sala A., *Radiant Properties of materials*, PWN-Polish Scientific Publishers, Warsaw & Elsevier Amsterdam-Oxford (1986).
12. www.FSI.com/meas.html (1998)
13. Seyrafi Khalil, Hovanessian S.A., *Introduction to electro-optical imaging and tracking systems*, Artech House, Norwood (1993).

3. Methods of non-contact temperature measurement

In Chapter 1 we presented seven criteria of describing the systems for non-contact temperature measurement: human role in measurement, presence of an additional source in measurement process, location of spectral bands, number of system spectral bands, width of spectral bands, transmission media and number of measurement points [Fig.1.1]. Every non-contact thermometer can be relatively precisely characterized by a combination of 7 adjectives and nouns, for example "an objective passive infrared singleband broadband atmosphere pyrometer". It is theoretically possible to distinguish 648 different types of these systems. It is probably practically possible to design over 100 different types of these thermometers. However, only a few types of non-contact thermometers are used in practical applications. It seems that only 6 different types of non-contact thermometers are manufactured in relatively high numbers and used in numerous applications:

1. objective passive infrared singleband broadband atmosphere pyrometers (50%),
2. objective passive infrared singleband narrow-band atmosphere pyrometers (38%),
3. objective passive infrared dualband narrow-band atmosphere pyrometers (4 %),
4. objective passive infrared singleband narrow-band fiber pyrometers (4.5 %)
5. objective passive infrared singleband broadband atmosphere thermal cameras (3 %),
6. objective passive infrared singleband broadband atmosphere thermal scanners (0.5%),
7. others (about 1%).

Figures of exemplary systems from six mentioned above groups are presented in Figs.3.1-3.6. As we can see, all the commonly used systems are objective passive infrared systems. Therefore, the three adjectives "objective passive infrared" will not be later used in description of these systems.

It is difficult, almost impossible, to present precise proportions between the mentioned above groups of thermometers. Therefore, the values in the brackets should be treated only as estimates of real values. These values are not based on market research and represent only a private opinion of the author of this book based on a certain experience in this area. Next, it must be emphasized that the borders between different types of the presented above systems are sometimes fluid as there are commercially available non-contact thermometers that are offered in different versions.



Fig. 3.1. Singleband broadband atmosphere pyrometer: Mikron IR Man[®]



Fig. 3.4. Singleband broadband fiber pyrometer: Infrared Fibre Transmitter M50 manufactured by MIKRON Instruments[®]



Fig. 3.2. Singleband narrowband atmosphere pyrometer: Modline 3 manufactured by IRCON^{5®}



Fig. 3.5. Singleband broadband atmosphere thermal camera: ThermoCAM manufactured by Inframetrics Inc[®]



Fig. 3.3. Dualband narrow-band atmosphere pyrometer: DICHROMA manufactured by E²T[®]



Fig. 3.6. Singleband broadband atmosphere thermal scanner: Thermo Profile TM Infrared Line Scanner manufactured by FLIR Systems[®]

⁵ Modline 3 is also available as fiber optics pyrometers.

The thermometers from the first two groups (singleband broadband pyrometers and singleband narrowband pyrometers) clearly dominate the market. They are widely used in numerous applications as independent portable devices or blocks of automated systems mostly because of their low cost and easiness of use.

The dualband thermometers from the third group are advertised by manufacturers as immune to error caused by emissivity changes in target material and bursts of steam, dust, etc. in the sight path. They are usually more expensive than the earlier discussed singleband thermometers. Additionally, there are applications when they offer accuracy comparable to accuracy of the latter thermometers, or even worse. Therefore, the dualband pyrometers are much less numerous than the singleband pyrometers.

The fiber thermometers from the fourth group are specially targeted for applications when direct sighting due to obstructions is impossible, significant RF and EMI interference is present and electronics must be placed at a safe distance, or very high temperatures exist. They can be also used in other applications. Because of flexibility they offer and resistance to the mentioned earlier effects, they are becoming nowadays more and more popular. However, they are still rather rarely met in comparison to the singleband atmosphere thermometers.

Thermal cameras from the fifth group represent only a small fraction of all non-contact thermometers. They are much less numerous than pyrometers as they are much more expensive than the latter devices.

Finally, the thermal scanners from the sixth group are at the end of the column because of two reasons. First, because they can generate a two dimensional thermal image only in case of moving targets and they can be used only in limited number of applications. Second, price of a thermal scanner is not significantly lower than price of a thermal camera and people have a tendency to buy thermal cameras due to their higher capabilities.

Apart from the mentioned earlier 6 types of mass-use non-contact thermometers there are 3 additional types that found some applications mostly in limited number of applications:

1. subjective passive visible singleband narrow-band atmosphere pyrometers,
2. objective active infrared singleband narrow-band atmosphere pyrometers,
3. objective passive infrared singleband total radiation atmosphere pyrometers.

Subjective pyrometers from the first group are nowadays very rarely used in industrial applications because due to subjective character of the measurement process they are slow, time consuming for their users and cannot be used in present day automated technological processes etc. However, they offer high measurement accuracy if used by experienced users and are sometimes used in research laboratories for control of other types of non-contact thermometers or in other applications that require high accuracy.

Active singleband pyrometers from the second group have not so far been successful on market. However, there are active pyrometers manufactured as classical passive singleband pyrometers integrated with lasers working as radiation sources [1]. The price of such systems is still relatively high and accuracy gains are significant only in a few applications.

Total radiation pyrometers have the advantage over broadband 8-12 μm pyrometers due to a bit higher output signal because of a wider spectral band. However, they are more vulnerable to variation of transmittance of the atmosphere. Therefore, they are used only in short distance applications.

There are also 5 types of systems that so far have been developed only in research laboratories. At present, they are not available commercially but they could be in future:

1. objective passive infrared multiband narrow-band atmosphere pyrometers,
2. objective passive infrared multiband narrow-band atmosphere cameras,
3. objective active infrared dualband narrow-band atmosphere pyrometers,
4. objective active infrared multiband narrow-band atmosphere pyrometers,
5. objective passive microwave singleband broadband atmosphere pyrometers.

Indications of passive multiband thermometers do not depend theoretically on object emissivity even when the latter parameter depends significantly on wavelength and changes during technological process. There have been published the reports about successful designs of a few passive multiband pyrometers or cameras [2,3,4,5,6,7,8].

Active dualband or multiband pyrometers represent another possible solution to ensure better temperature measurement accuracy. There have been published also some reports about research in this area [9,10].

All the discussed earlier types of non-contact thermometers enable generally temperature measurement on surfaces of objects of interest as most materials are opaque in visible and infrared range. However, most materials transmit relatively well microwave radiation. It means that microwave thermometers can measure temperature under a surface that could be very useful in some applications. There have been published a few papers informing about progress in development of microwave thermometers [11,12].

As it was presented earlier, there are many different types of non-contact thermometers. However, there are only a few different methods of non-contact temperature measurement as many types of thermometers use the same measurement method. There is, for example, no significant differences between measurement methods used by pyrometers, thermal scanners or thermal cameras. Similarly, thermometers that differ because of different spectral range (visible, infrared, microwave) can use the same method of temperature measurement. Next, both fiber thermometers and atmosphere thermometers can use the same measurement method.

It seems that it is possible to distinguish 7 different methods of temperature measurement used by earlier presented non-contact radiation thermometers:

1. objective passive *singleband* method,
2. objective passive *dualband* method,
3. objective passive *multiband* method,
4. objective *active* singleband method,
5. objective *active* dualband method,
6. objective *active* multiband method,
7. *subjective* passive singleband method.

Further analysis will be limited to the first four of the mentioned above methods. Single and dualband passive methods were included to the analyzed group because almost all available on the market non-contact thermometers use one of these methods. Active singleband method was also included because a few such thermometers are commercially available and their number may increase in future. Systems using the passive multiband methods are so far not commercially available. However, there is a significant interest in these systems and there are quite a few reports in literature about such systems. Therefore, it is a good place to present this method, too.

The active dualband method and the active multiband method were excluded from the analyzed group because so far the systems using these methods are not commercially available and there are very few reports in literature about research in this area. Finally, the subjective passive singleband method was also excluded because they are being nowadays replaced with objective thermometers.

3.1 *Passive methods*

3.1.1 *Singleband method*

Singleband method of non-contact temperature measurement is based on a phenomenon of dependence of the radiant flux emitted by the tested object on object's temperature. As we can see in Fig. 3.7 there exists one-to-one correspondence between the exitance M and the object temperature T for any wavelength λ . This correspondence creates possibility of determination the object temperature T when the exitance M is known.

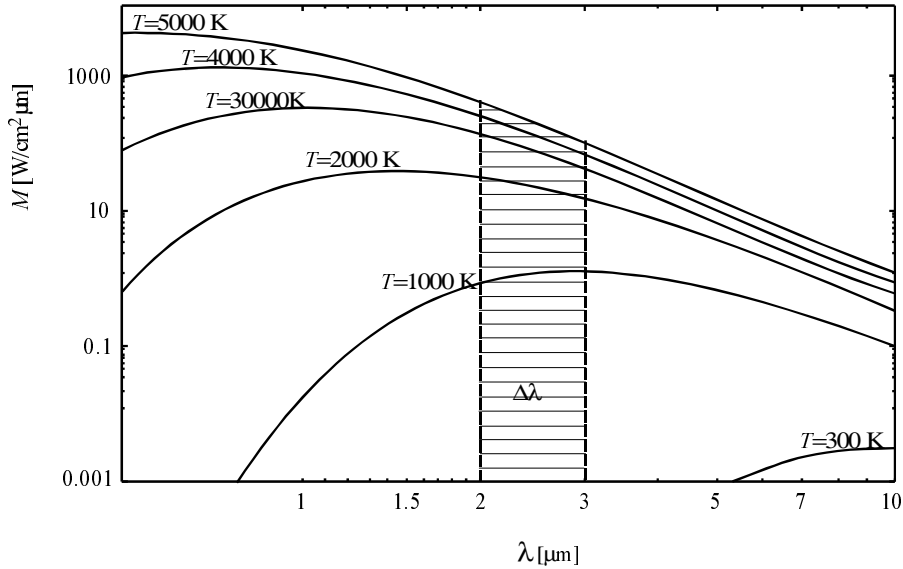


Fig. 3.7. Dependence of the radiant exitance M of a blackbody on wavelength λ for different temperatures T

3.1.1.1 Measurement procedure

Singleband systems measure temperature indirectly from radiant flux of radiation incident on the detector in one spectral band. It is possible to determine temperature of the tested object on the basis of the output signal caused by radiation emitted by the object within the thermometer spectral band, using different theoretically derived analytical functions [13,14,15]. However, in case of most commercially available non-contact thermometers, the output temperature is determined on the basis of the absolute value of the output electrical signal, the measurement conditions assumed by the user, and an experimentally determined calibration characteristic of the thermometer. The function represent dependence of the device output signal on temperature of a blackbody.

Most singleband thermometers employ a following 4 step measurement procedure to determine temperature of the tested object.

1. Measurement of the calibration characteristic $S_{bb}=f(T_{bb})$ at the discrete temperatures T_{bb} . On the basis of the measurement results and using different approximation functions the inverse calibration function $T_{bb}=f(S_{bb})$ is calculated.
2. Measurement of the real output signal S_r generated by tested object of the temperature T_{ob} .

3. Correction of the measured signal S_r to the new value S_{cor} using a certain mathematical model of the measurement process and assumed by the user measurement conditions (effective object emissivity, effective background temperature, and sometimes effective atmospheric transmittance and temperature of the optical components).

Different thermometers require from the user to input to camera microcomputer different measurement conditions. The mentioned above set of the measurement conditions should be treated as the most general. However, we must remember that in case of some simple non-adjustable pyrometers the user is not required to make any assumptions about the measurement process. The output temperature is determined directly on the basis of the real signal. Next, there are thermal cameras that require from the user to input to camera microcomputer not the effective atmospheric transmittance but the relative humidity and the temperature of the atmosphere and distance to the tested object and calculate the effective emissivity. Further on, the user is not required to estimate temperature of the optical elements as this temperature is measured automatically in case of modern thermal cameras.

4. Calculation of the output temperature on the basis of the value of the corrected signal S_{cor} using the inverse calibration chart $T_{bb}=f(S_{bb})$.

In fact, the first step of this procedure is usually carried out in the factory, and later is repeated very rarely. However, the three steps 2-4 are made during every measurement as graphically shown in Fig. 3.8.

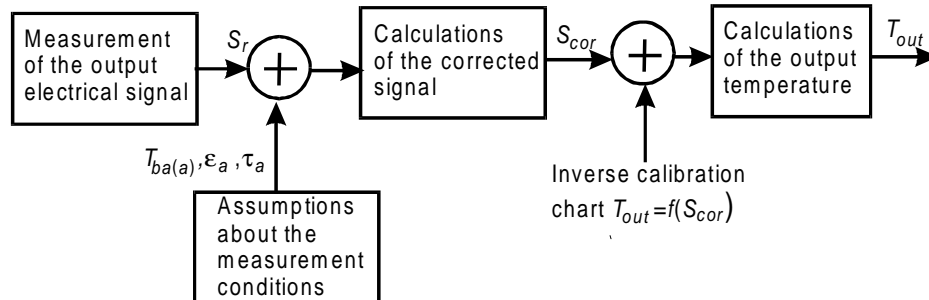


Fig. 3.8. Measurement procedure with passive singleband systems

Now, we shall model mathematically the procedure to enable determination of the output temperature T_{out} shown above.

3.1.1.2 Calibration characteristic

The calibration characteristic $S_{bb}=f(T_{bb})$ is usually determined experimentally using a blackbody as a reference object. As blackbody reflectance is almost zero, then the signal emitted by the background and reflected the blackbody is negligible. Next, the distance between the system and the blackbody is short during the calibration process and the influence of the atmosphere on the measured signal S_{lab} is negligible, too. Therefore, the signal S_{lab} measured during calibration process

when a blackbody is a tested object, is a sum of two signals: the signal generated by the radiation emitted by the blackbody S_{bb} and the signal caused by the radiation emitted by the optical blocks (optical objective, scanning systems, optical filters)

$$S_{lab}(T_{bb}) = S_{bb}(T_{bb}) + S_{op(c)}. \quad (3.1)$$

The signal generated by the blackbody S_{bb} is modeled mathematically as

$$S_{bb}(T_{bb}) = g \frac{R^* A_d \tau_o \tau_{sc}}{4F^2 + 1} \int_{\lambda_1}^{\lambda_2} M(T_{bb}, \lambda) \tau_F(\lambda) s(\lambda) d\lambda, \quad (3.2)$$

where g is the amplification of the electronic block, R^* is the peak detector spectral sensitivity, A_d is the detector area, and F is the optics F-number (ratio of focal length f' of the optical objective to diameter D of the objective), λ_1 and λ_2 are the limits of the detector spectral band, $M(T, \lambda)$ is the spectral exitance at the temperature T and wavelength λ , τ_o is the transmittance of the optical objective, τ_{sc} is the transmittance of the scanning block⁶, τ_F is the transmittance of the filter⁷, and $s(\lambda)$ is the detector relative spectral detectivity function.

The function $S_{bb}(T_{bb})$ is usually used as the calibration characteristic of the thermometer. However, for the non-contact thermometers having exchangeable optical objectives it is desirable to know the signal generated by a blackbody without any optical objectives (or having an ideal objective of transmittance equal to one). For such systems the function $S_{bb}(T_{bb})/\tau_o$ is used as the calibration characteristic.

The signal caused by the radiation emitted by the optical blocks $S_{op(c)}$ during calibration can be presented as

$$S_{op(c)} = \varepsilon_{opt} \frac{gR^* A_d}{4F^2 + 1} \int_{\lambda_1}^{\lambda_2} M(T_{op(c)}, \lambda) s(\lambda) d\lambda, \quad (3.3)$$

where ε_{opt} is the effective emissivity of the optical blocks and $T_{op(c)}$ is the temperature of the optical components of the thermometer during calibration.

Example 1. Calculate the signals S_{lab} , S_{bb} , $S_{op(c)}$ using formulas (3.1-3.3) for case of an infrared singleband broadband atmosphere pyrometer. Such pyrometers are built using thermal detectors (typically thermocouples or thermopiles) with an optical filter of 8-12 μm spectral band. We will assume following parameters of this thermometer:

$$\begin{array}{lllll} g = 1000 & R^* = 9 \text{ V/W} & A_d = 0.01 \text{ cm}^2 & F = 2 & \tau_o = 0.9 \\ \varepsilon_{opt} = 0.3 & T_{op(c)} = 300 \text{ K} & \tau_F = 0.6 \text{ for } 8 \mu\text{m} < \lambda < 12 \mu\text{m} \text{ and } 0 \text{ outside} & & \end{array}$$

⁶ For pyrometers, thermal scanners or thermal cameras without scanning block the τ_{sc} component should be removed from formula (3.44).

⁷ For thermometers without optical filters the τ_F component should be removed from formula (3.44).

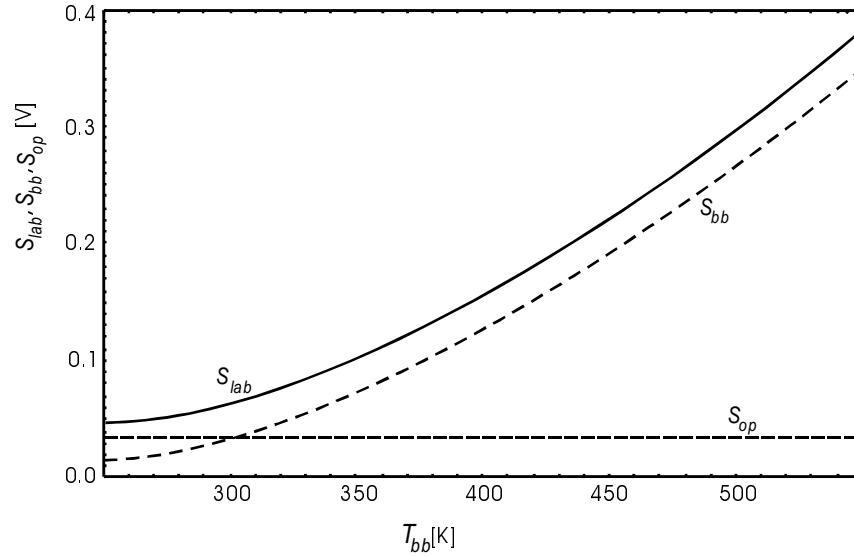


Fig. 3.9. Calibration characteristic of an example infrared singleband broadband pyrometer

The signals S_{cal} , S_{bb} , S_{op} are presented in Fig. 3.9 in *Volts* units. However, they can be presented also in other electrical units or in relative units chosen by a manufacturer.

As we can see in Fig. 3.9 the signal S_{op} does not depend on temperature of the blackbody T_{bb} ; it depends only on temperature of the optical components $T_{op(c)}$. Changes of the signal S_{cal} are caused by changes of the signal S_{bb} that depends on the temperature T_{bb} of the blackbody.

It is theoretically possible to determine very accurately both S_{lab} , S_{bb} , and $S_{op(c)}$ signals using formulas (3.1-3.3) or their modified versions. However, it is difficult to predict accurately these signals; it is particularly difficult to predict the signal caused by the radiation emitted by the optical components $S_{op(c)}$. Therefore, these signals are typically determined experimentally during a calibration process using an external blackbody as a simulated tested object.

First, the output signal S_{lab} is measured when a blackbody is a tested object for different temperatures T_{bb} and we determine the function $S_{lab}(T_{bb})$. Next, the signal $S_{op(c)}$ is measured by putting, for example, a very cold object in thermometer field of view. Further on, the function $S_{bb}(T_{bb})$ is calculated as difference of the $S_{lab}(T_{bb})$ minus $S_{op(c)}$.

The calibration characteristic or the calibration chart of the thermometer is usually understood as the function $S_{bb}=f(T_{bb})$. However, in fact the inverse calibration characteristic $T_{bb}=f_{inv}(S_{bb})$ is used in the measurement procedure because it is necessary to determine the output temperature T_{out} on the basis of the value of the corrected signal S_{cor} [Fig. 3.10].

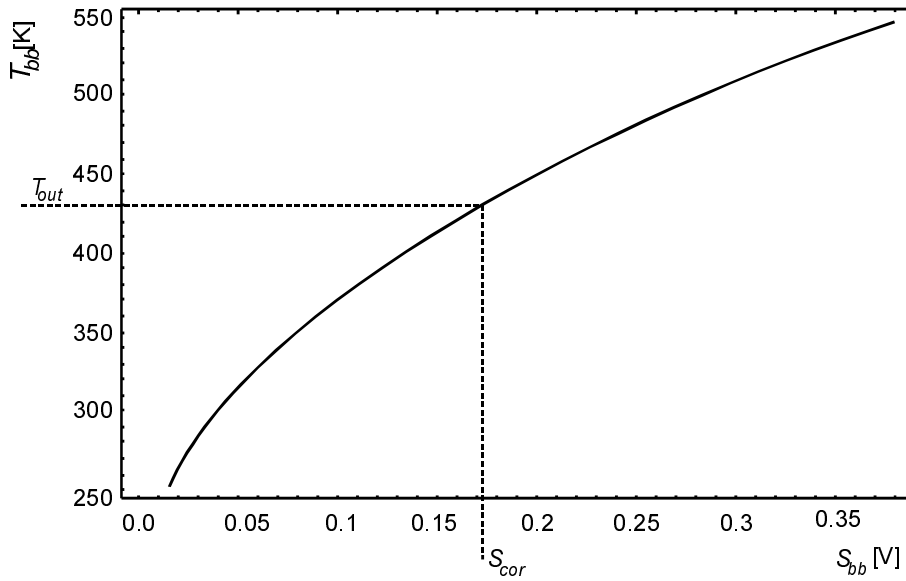


Fig. 3.10. Inverse calibration characteristic

3.1.1.3 Real output signal

During the second step of the measurement procedure presented earlier, the signal S_r generated by the real object of temperature T_{ob} is measured. The formula enabling determination of this signal will be derived in Chapter 4. Now, let us simply assume that the signal S_r was measured.

3.1.1.4 Corrected output signal

Due to difference between the real measurement conditions and the calibration conditions, the signal S_r usually differs from the signal S_{bb} generated by a blackbody of temperature equal to the object the temperature T_{ob} . This means that if we determine the output temperature T_{out} using the inverse calibration chart as $T_{out}=f_{inv}(S_r)$ then there will be difference between thermometer indication T_{out} and the true object temperature T_{ob} . Therefore, to avoid this possibility, the signal S_r must be corrected to the new signal S_{cor} that would be generated by a blackbody of temperature equal to the object temperature T_{ob} in laboratory conditions.

The correction is made using a mathematical model of a measurement channel between the object and the output of the electronic blocks and a few values of measurement conditions (object effective emissivity, effective background temperature and effective transmittance of the atmosphere) determined by the user.

The model typically assumes that the signal recorded when the object of temperature T_{ob} is a tested object can be presented as a sum of three components: the signal caused by the radiation emitted by the object $S_{em(a)}$, the signal emitted by

the environment and reflected by the object $S_{re(a)}$ and the signal from the radiation emitted by the optical components $S_{op(a)}$

$$S_a = S_{em(a)} + S_{re(a)} + S_{op(a)}. \quad (3.4)$$

The signal $S_{em(a)}$ is assumed to be

$$S_{em(a)}(T_{ob}) = \varepsilon_a \tau_{a(a)} S_{bb}(T_{ob}), \quad (3.5)$$

where ε_a is the assumed object effective emissivity, $\tau_{a(a)}$ is the assumed effective atmospheric transmittance.

Object emissivity and atmospheric transmittance are usually functions of wavelength λ . Users of singleband thermometers usually do not know these functions. However, they can usually estimate object effective emissivity and effective atmospheric transmittance: one value parameters that represent the influence of object emissivity and limited atmospheric transmittance on the measured signal. The assumed parameters ε_a and $\tau_{a(a)}$ represent these influences and are termed using the word "effective" to make difference with object emissivity and atmospheric transmittance understood as functions of the wavelength λ .

The effective emissivity ε_a can be defined as an emissivity of a greybody of the same temperature as the tested object that produces the same signal at the output of the detector as the real object does and can be calculated as was presented in [16]

$$\varepsilon_a = \frac{\int_{\lambda_1}^{\lambda_2} \varepsilon(\lambda) L(\lambda, T_{ob}) \tau_o(\lambda) \tau_F(\lambda) s(\lambda) d\lambda}{\int_{\lambda_1}^{\lambda_2} L(\lambda, T_{ob}) \tau_o(\lambda) \tau_F(\lambda) s(\lambda) d\lambda}, \quad (3.6)$$

where $\varepsilon(\lambda)$ is the true object emissivity and $L(\lambda, T)$ is the object radiance for the wavelength λ and the temperature T .

There are two cases when formula (3.6) can be significantly simplified. For graybody objects the effective emissivity ε_a equals the object emissivity ε that in this case does not depend on the wavelength. For selective objects but measured with systems of sensitivity not dependent on wavelength (it often occurs when thermal detectors are used), the object effective emissivity ε_{ef} is equal to mean value of the object emissivity $\varepsilon(\lambda)$ within the system spectral band λ_2, λ_1 .

If results from Eq.(3.6) that the object effective emissivity ε_a depends not only on wavelength dependent emissivity $\varepsilon_{ob}(\lambda)$ and systems parameters $s(\lambda)$, $\tau_o(\lambda)$ and $\tau_F(\lambda)$ but also on object temperature T_{ob} . Fortunately, this dependence is relatively significant only in case when system sensitivity $s(\lambda)$ and the object's emissivity $\varepsilon(\lambda)$ strongly depends on the wavelength λ [16]. For typical objects and systems the dependence of the effective emissivity ε_a on the object temperature T_{ob}

is small and often the effective emissivity ε_a can be considered as independent on object temperature.

Many methods of determination of the effective emissivity of the tested object can be found in literature. However, now, we will only comment that there is no a perfect method to determine this parameter. Limited accuracy of determination of the effective emissivity is often a significant source of errors of determination of object's temperature.

The effective atmospheric transmittance $\tau_{a(a)}$ can be defined in a similar manner as the effective emissivity and calculated by a formula

$$\tau_{a(a)} = \frac{\int_{\lambda_1}^{\lambda_2} \tau_a(\lambda) L(\lambda, T_{ob}) \tau_o(\lambda) \tau_F(\lambda) s(\lambda) d\lambda}{\int_{\lambda_1}^{\lambda_2} L(\lambda, T_{ob}) \tau_o(\lambda) \tau_F(\lambda) s(\lambda) d\lambda}, \quad (3.7)$$

where $\tau_a(\lambda)$ is the true atmospheric transmittance that depends on wavelength.

Most pyrometers and also some thermal cameras use the method of determination of output temperature assuming that the effective atmospheric transmittance $\tau_{a(a)}$ equals one. This means, that the calculation methods used by most non-contact thermometers do not even try to correct⁸ the influence of the limited transmittance of the atmosphere on measurement results. However, most modern thermal cameras enable correction of the atmosphere on measurement results. These systems require from the user to determine the distance between the object and the front lens of the camera r and the relative humidity of the atmosphere RH . These two parameters are used to calculate the effective atmospheric transmittance $\tau_{a(a)}$ using different simplified models of atmospheric transmittance.

The signal $S_{re(a)}$ is assumed as equal to

$$S_{re}(T_{ba(a)}) = (1 - \varepsilon_a) \tau_{a(a)} S_{bb}(T_{ba(a)}), \quad (3.8)$$

where $T_{ba(a)}$ is the assumed effective background temperature.

The effective background temperature T_{ba} is the temperature of a blackbody that when put in the place of the real background would produce the same output signal as the real background does. In case of a uniform high emissivity background the effective background temperature T_{ba} equals true background temperature.

The signal $S_{op(a)}$ is

$$S_{op(a)} = f_{op}(T_{op(a)}), \quad (3.9)$$

where $T_{op(a)}$ is the assumed temperature of the optical components and f_{op} is the function that represents dependence of the output signal due to radiation emitted by optical components on their temperature $T_{op(a)}$. The function $f_{op}(T_{op(a)})$

⁸ It will be shown in Chapt. 4 that in many cases it is not necessary to correct influence of the atmosphere because this influence can be considered negligible.

is usually determined experimentally by changing temperature of the optical components and recording the signal S_{op} .

For simpler MIR and FIR thermal cameras⁹, the value of the $T_{op(a)}$ is determined by the user, in case of more sophisticated cameras it is automatically measured using temperature sensitive elements placed in the optical components.

Finally, the whole assumed signal S_a can be presented using a formula

$$S_a = \varepsilon_a \tau_{a(a)} S_{bb}(T_{ob}) + (1 - \varepsilon_a) \tau_{a(a)} S_{bb}(T_{ba(a)}) + S_{op}(T_{op(a)}). \quad (3.10)$$

Formula (3.10) represents the assumed model of the measurement channel that is used to derive the formula for correction of the real measured signal S_r . It is assumed that the measured signal S_r is equal to the assumed signal S_a . and then the corrected signal S_{cor} can be obtained as

$$S_{cor} = \frac{S_r - (1 - \varepsilon_a) \tau_{a(a)} S_{bb}(T_{ba(a)}) - S_{op}(T_{op(a)})}{\varepsilon_a \tau_{a(a)}}. \quad (3.11)$$

Example 2: Determine the corrected signal S_{cor} for a following case:

$$S_r = 0.2,$$

$$\varepsilon_a \in (0.5, 1),$$

$$\tau_a = 0.9,$$

$$T_{ba} = 250 \text{ K},$$

$$T_{op(a)} = 300 \text{ K}.$$

Solution: Let us assume that the functions $S_{bb}(T)$ and $S_{op}(T_{op(a)})$ can be determined using formulas (3.2-3.3) although practically they are determined experimentally. Next, we can determine the corrected signal S_{cor} for the assumed measurement conditions (ε_a , τ_a , T_{ba} , $T_{op(a)}$) using the formula (3.11). The values of the corrected signal S_r are shown in Fig. 3.11. As can we see in this figure, the signal S_{cor} strongly depends on value of the assumed effective emissivity ε_a . If we made calculations of the S_{cor} for different values of $\tau_{a(a)}$, $T_{ba(a)}$ and $T_{op(a)}$ then we would find that the S_{cor} depends significantly on the assumed values of the effective atmospheric transmittance $\tau_{a(a)}$, the effective background temperature $T_{ba(a)}$ and the assumed optics temperature $T_{op(a)}$.

⁹ For VNIR and NIR thermometers the influence of the radiation emitted by the optical elements is negligible.

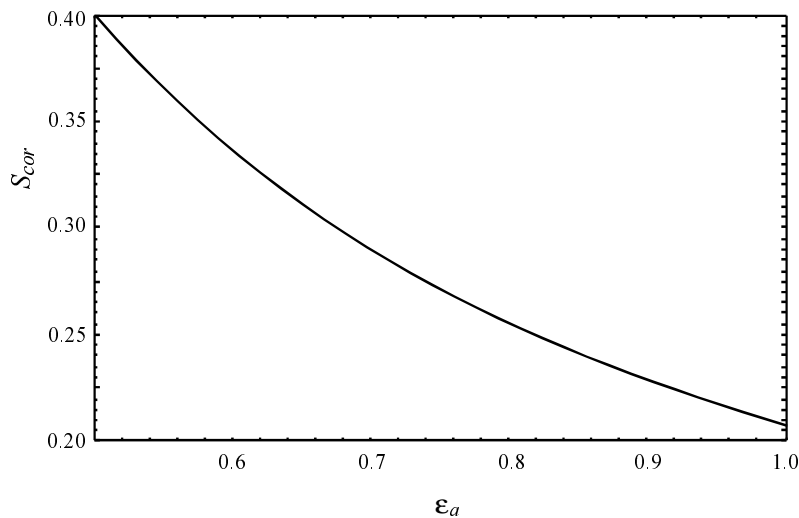


Fig. 3.11. Dependence of the corrected signal S_{cor} on the assumed object effective emissivity ϵ_a

3.1.1.5 Output temperature

Finally, the output temperature T_{out} is calculated on the basis of the determined value of the corrected signal S_{cor} and the inverse calibration characteristic during the fourth step of the measurement procedure by the formula

$$T_{out} = f_{inv}(S_{cor}). \quad (3.12)$$

Example 3. Determine the output temperature T_{out} for the case when the corrected signal equals $S_{cor}=0.172$.

Solution: Using the inverse calibration characteristic $T_{bb}=f_{inv}(S_{bb})$ we can determine the output temperature $T_{out} = 430$ K.

3.1.2 Dualband method

Dualband method determines temperature of the tested object on the basis of the ratio between two radiometric signals measured in two spectral bands. The method can be treated as valid when the ratio of these two signals does not depend on the object emissivity, and exists one-to-one correspondence between the ratio and the object temperature.

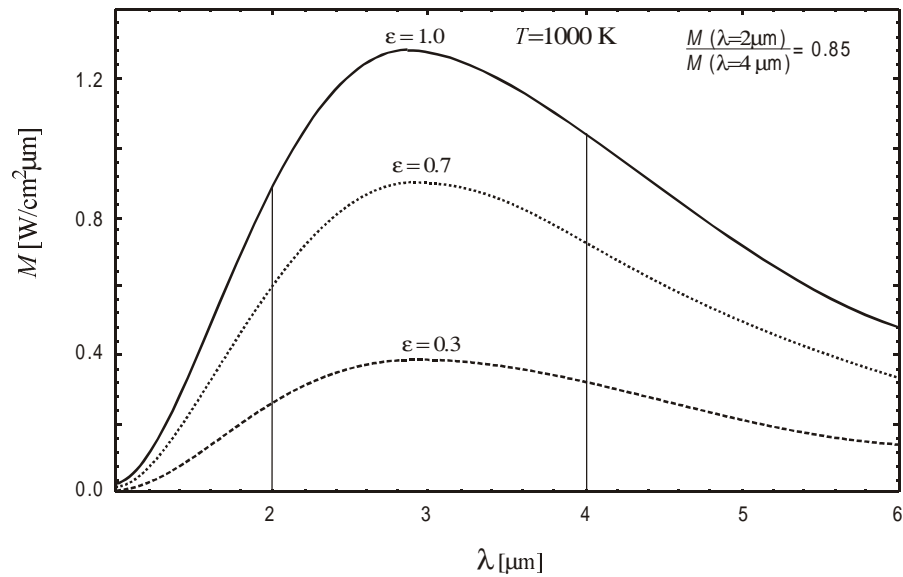


Fig. 3.12. Radiant exitance M of graybodies of different emissivities

Validity of the dualband method is evident when the spectral bands of the system are infinitesimally narrow and a graybody is the tested object [Fig. 3.12]. Real systems use spectral bands of finite widths. However, it was shown in Ref.[17] that the dualband method is valid (there exists one-to-one correspondence between the ratio and the graybody temperature; and the ratio does not depend on the object emissivity) for a more general case when neither spectral band is contained totally within the other. This gives theoretically possibility to design dualband systems of wide spectral bands (strong signals) located within infrared range. However, it was shown in Ref.[18] that in case of systems of spectral bands located in wavelengths longer than about $3 \mu\text{m}$, where the signal caused by the radiation emitted by the optical components becomes significant, the mentioned above conditions do not have to be always valid. The conditions are also typically not valid in case of wide partially overlapping spectral bands.

The problem with the non-validity of the mentioned above conditions for systems of spectral bands located in the middle and far infrared can be eliminated by using correction of the signal caused by the radiation emitted by the optical elements on the output signal. However, practically it is rarely needed as almost all commercially available dualband infrared pyrometers have narrow spectral bands located in the near infrared range where the signal due to radiation from the optical elements is negligible.

Dualband systems are the oldest alternative solution to the classical single-band systems. They have been manufactured as dualband pyrometers for over half a century. Manufacturers of dual band systems advertise them as not sensitive to

changes of emissivity of the tested object and changes of atmospheric transmittance due to bursts of steam, dust, etc. in the sight path.

The dualband thermometers can be designed in many different ways. However, in general, these systems can be divided into two groups. The first group contains the systems with two completely different optical-electronic channels (two blocks of optics, two detectors, two electronic blocks etc.) which continuously measure two different radiometric signals. The selection of a proper spectral band is achieved by using detectors of different spectral sensitivity bands or optical filters of different spectral bands [Fig. 3.13].

The second group contains systems with a single optical-electronic channel (common optics, detector, electronics). The two radiometric signals are selected by optical filters and they are measured alternatively. An example of such a system is shown in Fig. 3.14 [20]. Infrared radiation from the tested object is focused on the IR detector by the optical objective. The radiation on the way from the objective to the detector is modulated spectrally by rotating plate with two narrow-band optical filters. The detector converts the optical signals into the electrical signal that is amplified by a low noise preamplifier. Next, the electrical signals are transformed into more convenient form and digitized. Finally, the digitized signals from the two spectral bands are sent to microprocessor and visualization block.

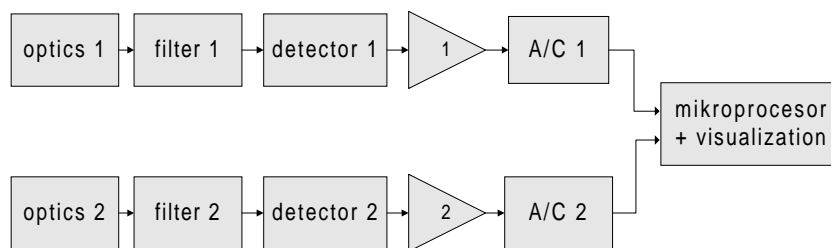


Fig. 3.13. Diagram of a dualband thermometer with two separate channels

Single-channel thermometers use only a single optical objective, a single detector, and a single electronic block. This is a significant advantage due to lower costs of these blocks. However, a moving element in form of rotating wheel with fitted filters is needed in single-channel thermometers. This solution limits measurement speed, decreases thermometer reliability and increases its sizes and mass. Therefore, the single-channel design is an especially interesting solution for dualband pyrometers of spectral bands located in the range of wavelengths longer than $3\ \mu\text{m}$ when the cost of a photoelectric detector is high. Typical dualband pyrometers of spectral bands located in the range of wavelengths shorter than $3\ \mu\text{m}$ use typically dual-channel design with one modification: they have a common optical block. We are going to assume this configuration in further investigations.

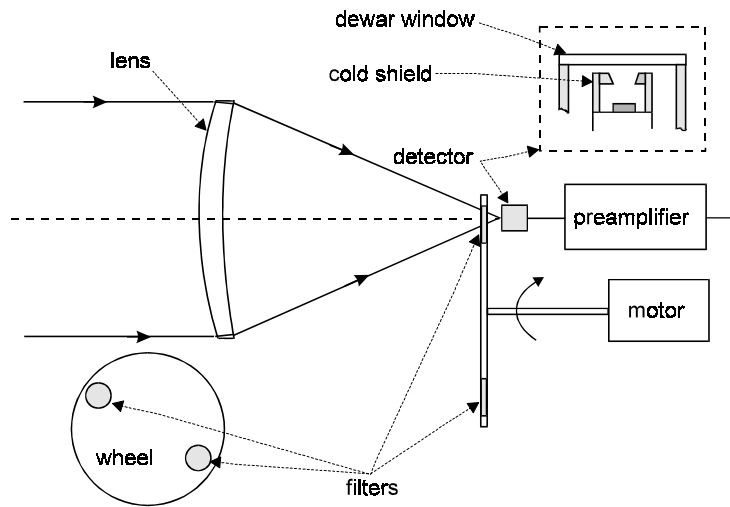


Fig. 3.14. Block diagram of a single channel dualband pyrometer

It is possible to measure temperature with dualband systems by using analytical methods. The so called reference-wavelength method provides high accuracy of temperature measurement [19]. Other analytical methods can be found in radiometric literature, too [15]. Another possible variation of the dualband method is so called multiple-pair method [21]. This method assumes an almost continuous measurement of the object spectrum. Temperature is then calculated for many individual pairs of wavelengths. Although the calculated temperature for individual pairs can exhibit considerable variation, the measured temperature tends to be quite accurate if data from enough pairs are averaged over [21].

In spite of possibility to determine output temperature using different analytical formulas, practical dualband systems do it usually using a presented below four- step measurement procedure based on the thermometer calibration chart.

- 1 Determination of the calibration characteristic $R_{bb}=f(T_{bb})$
- 2 Measurement of the real output signals S_{r1} and S_{r2} in two spectral bands and calculation of the ratio of the two measured signal $R_r= S_{r1} / S_{r2}$.
- 3 Correction of the ratio R_r is to the new value R_{cor} on the basis of the assumed ratio of object emissivity in the two spectral bands $\varepsilon(\lambda_1)/\varepsilon(\lambda_2)$ (this step is conditional).
- 4 Calculation of the output temperature T_{out} on the basis of the value of the measured ratio R_r or the corrected ratio R_{cor} .

Step 3 is used in minority of dualband pyrometers. It potentially enables improvement in measurement accuracy. However, at the same time it is inconvenient for the users, as it requires from them some knowledge about radiant properties of the tested object.

The output signal during calibration at any of the two spectral bands is a sum of the signal generated by radiation emitted by the blackbody and the signal due to radiation emitted by the optical elements. Therefore, the ratio of two output signals during calibration R_{bb} can be calculated as

$$R_{bb}(T_{bb}) = \frac{S_{b1}(T_{ob}) + S_{op1}}{S_{b2}(T_{ob}) + S_{op2}}, \quad (3.13)$$

where the S_{b1} and S_{b2} are the signals generated in the two spectral bands by a blackbody of the temperature T_{bb} during the calibration process, and the S_{op1} , S_{op2} are the signals due to radiation emitted by optical elements in the two spectral channels. Finally, the ratio R_{bb} can be modeled mathematically by the formula

$$R_{bb}(T_{bb}) = \frac{\frac{R_1^* g_1 A_{d1}}{4F_1^2 + 1} \left[\tau_{o1} \int_{\Delta\lambda_1} M(T_{bb}, \lambda) \tau_{F1}(\lambda) s_1(\lambda) d\lambda + \varepsilon_{opt1} \int_{\Delta\lambda_{d1}} M(T_{op(c)}, \lambda) s_1(\lambda) d\lambda \right]}{\frac{R_2^* g_2 A_{d2}}{4F_2^2 + 1} \left[\tau_{o2} \int_{\Delta\lambda_2} M(T_{bb}, \lambda) \tau_{F2}(\lambda) s_2(\lambda) d\lambda + \varepsilon_{opt2} \int_{\Delta\lambda_{d2}} M(T_{op(c)}, \lambda) s_2(\lambda) d\lambda \right]} \quad (3.14)$$

where R_n^* is the peak spectral sensitivity of the detector at n -th spectral channel, g_n is the amplification of electronic block at n spectral channel, A_{dn} is the area of the detector at n spectral channel, and F_n is the F-number of the optical objective optics at n spectral channel, $\Delta\lambda_n$ is the width of the n spectral band, τ_{on} is transmittance of the optical objective at n spectral channel, τ_{fn} is the transmittance of the filter used in n spectral channel and $s_n(\lambda)$ is the relative spectral sensitivity of the detector at n spectral channel, ε_{optn} is the effective emissivity of the optical block in n spectral channel and $T_{op(c)}$ is the temperature of optical components of the thermometers during calibration.

For the single channel system, such parameters like F -number, τ_o , R^* , g , A_d , $s(\lambda)$ are the same for both channels and formula (3.14) can be significantly simplified.

Example 4. Calculate the calibration chart $R_{bb}(T_{bb})$ of an example infrared dualband atmosphere pyrometer built using two identical non-cooled Ge photodiodes. Selection of spectral bands is done by using two different optical filters of the following parameters: $\lambda_1=1.53$, $\Delta\lambda_1=0.03$, $\tau_{F1} = 0.6$, $\lambda_2=1.3$, $\Delta\lambda_2=0.03$, $\tau_{F2}=0.6$. Other parameters of the thermometer are presented below.

$$\begin{aligned} R_1^* = R_2^* = 3 \text{ A/W} & \quad g_1 = g_2 = 1000 \text{ V/A} & \quad A_{d1} = A_{d2} = 0.01 \text{ cm}^2 & \quad F_1 = F_2 = 2 \\ \tau_{o1} = \tau_{o2} = 0.9 & \quad s(\lambda_1) = 0.98 & \quad s(\lambda_2) = 0.75 & \end{aligned}$$

Solution: Using formula (14) we can determine calibration chart $R_{bb}(T_{bb})$ presented in Fig. 3.15.

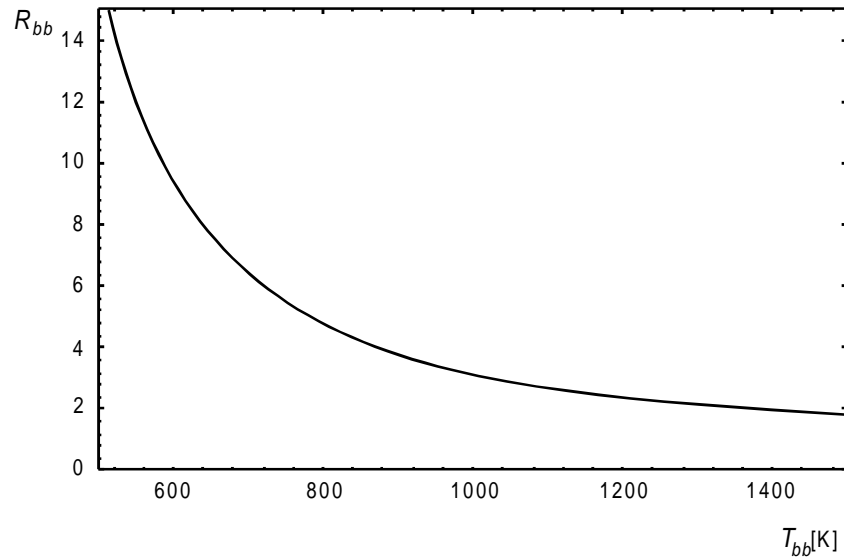


Fig. 3.15. Calibration characteristic of an example infrared dualband pyrometer

During the second step of the presented above measurement procedure the ratio R_r of the two output signals caused by the radiation emitted by tested object in two spectral bands S_{r1} and S_{r2} . The formula enabling determination of the ratio R_r will be derived in Chapt. 5. Now, let us simply assume that the signal S_r was measured.

That ratio R_r does not depend on the object temperature T_{ob} , when the object is a graybody. Generally, there are few objects that can be strictly treated as graybodies. Therefore, to extend the area of applications of dualband systems some dualband systems offer possibility of correction of the ratio R_r to a new value when a selective body is measured by using a formula

$$R_{cor} = R_r \cdot ra, \quad (3.15)$$

where ra is the assumed ratio of object emissivity in the two spectral bands that equals

$$ra = \frac{\varepsilon_2}{\varepsilon_1}.$$

Correction of the calibration chart R_{bb} in the third step of the measurement procedure extends the application area of the dualband pyrometers on both graybodies and selective bodies. However, it requires from the user knowledge about object emissive properties what is a disadvantage of the systems using this step of the procedure.

system spectral band can be interpolated by the two degree polynomial $\varepsilon_{ob}(\lambda) = a_0 + a_1\lambda + a_2\lambda^2$.

The measured output signals are the following: $S_1=0.02531$ V, $S_2=0.22216$ V, $S_3=0.96271$ V, $S_4=1.4303$ V. The parameters of the optical and electrical blocks are the same for all spectral channels and are presented in Tab. 3.1. Calculate the output temperature T_{out} and the emissivity coefficients a_0, a_1, a_2 .

Tab. 3.1. The system parameters used in the calculations

detector type	g[V/A]	$R(\lambda_{peak})$ [A/W]	τ_o	τ_F	F	A_d [cm ²]	$s(\lambda)$
thermoelectrically cooled Ge photodiode	10000	10	0.9	0.7	2	0.01	$s(\lambda=1 \mu\text{m})=0.35$ $s(\lambda=1.2 \mu\text{m})=0.6$ $s(\lambda=1.4 \mu\text{m})=0.87$ $s(\lambda=1.6 \mu\text{m})=0.6$

Solution: For the situation described in the example we obtain the following set of equations

$$\left\{ \begin{array}{l} 0.02531 = \frac{48529.459}{\left(e^{\frac{14388}{T_{out}}} - 1\right)} (a_0 + a_1 + a_2) \\ 0.22216 = \frac{83193.353}{\left(2.48832e^{\frac{11990}{T_{out}}} - 2.48832\right)} (a_0 + a_1 \cdot 1.2 + a_2 \cdot (1.2)^2) \\ 0.96271 = \frac{120630.36}{\left(5.378e^{\frac{10277.143}{T_{out}}} - 5.378\right)} (a_0 + a_1 \cdot 1.4 + a_2 \cdot (1.4)^2) \\ 1.4303 = \frac{83193.353}{\left(10.486e^{\frac{8992.5}{T_{out}}} - 10.486\right)} (a_0 + a_1 \cdot 1.6 + a_2 \cdot (1.6)^2) \end{array} \right. \quad (3.23)$$

The set of equations (3.23) cannot be solved analytically. It can be solved numerically using a few methods. The least square method was chosen to calculate unknown parameters T_{out}, a_0, a_1, a_2 and following results were obtained:
 $T_{out}=1100\text{K}$ $a_0=0$, $a_1=0$, $a_2=0.25$.

After putting the emissivity coefficients a_0, a_1, a_2 into the interpolating polynomial (3.19) we obtain the function $\varepsilon(\lambda)$ shown in Fig. 3.16 and the following emissivity values into the system spectral bands $\varepsilon(\lambda=1 \mu\text{m})=0.25$; $\varepsilon(\lambda=1.2 \mu\text{m})=0.36$; $\varepsilon(\lambda=1.4 \mu\text{m})=0.49$; $\varepsilon(\lambda=1.6 \mu\text{m})=0.64$.

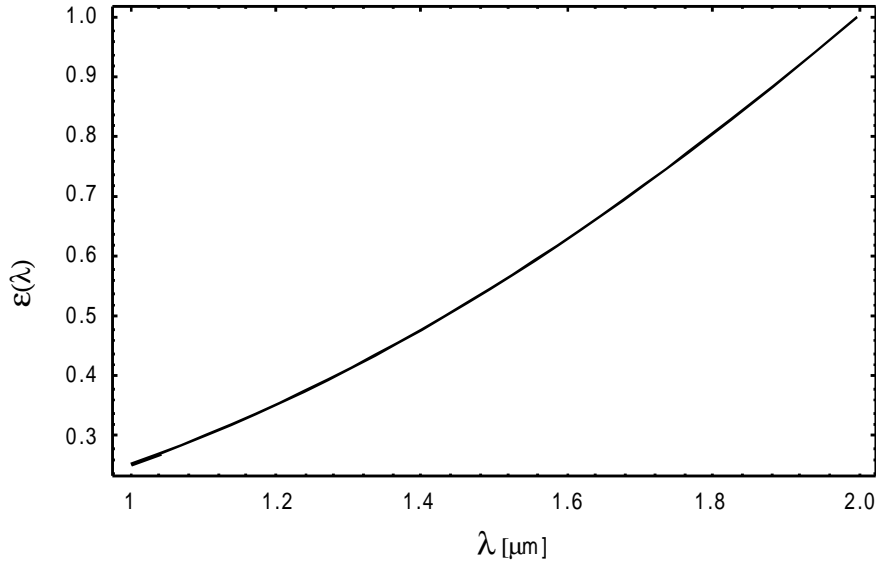


Fig. 3.16. Emissivity function $\epsilon(\lambda)$ of the tested object in example (6)

As can we see in Fig. 3.16 the multiband systems enable not only determination of temperature but also the object emissivity function $\epsilon(\lambda)$ even in case of significantly selective objects. This is a very significant advantage of the passive multiband systems. Unfortunately, they are also characterized by a few disadvantages that will be discussed in Chapt. 6 dealing with the problem of accuracy of these systems.

3.2 Active methods

It is possible to design both active single- dual- and multiband thermometers. At present, only active singleband pyrometers are commercially available [1]. At the same time, in contrast to numerous literature about passive multiband systems, there are few publications on active dual- and multiband systems. At present time the author of this book is aware of only two reports about development of active dual- and multiband systems [9,10]. Therefore in this section only the active singleband method will be discussed.

3.2.1 Singleband method

As it was presented in Section 2.4 in case of opaque objects there exist a following relationship between the directional spectral emissivity $\epsilon_{\lambda,\varphi}$ and the directional-hemispherical spectral reflectance $\rho_{\lambda,\varphi}$

$$\epsilon_{\lambda,\varphi} = 1 - \rho_{\lambda,\varphi}. \quad (3.24)$$

Formula (3.24) suggests an indirect way of determination of directional spectral emissivity $\varepsilon_{\lambda,\varphi}$ by measuring its directional-hemispherical spectral reflectance $\rho_{\lambda,\varphi}$. This way seems very attractive, especially because in many books or papers relationship (3.24) is presented in an improper form

$$\varepsilon = 1 - \rho, \quad (3.25)$$

without any information about types of emissivity and reflectance that are related.

Active singleband systems try to use equation (3.24) to determine object emissivity. These systems consist of an emitter that irradiates the tested objects and the receiver that measures radiation both emitted and reflected by the object. During the last half a century many papers about development of active singleband systems have been published. These reported in literature systems were designed using numerous solutions. However, here we are to discuss only a measurement method and design of a modern commercially available pyrometer built as an infrared laser integrated with a typical passive singleband pyrometer [1]. It is manufactured by the Pyrometer Instrument Co. and sold under the name Pyrolaser® [1]. The device consists of a laser emitting impulses of radiation of known power on wavelength $0.865 \mu\text{m}$ and a classical passive singleband pyrometer. It enables automatic measurement of both emissivity and temperature within the following ranges: emissivity 0.05-1, and temperature 600°C - 1500°C .

There is little available information about measurement method used by these active pyrometers. However, it seems that it uses the following measurement method.

The emitter (the laser) emits modulated IR radiation of known maximal power. The radiation that comes to the surface of the tested object is reflected in different directions within a hemisphere, among others into direction of the receiver [Fig. 3.17]. The receiver measures both the radiation emitted by the laser and reflected by the tested object and the radiation emitted by the object. However, on the basis of known frequency and/or phase of the modulated radiation it is possible to separate electronically the reflected signal from the emitted signal.

Next, the object reflectance in direction of the receiver $\rho_{ob,d}$ is calculated as

$$\rho_{ob,d} = a \frac{P_r}{P_e}, \quad (3.26)$$

where P_r is the reflected radiant flux measured by the receiver, P_e is the radiant flux emitted by the emitter, and a is the coefficient that depends on design parameter of the pyrometer which can be determined experimentally.

Further on, the object emissivity ε_{ob} is calculated as

$$\varepsilon_{ob} = 1 - \rho_{ob,d}. \quad (3.27)$$

Finally, a typical measurement procedure used by classical passive singleband systems is employed to calculate object's temperature.

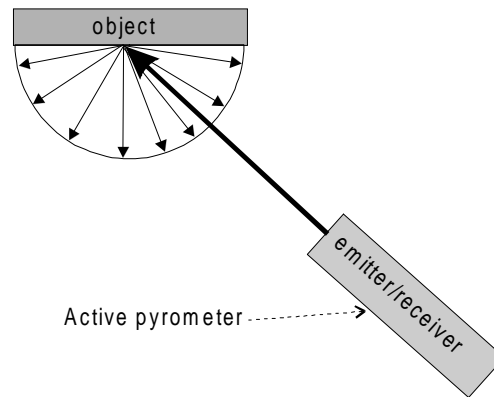


Fig. 3.17. Distribution of reflected radiation in case of diffusive surface of the tested object

Active singleband pyrometer designed as a classical passive pyrometer integrated with a laser is a small mobile device that can measure temperature of any objects. At the same time its user do not have to know object emissivity. However, unfortunately, as it will be presented in Chapt.7, accuracy of active singleband systems can be relatively high only in limited number of applications.

3.3 References

1. The Pyrometer Instrument Co., Inc., Manual for the Pyrolaser®
2. Tank V, Dietl H. Multispectral Infrared Pyrometer For Temperature Measurement With Automatic Correction Of The Influence Of Emissivity, *Infrared Phys.* 30, 331-342 (1990).
3. Khan N.A., Allemand C., Eagar T.W., Non-contact temperature measurement: least squares based techniques, *Rev. Sci. Instrum.*, 62, 403-409 (1991)
4. Levendis Y.A., Estrada K.R., Hottel H.C., Development of multicolor pyrometers to monitor transient response of burning carbonaceous particles, *Rev. Sci. Instrum.*, 63, 7, 3608-3621(1992).
5. Hejazi S., Wobschall D.C., Spangler R.A., Anbar M., Scope and limitation of thermal imaging using multiwavelength infrared detection, *Opt. Eng.*, 31, 2383-2392 (1992).
6. Hunter C.D., Prototype device for multiwavelength pyrometry, *Opt. Eng.*, 25, 11, 1222-1231 (1986).
7. Jiang H., Qian Y., High-speed multispectral infrared imaging, *Opt. Eng.*, 32, 6, 1281-1289 (1993).
8. Kosonocky W. F., Kaplinsky M. B., McCaffrey N. J., Multi-Wavelength imaging pyrometer, SPIE Vol. 2225 Infrared Detectors and Focal Plane Arrays III, 26-43 (1994).
9. Kostka G., Reger J., Aktive Zwei-Wellenlangen-Pyrometrie, VDI/VDE Gesellschaft Mess-Und Automatisierungstechnik TEMPERATUR '98, VDI Berichte 1379, p.227-232, 1998 (in German).
10. Daniel N., Williams D., Full spectrum multiwavelength pyrometry for non-grey surfaces, SPIE, Vol. 1682, p. 260-270, 1992.

11. Dubois L., Pribetich, J., Falbre J., Chive J., Moschetto Y., Non-invasive microwave multifrequency radiometry used in microwave hyperthermia for bidimensional reconstruction of temperature patterns, *Int. Journal of Hyperthermia*, Vol. 9, 415-431, 1993
12. Mizushina S., Shimizu T., Suzuki K., Kinomura K., Ohba K., Sugiura T., Retrieval of temperature-depth profiles in biological objects from multi-frequency microwave radiometric data, *Journal of Electromagnetic Waves and Applications*, Vol. 7, 1515-1548, 1993.
13. Temperature measurement in industry: Radiation Thermometry, VDI/VDE 3511 Part 4, Verein Deutscher Ingenieure, Dusseldorf, 1995.
14. Coates P. B., Wavelength specification in optical and photoelectric pyrometry, *Metrologia*, 13,1-5 (1977).
15. Barani G., Tofani A., Comparison of some algorithms commonly used in infrared pyrometry: computer simulation, in *Thermosense XIII*, ed. George S. Baird, Proc. SPIE 1467, 458-468 (1991).
16. Chrzanowski K., Problem of determination of effective emissivity of some materials, *Infrared Physics and Technology*, 36, 679-684 (1995).
17. Fehribah J.D. and Johnson R.B., "Temperature measurement validity for dual spectral-band radiometrics techniques," *Opt. Eng.*, 28 (12), 1255-1259 (1989).
18. Chrzanowski K., Limitation of temperature measurement validity for doublespectral systems of middle infrared range, *Optica Applicata*, 25,1, 57-63 (1995).
19. Hahn J.W., Rhee C., Reference wavelength method for a two-color pyrometer, *App. Opt.*, 26, 5276-5278 (1987)
20. Chrzanowski K., Madura H., Polakowski H. and Pawlowski M., A Doublespectral Fast Infrared Pyrometer, in *Quantitative Infrared Thermography Conference QIRT-94*, Editionse Europeennes Thermique et Industrie, 1994
21. Andreic A., Numerical evaluation of the multiple-pair method of calculating temperature from a measured continuous spectrum, *App. Opt.*, 27,4073-4075 (1988).
22. Tank V., Infrared temperature measurement with automatic correction of the influence of emissivity, *Infrared Phys.* 29, 211-212 (1989).
23. Hunter G.B., Allemand C. D., Eagar T.W., Multiwavelength pyrometry : an improved method, *Opt. Eng.*, 24, 1081-1085 (1985).
24. Duvaut T., Georgeault D., Beaudoin J., Multiwavelength infrared pyrometry: optimization and computer simulations, *Infrared Phys. & Technology*, 36, 1089-1103 (1995).

4. Errors of passive singleband thermometers

4.1 Mathematical model

Power of radiation emitted by tested objects carries information about object temperature. This radiation represents a certain radiometric signal that comes to IR detector and is converted into an electronic signal. Next, the latter one is amplified and transformed into a more convenient output form. Object temperature is determined on the basis of the value of the output electronic signal using this four-step measurement procedure described in detail in Chapt 3:

1. Determination of the calibration characteristic $S_{bb}=f(T_{bb})$
2. Measurement of the real output signal S_r generated by the tested object of the temperature T_{ob} .
3. Correction of the measured signal S_r to the new value S_{cor} on the basis of the assumed measurement conditions (the object effective emissivity ϵ , the background effective temperature T_{back} , and sometimes the effective atmospheric transmittance τ_a) assumed by a user of the system.
4. Calculation of the output temperature on the basis of the value of the corrected signal S_{cor} using the inverse calibration chart $T_{out}=f(S_{cor})$.

The presented above measurement procedure is typically used in most singleband thermometers. However, there is no clear connection between the output temperature T_{out} and the true object temperature T_{ob} in this procedure. A single analytical formula that would connect these two quantities would be very useful for any errors analysis of the measurement process.

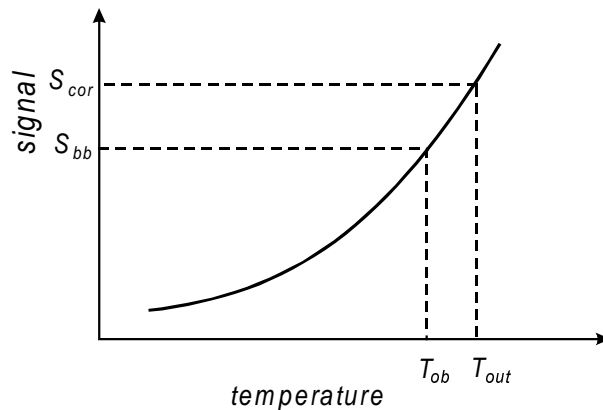


Fig. 4.1. Relationship between the output temperature T_{out} , the true object temperature T_{ob} , the corrected signal S_{cor} and the calibration signal S_{bb}

Assuming that the difference between the corrected signal S_{cor} for the object temperature T_{ob} and the signal S_{bb} for the same temperature is not high then on

the basis of the Fig. 4.1 the relationship between T_{ob} and T_{out} can be presented in the following form

$$T_{out} = T_{ob} + \frac{(S_{cor}(T_{ob}) - S_{bb}(T_{ob}))}{\left. \frac{dS_{bb}}{dT} \right|_{T=T_{ob}}}. \quad (4.1)$$

Formula (4.1) is a simple and convenient for calculations of the output temperature T_{out} when the true object temperature T_{ob} is known. However, we must always remember that it represents only a simplified relationship between T_{out} and T_{ob} that should be used only when the difference between the corrected signal S_{cor} for the object temperature T_{ob} and the signal S_{bb} for the same temperature is not significant. If it is not the case then it should not be used for error analysis.

Using Eq.(4.1) the error of temperature measurement ΔT that equals to the difference between the output temperature T_{out} and the true object temperature T_{ob} .

$$\Delta T = T_{out} - T_{ob} = \frac{(S_{cor}(T_{ob}) - S_{bb}(T_{ob}))}{\frac{dS_{bb}}{dT_{ob}}}. \quad (4.2)$$

As can we see in formula (4.2) when the signal $S_{cor}(T_{ob})$ equals the signal $S_{bb}(T_{ob})$ then the output temperature T_{out} equals T_{ob} what means that the measurement error ΔT is zero. When the equality $S_{cor}(T_{ob}) = S_{bb}(T_{ob})$ is not fulfilled then a difference between T_{out} and T_{ob} exists. This means that difference between the signals $S_{cor}(T_{ob})$ and $S_{bb}(T_{ob})$ generates errors of temperature measurement with singleband systems.

Let us analyze the presented above measurement procedure to find reasons that cause that difference between the signals $S_{cor}(T_{ob})$ and $S_{bb}(T_{ob})$ and generate the errors of temperature measurement ΔT with singleband systems. The difference between the signal $S_{cor}(T_{ob})$ and the signal $S_{bb}(T_{ob})$ is when the calibration characteristic $S_{bb}=f(T_{bb})$ is determined with limited accuracy and/or the corrected signal S_{cor} is determined with some errors.

The calibration characteristic $S_{bb}=f(T_{bb})$ can be determined with some errors during the first step of the presented earlier measurement procedure due to limited accuracy of the blackbody used during calibration, limited number of the calibration points, errors of the interpolation algorithm and internal errors of the electronic block of the thermometer. The errors of determination of the calibration characteristic $S_{bb}=f(T_{bb})$ due to limited number of the calibration points and errors of the interpolation algorithm are typically negligible in comparison to errors due to limited accuracy of the blackbody. The errors determination of the calibration characteristic $S_{bb}=f(T_{bb})$ due system internal disturbances are also negligible in most situations as during calibration it is possible to use special techniques to reduce the influence of these internal electronic disturbances. Therefore the limited accuracy

of the blackbody used during calibration is usually the main source of errors of determination of the calibration characteristic $S_{bb=f}(T_{bb})$.

Manufactures of blackbodies usually state the interval $T_{bb} \pm \Delta T_{bb}$ (T_{bb} - indicated blackbody temperature) within which the true blackbody temperature is located with 100% probability. Let us assume uniform distribution of true blackbody temperature within range $[T_{bb} - \Delta T_{bb}; T_{bb} + \Delta T_{bb}]$ where ΔT_{bb} is the limit error of the indicated blackbody temperature. Next, we will additionally assume that limited accuracy of the blackbody is the only source of calibration errors and we can present the signal S_{bb} as

$$S_{bb}(T_{bb}) = g \frac{R^* A_d \tau_{sc}}{4F^2 + 1} \int_{\lambda_1}^{\lambda_2} M(T_{bb} \pm \Delta T_{bb}, \lambda) \tau_F(\lambda) s(\lambda) d\lambda, \quad (4.3)$$

where g is the amplification of the electronic block, R^* is the peak detector sensitivity, A_d is the detector area, and F is the optics F-number (ratio of focal length f' of the optical objective to diameter D of the objective), λ_1 and λ_2 are the limits of the detector spectral band, $M(T, \lambda)$ is the spectral exitance at the temperature T and the wavelength λ , τ_o is the transmittance of the optical objective, τ_{sc} is the transmittance of the scanning block¹⁰, τ_F is the transmittance of the filter¹¹, $s(\lambda)$ is the detector relative spectral sensitivity.

Now, let us find reasons why the corrected signal is determined with some errors. As it was shown in Chapt. 3 the formula for the corrected signal S_{cor} can be presented in the following form

$$S_{cor} = \frac{S_r - (1 - \varepsilon_a) \tau_{a(a)} S_{bb}(T_{ba(a)}) - S_{op}(T_{op(a)})}{\varepsilon_a \tau_{a(a)}}. \quad (4.4)$$

where S_r is the signal measured during real measurement conditions, ε_a is the assumed object effective emissivity, $\tau_{a(a)}$ is the assumed effective atmospheric transmittance, $T_{ba(a)}$ is the effective background temperature and $S_{op}(T_{op(a)})$ is the signal generated by the radiation emitted by the optics of temperature of the optical components equal to the temperature $T_{op(a)}$ assumed by the user.

Let us define the term "effective" before the quantities ε_a , $\tau_{a(a)}$ and $T_{ba(a)}$ in order to interpret Eq. (4.4).

Object emissivity and atmospheric transmittance are usually not only unknown but also wavelength dependent. It would be very difficult and inconvenient for the user to estimate the functions $\varepsilon(\lambda)$ and $\tau_a(\lambda)$. Next, the background of the tested object often consists of the areas of different temperatures. The temperature distribution

¹⁰ For pyrometers, thermal scanners or thermal cameras without scanning block τ_{sc} component should be removed from formula (44).

¹¹ For thermometers without optical filters τ_F component should be removed from the formula.

of the background and distribution of emissivity of the background are very difficult to estimate for the user. Therefore, the user is required in the measurement procedure to estimate only numbers: the effective emissivity ε_a , the effective transmittance τ_a and the effective background temperature T_{ba} .

The effective emissivity ε is defined as emissivity of the graybody of the same temperature as the tested object, that produces the same signal at the output of the detector as the real object does. It can be calculated as the mean value of the function of the spectrally variable emissivity $\varepsilon(\lambda)$ weighted by the product of the function of the object radiance $L(T_{ob}, \lambda)$, the camera relative sensitivity $sys(\lambda)$ [1]

$$\varepsilon = \frac{\int_{\lambda_1}^{\lambda_2} \varepsilon(\lambda) L(\lambda, T_{ob}) sys(\lambda) d\lambda}{\int_{\lambda_1}^{\lambda_2} L(\lambda, T_{ob}) sys(\lambda) d\lambda}. \quad (4.5)$$

Similarly, the effective transmittance τ_a can be defined as a non-dependent on wavelength transmittance of a transparent media that suppress the radiometric signal in the same way as the real atmosphere does. It can be calculated as the mean value of the function of the spectrally variable atmospheric transmittance $\tau_a(\lambda)$ weighted by the product of the function of the object radiance $L(T_{ob}, \lambda)$, the camera relative sensitivity $sys(\lambda)$

$$\tau_a = \frac{\int_{\lambda_1}^{\lambda_2} \tau_a(\lambda) L(\lambda, T_{ob}) sys(\lambda) d\lambda}{\int_{\lambda_1}^{\lambda_2} L(\lambda, T_{ob}) sys d\lambda}. \quad (4.6)$$

The effective background temperature T_{ba} is defined as a temperature of a blackbody of infinite sizes around the tested object that would generate the same output signal caused by the reflected from the object radiation as the real background does.

The errors of determination of the corrected signal S_{cor} arise during the second step and the third step of the measurement procedure. First, the signal S_r measured during the second step is determined with a limited accuracy because of disturbances in electronic channel of the system which distort the radiometric signal that comes to the detector. Second, there are usually some differences between the assumed values of measurement conditions and the real conditions (the effective emissivity ε_a and true the object effective emissivity ε_{ef} , the assumed effective atmospheric transmittance $\tau_{a(a)}$ and the true value $\tau_{a(ef)}$, the assumed effective background temperature $T_{ba(a)}$ and the true value T_{back} , the assumed temperature of the optical components $T_{op(a)}$ and the true temperature $T_{op(r)}$).

If we analyze the measurement process from the detector to the system output then we will find that there are many possible sources of errors generated in electronic channel. These errors can be caused by noise in the detector or other

analog electronic blocks, limited stability of cooling system, variation of the preamplifier gain and offset, limited resolution and limited linearity of analogue/digital converters etc.

The real signal S_r at the output of the electronic channel can be calculated using two alternative formulas producing identical results

$$\begin{aligned}
 S_r = & \left\{ \left[\varepsilon_r \tau_{a(r)} \tau_o \int_{\Delta\lambda_d} M(T_{ob}, \lambda) \tau_F(\lambda) s(\lambda) d\lambda \right. \right. \\
 & + (1 - \varepsilon_{ob(r)}) \tau_{a(r)} \tau_o \int_{\Delta\lambda_d} M(T_{ba(r)}, \lambda) \tau_F(\lambda) s(\lambda) d\lambda \\
 & \left. \left. + \int_{\Delta\lambda_d} M(T_{op(r)}, \lambda) \varepsilon_{op}(\lambda) s(\lambda) d\lambda \right] \times \frac{(R^* \pm \sigma R^*) A_d}{4F^2 + 1} (g \pm \sigma g) \right\} \pm V_a \pm V_d
 \end{aligned} \quad , \quad (4.7)$$

or

$$\begin{aligned}
 S_r = & \left\{ \left[\int_{\Delta\lambda_d} \varepsilon_{ob}(\lambda) M(T_{ob}, \lambda) \tau_o(\lambda) \tau_a(\lambda) \tau_F(\lambda) s(\lambda) d\lambda \right. \right. \\
 & + \int_{\Delta\lambda_d} (1 - \varepsilon_{ob}(\lambda)) M(T_{ba(r)}, \lambda) \tau_a(\lambda) \tau_o(\lambda) \tau_F(\lambda) s(\lambda) d\lambda \\
 & \left. \left. + \int_{\Delta\lambda_d} M(T_{op(r)}, \lambda) \varepsilon_{opt}(\lambda) s(\lambda) d\lambda \right] \times \frac{(R^* \pm \sigma R^*) A_d}{4F^2 + 1} (g \pm \sigma g) \right\} \pm V_a \pm V_d
 \end{aligned} \quad , \quad (4.8)$$

where $\varepsilon_{ef(r)}$ is the true object effective emissivity, $\varepsilon_{ob}(\lambda)$ is the real object emissivity at the wavelength λ , $\tau_{aef(r)}$ is the true atmospheric effective transmittance, $\tau_a(\lambda)$ is the atmospheric transmittance at the wavelength λ , $T_{ba(r)}$ is the true background effective temperature, $T_{op(r)}$ is the temperature of the optics at real measurement conditions, V_a is the random variable simulating the noise at the output of the analog channel, V_d is the random variable of rectangular probability distribution within range determined by least significant bit LSB of the A/D converter, σg is the standard deviation of the gain g of the analog electronic channel treated as a random variable, σR^* is the standard deviation of the detector peak responsivity R^* treated as a random variable.

The standard deviation V_a in Eq. (4.8) represents rms value of the noise at output of analog electronic channel. This output noise consists of two components: the noise generated by the detector and amplified by electronic blocks and the additional noise generated by the analog electronic blocks. For a well designed electronics the noise caused by preamplifier and other analog electronic

blocks is comparable to the noise generated by the detector. It is difficult to make an assumption about exact proportion between these two noise components that would be valid for all systems. Therefore let us assume that V_{an} equals the multiplication of the coefficient u and the rms value of the noise caused by the detector, where u can change from 1 to about 10. Now, the V_{an} can be calculated as

$$V_a = u \times g \frac{R^* \sqrt{A_d \Delta f}}{D^*} \quad (4.9).$$

where D^* is the peak normalized spectral detectivity of the detector and Δf is the noise equivalent bandwidth to the output of the n analog channel.

The V_d that represents in Eq. (4.10) errors generated by limited resolution of the digitization system can be calculated as standard deviation of rectangular probability distribution within range determined by least significant bit LSB of the converter

$$V_d = \frac{LSB}{\sqrt{12}} \quad (4.11).$$

LSB can be determined as

$$LSB = \frac{FSR}{2^k} = \frac{S_{max} - S_{min}}{2^k}, \quad (4.12)$$

where FSR is the full scale range of A/D converter, the S_{max} and S_{min} are maximal and minimal values of the analog signal to be digitized at electronic channel, and k is the bit number of the A/D converter.

The quantities σg and σR^* cannot be modeled mathematically similarly to V_a or V_d . However, for a well-defined system they can be usually estimated.

Using the formulas (4.3-4.8) we can calculate the difference S_{cor} minus S_{bb} that causes the temperature measurement error ΔT . However, to determine the error ΔT using the formula (4.2) we need to define the derivative $\partial S_{bb} / \partial T_{ob}$. The latter component of the formula (4.2) equals

$$S_{bb}(T_{ob}) = g \frac{R^* A_d \tau_o \tau_{sc}}{4F^2 + 1} \int_{\lambda_1}^{\lambda_2} \frac{\partial M(T_{ob}, \lambda)}{\partial T_{ob}} \tau_F(\lambda) s(\lambda) d\lambda. \quad (4.13)$$

Now, using the formulas (4.1-4.8) we can calculate the error ΔT that arise during measurements with a singleband system of known parameters on condition that the object temperature T_{ob} is known.

To summarize our discussion about sources of errors of temperature measurement with singleband systems we can say that the errors of temperature measurement with multiband IR systems, according to their source, can be generally

divided into three groups: the radiometric errors, the electronic errors and the calibration errors [Fig. 4.2]. The radiometric errors are caused by differences between the limited accuracy of the estimated by the user measurement conditions: the effective emissivity ε_a , the effective atmospheric transmittance $\tau_{a(a)}$, the effective background temperature $T_{ba(a)}$ and the temperature of the optical components $T_{op(a)}$. The electronic errors are the errors of the transformation of the radiometric signal into output electrical signal during real measurements. Calibration errors are caused by errors of determination of output signal due to non-accuracy of the blackbody at laboratory conditions.

The radiometric errors and electronic errors reduce accuracy of determination of the corrected signal S_{cor} . The calibration errors limit accuracy of determination of the calibration characteristic $S_{bb}(T_{ob.})$.

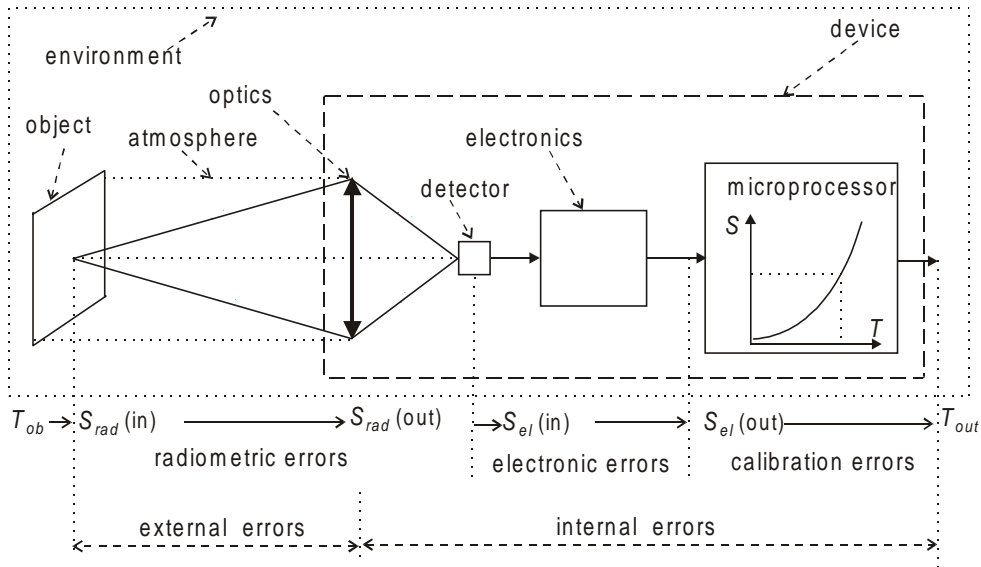


Fig. 4.2. Graphical presentation of the measurement process with singleband systems

The difference between the corrected signal S_{cor} and the signal S_{bb} can be treated as the error of the signal measurement ΔS . Therefore, using formula (4.2) we can present the relationship between the signal measurement error ΔS and the error of temperature measurement ΔT in the following form

$$\Delta T = T_{out} - T_{ob} = \frac{S_{cor} - S_{bb}}{ADRF} = \frac{\Delta S}{ADRF}, \quad (4.14)$$

where
$$ADRF = \frac{dS_{bb}}{dT_{ob}} = g \frac{R^* A_d \tau_o \tau_{sc}}{4F^2 + 1} c_1 c_2 \int_{\lambda_1}^{\lambda_2} \frac{\tau_F(\lambda) s(\lambda) \exp(c_2 / \lambda T_{ob})}{\lambda^6 T_{ob}^2 [\exp(c_2 / \lambda T_{ob}) - 1]^2} d\lambda \quad (4.15)$$

The new function $ADRF$ will be called the absolute disturbance resistance function ($ADRF$), because it represents the system resistance to the absolute errors of signal measurement that can be treated as disturbances of the measured signal. The $ADRF$ gives us information about how many times the absolute error of the temperature measurement ΔT is smaller than the absolute error of the signal measurement ΔS .

It is also possible to develop a relationship between the relative error of the temperature measurement $\Delta T/T$ and the relative error of the signal measurement by transforming formula (4.2) to this form

$$\frac{\Delta T}{T_{ob}} = \frac{\Delta S / S_{bb}}{RDRF}, \quad (4.16)$$

where

$$RDRF = \frac{\frac{dS_{bb}(T_{ob})}{dT_{ob}} T_{ob}}{S_{bb}(T_{ob})} = \frac{T_{ob} \int_{\lambda_1}^{\lambda_2} \frac{\tau_F(\lambda) s(\lambda) \exp(c_2 / \lambda T_{ob})}{\lambda^6 T_{ob}^2 [\exp(c_2 / \lambda T_{ob}) - 1]^2} d\lambda}{\int_{\lambda_1}^{\lambda_2} \frac{\tau_F(\lambda) s(\lambda)}{\lambda^5 [\exp(c_2 / \lambda T_{ob}) - 1]} d\lambda} \quad (4.17)$$

The new function $RDRF$ was termed the relative disturbance resistance function for similar reasons as the $ADRF$.

As we see in Eq. (4.15) the $ADRF$ depends on many system parameters. This means, that the same system for different values of gain in the electronic channel g etc. will have different $ADRF$ s. Therefore, the $ADRF$ is not a good measure for comparisons of different system or the same systems working in different configurations. However, the $RDRF$ depends only on wavelength dependent parameters like $s(\lambda)$ and $\tau_F(\lambda)$ and is an excellent measure for such comparisons.

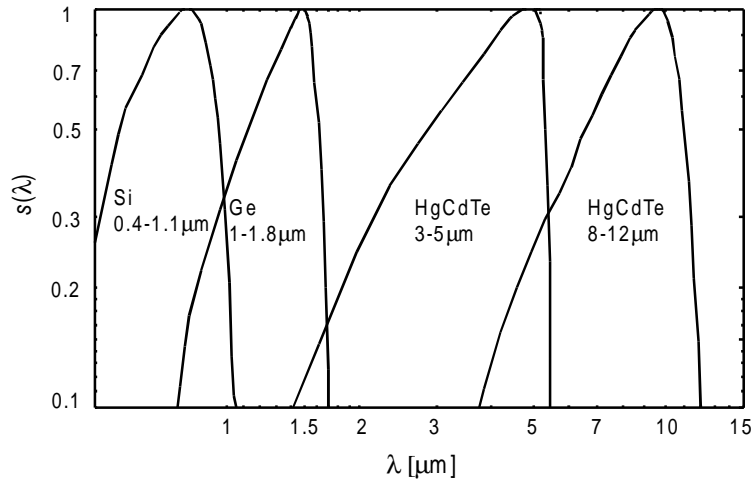


Fig. 4.3. Relative spectral sensitivity functions $s(\lambda)$ of the assumed detectors

Example 1: Calculate *RDRFs* of four singleband pyrometers built using these detectors: 1) cooled HgCdTe photoresistor optimized for 8-12 μm spectral band, cooled HgCdTe photoresistor optimized for 3-5 μm spectral band, non-cooled Ge photodiode for 1-1.8 μm band and non-cooled Si photodiode for 0.4-1.1 μm spectral range. The relative spectral sensitivity functions $s(\lambda)$ of the assumed detectors are shown in Fig. 4.3. The pyrometers do not use any optical filters.

Solution: The calculated *RDRFs* of four assumed singleband pyrometers using Eq.(4.17) are shown in Fig. 4.4.

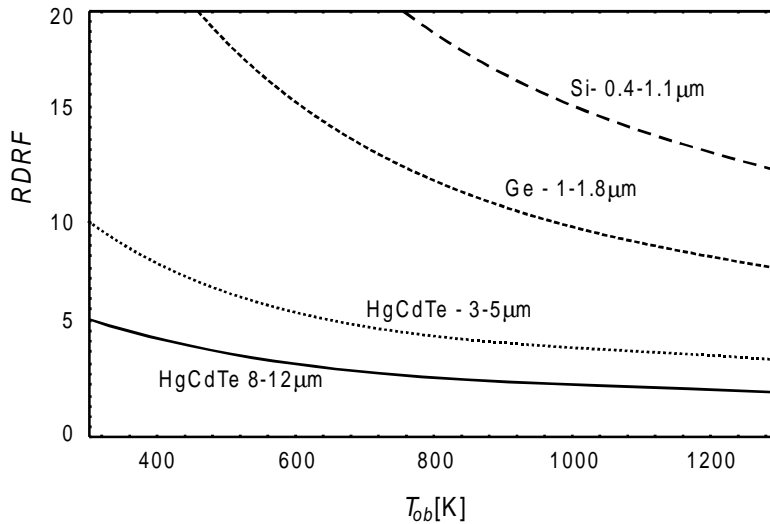


Fig. 4.4. *RDRFs* of four pyrometers described in the Example (1)

From analysis of the results presented in Fig. 4.4 we can develop two important conclusions. First, the *RDRF* depends on the object temperature T_{ob} . This means that the relative error of the temperature measurement $\Delta T/T$ depends not only on the relative error of the signal measurement $\Delta S/S$ but also on the object temperature T_{ob} . The same error $\Delta S/S$ causes higher error $\Delta T/T$ for the higher temperatures T_{ob} . Second, the *RDRF* depends significantly on location of system spectral bands. The shortwave systems have higher *DRF* than the longwave ones. This means, that the shortwave thermometers are more resistant on the errors of signal measurement than the longwave thermometers.

4.2 Calculations

The results of the calculations demonstrated in Fig. 4.4 clearly prefer the shortwave VNIR and NIR systems. However, accuracy of the temperature measurement depends not only on the system resistance to the signal errors but also on the level of these errors. The *RDRF* can be used as a useful figure of merit for thermometers comparison, but the most important figure of merit for comparing these systems

is the error of temperature measurement $\Delta T/T$ that can be determined using the earlier developed formulas (4.3-4.17).

As it was presented in subchapter 4.1 we can distinguish following main sources of errors of temperature measurement:

1. difference between the assumed by the user the object effective emissivity ε_a and the true object effective emissivity ε_r ,
2. difference between the assumed effective background temperature $T_{ba(a)}$ and the true value $T_{ba(r)}$,
3. difference between the assumed effective transmittance $\tau_{a(a)}$ and the true value $\tau_{a(r)}$,
4. difference between the assumed optics temperature $T_{op(a)}$ and the true value $T_{op(r)}$,
5. noise generated in detector or other analog electronic blocks,
6. variation of the detector peak responsivity R^* due limited stability of cooling system or other reasons,
7. variation of the preamplifier gain g ,
8. limited resolution of analogue/digital converter,
9. limited accuracy of the blackbody used during calibration.

The first 4 sources can be considered as the sources of radiometric errors, the next 4 sources we termed the sources of electronic errors and the last source is a source of the calibration errors.

Now, the influence of the mentioned above sources on temperature measurement accuracy with the analyzed systems will be calculated subsequently. To calculate the errors resulting from one source we will assume that the influence from the other sources is negligible. For example, to calculate temperature measurement error due to system noise we will assume that the influence of other sources is negligible: the values ε_a , $T_{ba(a)}$, $\tau_{a(a)}$, $T_{op(a)}$ were determined by the user without any error, there is no variation of R^* or g , a perfect ADC was used, and the a blackbody of perfect accuracy was used during calibration.

Singleband thermometers are built using different types of thermal detectors (thermocouples, pyroelectric) or photoelectric detectors (Si, Ge, InAsGa, PbS, PbSe, InSb, PtSi, HgCdTe). Next, some of the mentioned above the photoelectric detectors are available as photoresistors or photodiodes, as single or matrix detectors. Further on, the photoelectric detectors can be used as non-cooled or cooled detectors. However, to limit our discussion let us analyze only 5 systems. The first three are pyrometers built using 3 different detectors: a thermocouple with 8-12 μm filter, a non-cooled Si photodiode with a filter for 0.8-1 μm spectral band, and a non-cooled Ge photodiode with a filter for 1.5-1.7 μm spectral band. The latter two thermometers are thermal cameras designed using cryogenically cooled HgCdTe detector optimized for 3-5 μm (mercury cadmium tellury for middle wavelength range termed MCT-MW) and cryogenically cooled HgCdTe detector optimized for 8-12 μm (mercury cadmium telluric for long wavelength range termed MCT-LW).

The thermometer relative sensitivity $sys(\lambda)$ understood as product of the detector relative sensitivity $s(\lambda)$ and the filter transmittance $\tau_f(\lambda)$ of the assumed systems is presented in Fig. 4.5. Other parameters of the assumed pyrometers or thermal cameras are shown in Tab. 1.1.

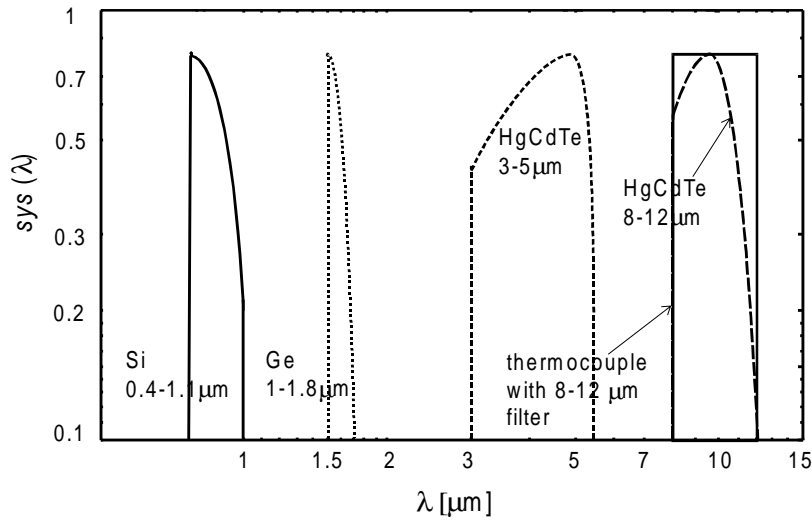


Fig. 4.5. System spectral sensitivity $sys(\lambda)$ functions of the assumed systems

Tab. 4.1. The parameters used in the calculations

Detector spectral band	Si pyrometer 0.4-1.1 μm (20°C)	Ge pyrometer 1-1.8 μm (20°C)	thermo- couple py- rometer (20°C)	3-5 μm thermal camera (77 K)	8-12 μm thermal camera (77 K)
D^* [cm Hz ^{1/2} /W]	2×10^{12}	2×10^{11}	$5 \cdot 10^8$	3×10^{11}	5×10^{10}
R^*	1 A/W	1 A/W	$5 \cdot 10^3$ V/W	$2 \cdot 10^5$ V/W	$1 \cdot 10^5$ V/W
g	1000 V/A	1000 V/A	200 V/V	100	100
τ_F	0.8 $\lambda \in (0.8; 1) \mu\text{m}$	0.8 $\lambda \in (1.5; 1.7) \mu\text{m}$	0.8 $\lambda \in (8; 12) \mu\text{m}$	0.8 $\lambda \in (3; 5) \mu\text{m}$	0.8 $\lambda \in (8; 12) \mu\text{m}$
A_d [cm ²]	0.01			0.00001	0.00001
Δf [kHz]	2			1000	
τ_o	0.9				
F	2				

Now, let us discuss the assumed parameters shown in Fig. 4.5 and Tab. 4.1 and explain reasons why specific values were chosen.

The relative detector spectral sensitivity $s(\lambda)$ of the assumed systems are the same as shown in Fig. 4.3. The curves shown in Fig. 4.5 differ significantly from the curves from Fig. 4.3 the assumed optical filters are used to limit detector spectral bands as it is often done in practical systems. The spectral bands of the pyrometers built with Si or Ge detectors are often limited using narrow band optical filters of bands similar to the assumed values. Next, thermocouples with a filter of 8-12 μm spectral band are manufactured in great numbers. Further on, almost all thermal cameras have their spectral bands limited to 3-5 μm or 8-12 μm bands.

Transmittance of the real filters can differ quite significantly. It was assumed a case of high transmittance filters.

The values of the detector normalized peak spectral detectivity D^* and the peak spectral responsivity R^* were taken from catalogs of detector manufactures.

The values of the gain in the electrical channel g were chosen to keep the output signals reasonably strong.

Pyrometers are designed using detectors of different sizes. The sizes can vary from about 0.25 mm to about 10 mm. However, a detector of 1mm diameter for a circular detector or 1 mm size for a rectangle detector can be considered as a typical case.

Detectors used in thermal cameras are much smaller than detectors used in pyrometers in order to achieve high spatial resolution. The assumed detector size can be treated as typical for thermal cameras built using a small linear matrix or a single detector. In case of thermal cameras built using a large number linear matrix or area matrix, the size of a single fotoelement can be a few times smaller than the assumed value.

The assumed values of the noise equivalent frequency band Δf can be treated as typical for fast pyrometers of a measurement time about a millisecond and thermal cameras built using a small (about 10 elements) linear matrix and frame rate about 25 Hz. It should be emphasized that the Δf is usually smaller than the assumed value for typical pyrometers. Next, the Δf is higher than the assumed value for thermal cameras built using a single detector.

The significant difference between values of the Δf for pyrometers and for thermal cameras is a consequence of the fact that in case of the assumed camera measurements of many thousands of points on the object surface are made during a fraction of second.

Both pyrometers and thermal cameras can use optical objectives of the different transmittance τ_o and F -number. However, the assumed values can be treated as typical for most systems.

We will start calculations from the analysis of electronic errors because one of sources of such errors - detector noise - determines the lower limit of the useful temperature range.

4.2.1 Electronic errors

4.2.1.1 Limited analog resolution

Noise in the analog electronic channel is a source of random dispersion of the measurement results and determines temperature resolution of the thermometer. A new measure of system temperature resolution called Noise Generated Error was recently proposed in literature [2,3]. It was defined as the standard deviation of the output temperature dispersion caused by noise of the detector used by the thermometer.

In case of noise of normal distribution, NGE is equal to the distribution standard deviation δ . Then, the probability density function $f(T_{out})$ equals

$$f(T_{out}) = \frac{1}{NGE\sqrt{2\pi}} \text{Exp}\left[-\frac{(T_{out} - T_{ob})^2}{2NGE^2}\right]. \quad (4.18)$$

In this case NGE shows temperature range around the true temperature T_{ob} within which the output temperature T_{out} lies with probability of 68% [Fig. 4.6]

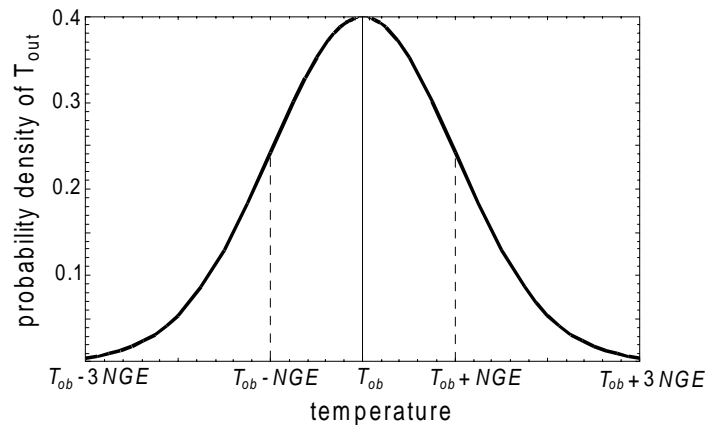


Fig. 4.6. Probability density function of the output temperature T_{out} during measurement of the true object temperature T_{ob} for the case of output temperature dispersion having a normal distribution

As the NGE definition is not based on signal parameters in a single channel, the NGE can be used to describe temperature resolution of single-, dual- and multi-band IR measurement systems. Generally, NGE enables comparison of non-contact thermometers on criterion of robustness to detector noise.

Temperature resolution NGE that is a measure of errors due to detector noise and can be determined as the standard deviation of dispersion of absolute error of temperature measurement ΔT using Eq.(4.14) if we simulate random noise in the analog channel of rms value calculated using Eq.(4.9). However, there are simpler ways of determining the NGE than by using Eq.(4.14).

First, for case of a singleband systems NGE can be calculated as ratio of rms value of noise in the electrical channel V_n and the slope of the system calibration curve $\partial S / \partial T$ [2]

$$NGE = \frac{V_n}{\partial S / \partial T} . \quad (4.19)$$

Assuming that the additional noise from preamplifier and other analog electronic blocks is negligible ($u=1$ in formula (4.9)) in comparison to the noise generated by the detector then the rms value of the noise in the electrical V_n channel can be calculated from a formula

$$V_n = g \frac{R^* \sqrt{A_d \Delta f}}{D^*} \quad (4.20)$$

where g is the amplification of the electronic channel, R^* is the detector peak responsivity, A_d is the detector area, D^* is the detector peak normalized detectivity, and Δf is the noise equivalent bandwidth to the output of analog output.

The slope of the calibration curve $\partial S / \partial T$ can be calculated using the formula

$$\frac{\partial S}{\partial T_{ob}} = g \frac{R^* A_d c_1 c_2}{4F^2 + 1} \int_{\Delta \lambda} \frac{\tau_o(\lambda) \tau_F(\lambda) s(\lambda) \exp(c_2 / \lambda T_{ob})}{\lambda^6 T_{ob}^2 [\exp(c_2 / \lambda T_{ob}) - 1]^2} d\lambda . \quad (4.21)$$

Second, as for case of singleband systems NGE equals to NETD [2] then a typical formula for the NETD can be used to calculate NGE .

$$NETD = \frac{(4F^2 + 1) \sqrt{\Delta f}}{\pi \tau_o \tau_F \sqrt{A_d} D^* \int_{\lambda_1}^{\lambda_2} s(\lambda) \frac{\partial L(T_{ob}, \lambda)}{\partial T_{ob}} d\lambda} . \quad (4.22)$$

It is not important which way to calculate the NGE we choose; the final results will always be the same. The calculated NGE functions of the systems of parameters shown in Fig. 4.5 and Tab. 4.1 are presented in Fig. 4.7 and Fig. 4.8. The noise on the analog channel is a source of random errors and they can be both positive or negative. Therefore, the NGE in Fig. 4.7 and Fig. 4.8 is a standard deviation of these errors treated as random variables.

It is typically considered that thermal resolution of any temperature measuring system should be below 0.1-0.2 K in the measurement range. On the basis of this criterion we see in Fig. 4.7 that the Si pyrometer can be used to measure objects of temperature over 720 K, Ge pyrometer - over 540 K and the pyrometer using the thermocouple can be used for measurement in the entire analyzed temperature range 300-1300K. It should be also noted that the temperature resolution NGE depends little on object temperature in case of the latter pyrometer. However, in case of Si pyrometer and Ge pyrometers NGE improves very quickly with object temperature.

The thermal camera of 8-12 μm spectral band fulfils the mentioned above criterion in the entire analyzed range 250-1300 K; thermal camera of 3-5 μm band does not fulfil it for temperatures below 290 K [Fig. 4.8]. It reflects a well known fact of snowy images when imaging low temperature objects with 3-5 μm thermal cameras. However, the NGE values are the same for both analyzed thermal cameras for temperatures about 300K. Next, the NGE is much better in case of 3-5 μm thermal camera for temperatures significantly over 300K.

Noise in the analog channel generates easily noticeable effect of "snow" in images of thermal cameras or quick, random variations of indications of pyrometers. Therefore, user of the non-contact thermometers often put great emphasis on this kind of errors and try to use systems of as low temperature resolution as possible. However, as we see in Fig. 4.7 and Fig. 4.8 the relative errors of temperature measurement due to the noise are typically below 0.1% of the measured object temperature and can be treated as negligible.

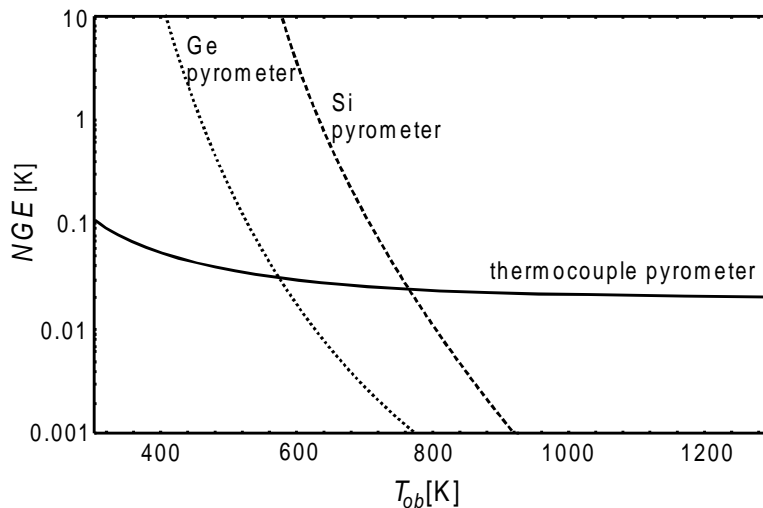


Fig. 4.7. NGE functions of the assumed pyrometers

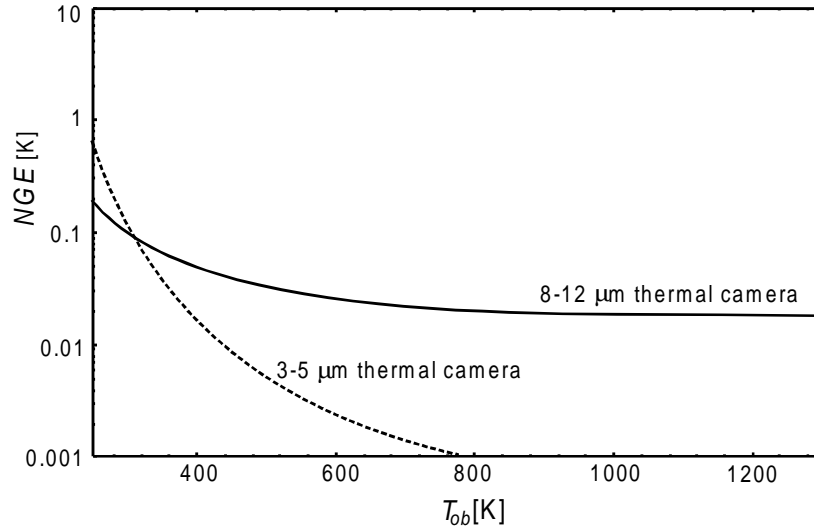


Fig. 4.8. NGE functions of the assumed thermal cameras

4.2.1.2 Limited digital resolution

Analog-to-digital converters ADC are typically used in modern non-contact thermometers in order to have the output electronic signal in a convenient digital form.

Every ADC is characterized by its resolution understood as the least significant bit *LSB*. As we see in the Eq.(4.12) the *LSB* depends on the bit number n and the full scale range *FSR* of the ACD, where the latter parameter equals the difference between the maximal analog signal and the minimal analog signal to be digitized.

Due to limited resolution of the ACD its indications will be the same for the analog signal S_a within the interval $(S_a - LSB/2; S_a + LSB/2)$. It is equally probable for the signal S_a to take any value within this interval and we can assume a case of uniform distribution. For such a case the standard deviation V_d of the random error caused by the ADC equals to *LSB* divided by the root square from 12 as shown in Eq.(4.11).

Let us assume that a 12-bit ACD is used to convert an analog signal within the range from $S_{min} = S_r(T_{ob}=0K, T_{op}=300K)$ up to $S_{max} = S_r(T_{ob}=1300K, T_{op}=300K)$. The *FSR* was calculated as difference of the two assumed signals S_r using Eq.(4.8). Next, the standard deviation V_d of the random errors of output signal measurement due to digitization were determined employing Eqs(4.11-4.12). Finally, the relative standard deviation of the random errors of the temperature measurement $\sigma T/T$ caused by limited resolution of the ADC were calculated using the Eqs(4.3,4.4,4.17) and the results are shown in Fig. 4.9.

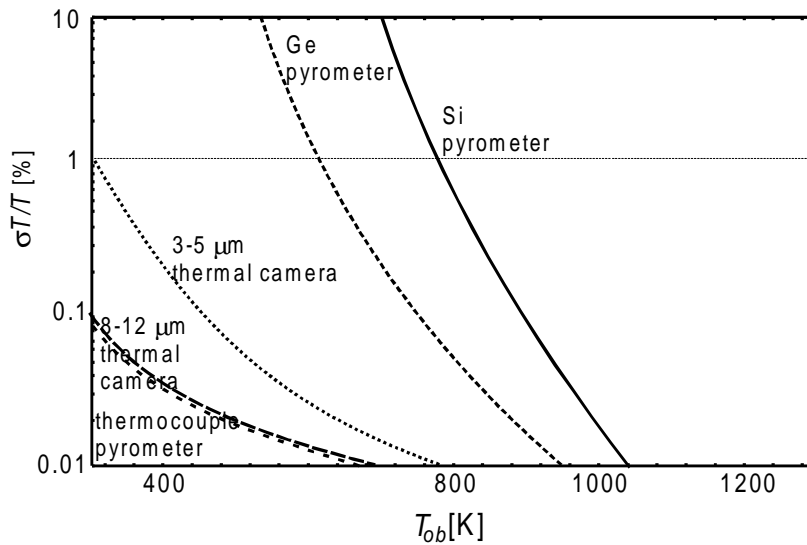


Fig. 4.9. The relative standard deviation of the random errors of temperature measurement $\sigma T/T$ caused by limited resolution of the ADC

Let us assume that a relative errors below 1% are acceptable. On the basis of this criterion there were determined following temperature measurement ranges: 300-1300K for the thermal cameras with MCT-LW and MCT-MW detectors and the pyrometer with thermocouple, 600-1300K for the pyrometers with Ge detector, 790-1300K for the pyrometers with Si detector.

High errors caused by ADC in case of the Si, Ge thermometers are generated by very high dynamic (the ratio of the FSR and the rms value of the noise in the analog channel V_a) of the output electronic signals over 10^6 in the assumed measurement ranges for these systems, when in case of the systems using the thermocouple or the MCT-LW detector the dynamic is only about $4 \cdot 10^4$.

There are a few ways to reduce the errors due to limited resolution of the digitization block. First, is by employing a special electronic system enabling changing automatically the FSR of the ADC during the measurement. Second, is by narrowing the measurement range of the system. It should be emphasized that it is difficult to find real systems that could offer measurement ranges as wide as the measurement ranges we analyzed.

There is also another simple way by using an ADC of better resolution. The 8-10 bit ADCs were typically used in older non-contact thermometers. Nowadays, a 12-bit ADC seems to a standard and for such a case we carried out our analysis. Probably in a few years time 14-16 bit ADCs will be commonly used and it will be possible to design systems of wider temperature measurement ranges.

4.2.1.3 Variations of gain of electronic channel and detector responsivity

Both variations of the detector responsivity R^* and the gain g generate variations of the output electronic signal. Therefore we will analyze these factors together.

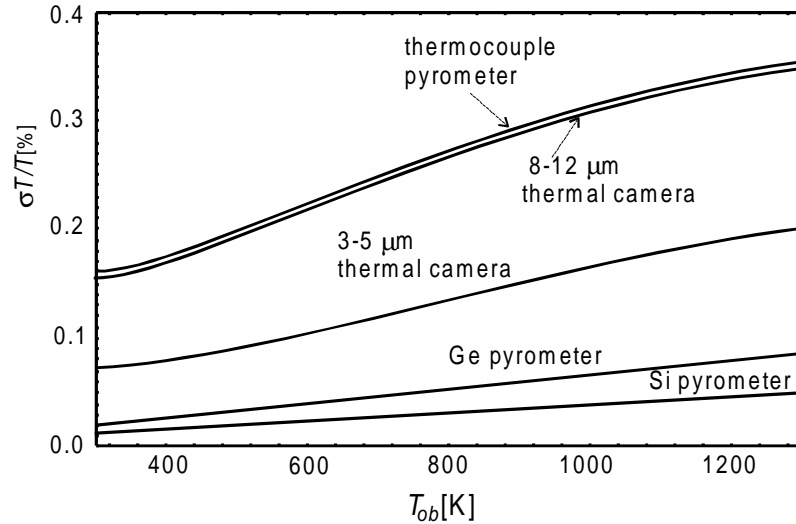


Fig. 4.10. The relative standard deviation of the random errors of the temperature measurement $\sigma T/T$ due to random variations of the detector responsivity R^* and the gain g

It seems that for most well designed singleband systems, the variations of the product of the quantities R^* and g are kept within the range $\pm 1\%$ $R^* g$. Assuming uniform distribution of the random variable R^* we can calculate the standard deviation of the random variable $R^* g$ equal to $0.0058 R^* g$. The relative standard deviation of the random errors of the temperature measurement $\sigma T/T$ caused by random variations of the random variable $R^* g$ are shown in Fig. 4.10. As we can see the errors due to analyzed source are for all the systems below the acceptable level of 0.4%. This means that the errors from the variations of the detector responsivity R^* and the gain g in well designed systems are not significant.

4.2.2 Radiometric errors

As it was mentioned earlier we can distinguish 4 sources of errors of temperature measurement in radiometric channel:

1. difference between the assumed by the user the object effective emissivity ϵ_a and the true object effective emissivity ϵ ,
2. difference between the assumed effective background temperature $T_{ba(a)}$ and the true value $T_{ba(r)}$,

3. difference between the assumed effective transmittance $\tau_{a(a)}$ and the true value $\tau_{a(r)}$,
4. difference between the assumed optics temperature $T_{op(a)}$ and the true value $T_{op(r)}$.

4.2.2.1 Errors of estimation of the effective emissivity

Difference between the assumed by the user the object effective emissivity ε_a and the true object effective emissivity ε_r is typically a source of significant errors of temperature measurement.

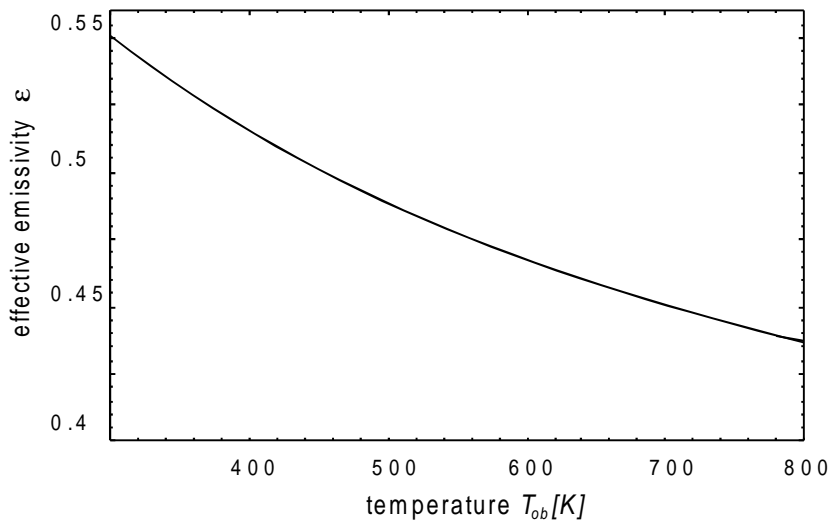


Fig. 4.11. Effective emissivity ε of an object of emissivity function $\varepsilon(\lambda)$ shown in Fig. 4.12 measured using a 3-5 μm thermal camera of the detector relative sensitivity $s(\lambda)$ shown in Fig. 4.3

Formula (4.5) shows that in case of selective object the effective emissivity can be exactly determined only when, the parameter we want to measure, the temperature of the tested object, is known. As shown in Fig. 4.12 the variations of the effective emissivity ε with object temperature can be sometimes quite significant [1]. As object temperature is not known this means that in case of selective objects we cannot determine exactly object effective emissivity.

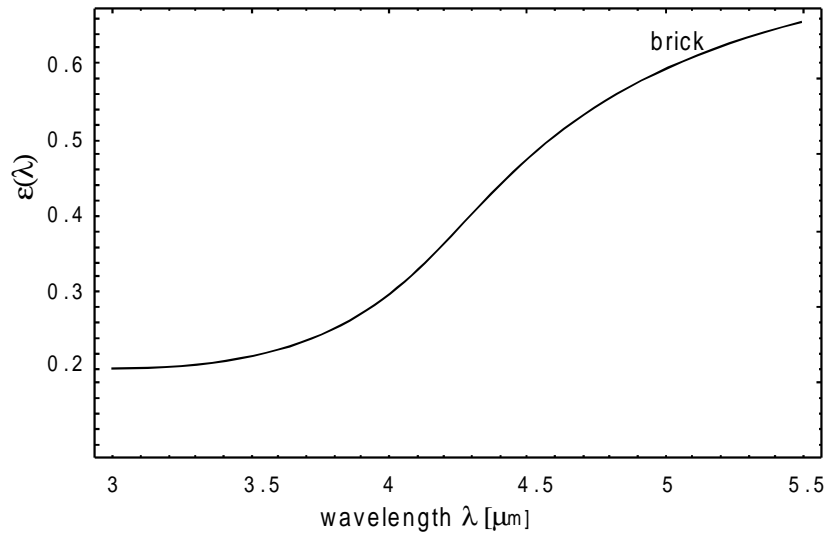


Fig. 4.12. Dependence of the emissivity function $\varepsilon(\lambda)$ of an example selective object (chamotte brick [4]) on wavelength λ

The variations of the effective emissivity with object temperature shown in Fig. 4.11 are about 10% in the analyzed temperature range and can be considered as quite significant. However, these results were calculated for a case of an object of emissivity $\varepsilon(\lambda)$ strongly dependent on wavelength presented in Fig. 4.12. Emissivity of most objects do not depend so strongly on wavelength [4]. We can estimate that the variations of the effective emissivity with object temperature are usually below the level of 2%.

The variations of the effective emissivity with object temperature are not negligible but they usually contribute little to the relative error of estimation of this parameter $(\varepsilon_a - \varepsilon_r)/\varepsilon_r$ by the user. The error $(\varepsilon_a - \varepsilon_r)/\varepsilon_r$ is often over 20% or more due to difficulties in accurate estimation of the spectral emissivity ε_λ because of a few reasons. First is that the data about spectral emissivity $\varepsilon_\lambda(\lambda)$ of many materials is not available (in many emissivity tables found in literature are published only the total hemispherical emissivity ε_T , directional total emissivity in the normal direction $\varepsilon_{T,n}$, spectral directional emissivity in the normal direction $\varepsilon_{\lambda,n}$). Second, even if such data is available it often cannot be trusted as the emissivity values differ quite significantly from one source to another. Third, the spectral emissivity ε_λ depends not only on wavelength but also on a shape of the surface and the angle of measurement.

Errors of temperature measurement due to relative error in estimation of the effective emissivity $(\varepsilon_a - \varepsilon_r)/\varepsilon_r$ of the 20% level are shown in Fig. 4.13. We can make two conclusions on the basis of this figure.

First, that the relative errors of temperature measurement due to the analyzed source rise with object temperature. This means that we can expect higher

errors due to improperly estimated object effective emissivity in higher temperature range.

Second, that the errors of temperature measurement that originate from the analyzed source are many times lower in case of the short wave Ge and Si pyrometers than in case of the long wave thermocouple pyrometer or the 8-12 μm thermal camera .

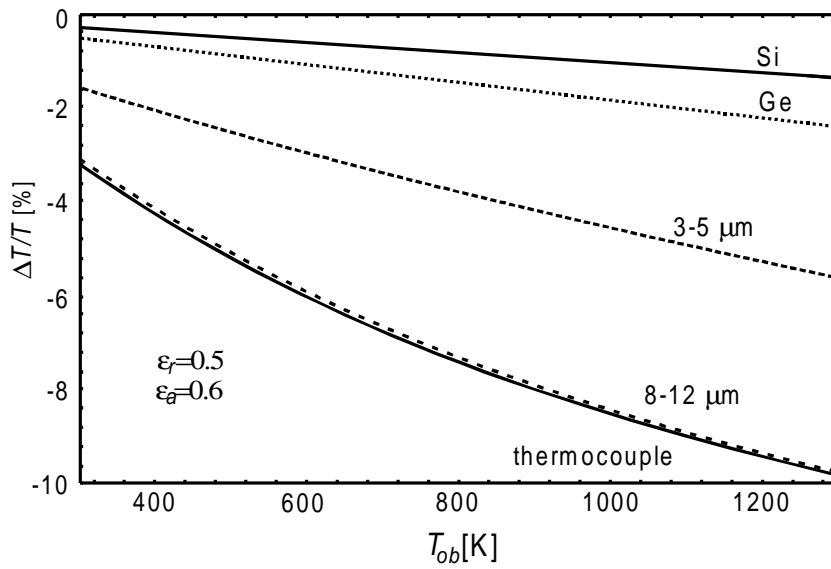


Fig. 4.13. Errors of temperature measurement due to difference between the assumed effective emissivity ε_a and the real effective emissivity ε_r

4.2.2.2 Non-accuracy of estimation of the effective background temperature

Operators of most singleband thermometers are required to estimate the effective background temperature that is the temperature of a blackbody that when put in the place of the real background would produce the same signal as the real background does.

It is easy to estimate the effective background temperature in the case of uniform high emissivity background when the effective background temperature T_{ba} equals true background temperature. The assumption about uniform background is sometimes fulfilled in indoor conditions. However, it is usually not fulfilled in outdoor conditions primarily because of the radiation from the Sun. Even in indoor conditions There are many applications when high temperature sources are mixed with low temperature ones and is difficult to estimate accurately the effective background temperature $T_{ba(a)}$.

The methods of background temperature measurement described in Ref. [5] and manuals of different non-contact thermometers are useful. However, their accu-

racy varies from one application to another. Additionally there are many situation when these methods cannot be used or the effective background temperature changes during the measurement process. Therefore, the accuracy of estimation of the effective background temperature can vary significantly.

We can generally distinguish two opposite cases of the influence of the reflected radiation on the measurement accuracy. First, the low background temperature case when the background temperature is below about 400K. Such background temperatures can be considered as typical in most applications. Second, the high background temperature case when the background temperature, for example in ovens, can reach even 1000K or more.

As can we see in Fig. 4.14 for the case of low temperature background the errors due to background radiation are significant only for low temperature objects below 400K measured using the MIR and the FIR systems. The errors are completely negligible for VNIR and NIR systems of spectral bands located below 3 μm . Next, we can conclude that the MIR systems are less vulnerable to the reflected background radiation than the FIR systems are.

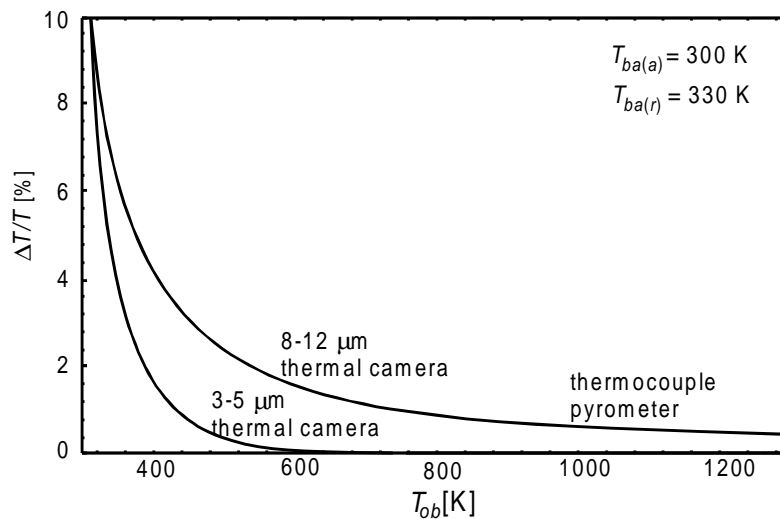


Fig. 4.14. Errors of temperature measurement for case of low temperature background

The situation presented in Fig. 4.14 prefers the VNIR and NIR as for these systems the errors due to radiation emitted by low temperature background are negligible. From Fig. 4.15 we can conclude that for the high-temperature case we have the same situation because the errors are the lowest for the VNIR thermometers and the highest for the FIR thermometers. Additionally, it is clear that for the case of high temperature object the errors due to improperly estimated effective background temperature are significantly higher for both analyzed cases when the real effective background temperature $T_{ba(r)}$ is higher than the object temperature T_{ob} .

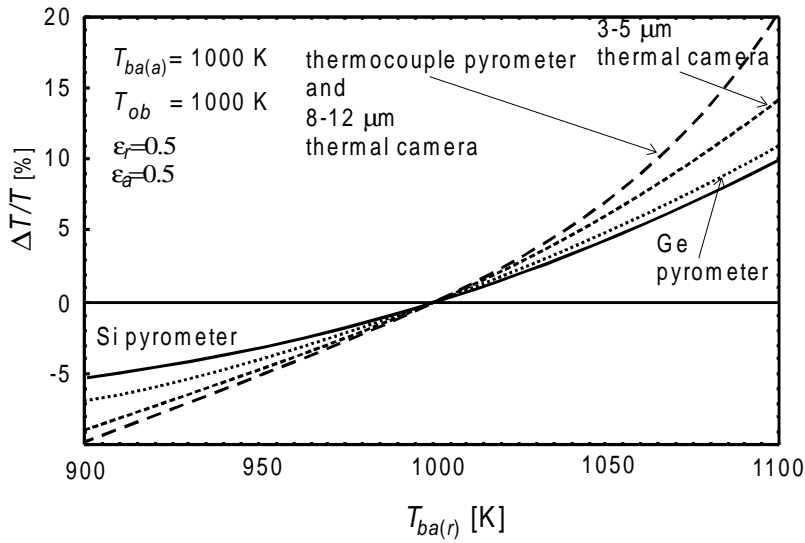


Fig. 4.15. Errors of temperature measurement for case of high temperature background

4.2.2.3 Errors of estimation of the effective atmospheric transmittance

Infrared radiation is always absorbed and scattered in the atmosphere. The analyzed non-contact thermometers operate in atmospheric windows where atmospheric transmittance is relatively good. However, independently of the spectral band, the atmosphere always suppresses the emitted and the reflected radiation. The atmosphere not only influences these two components, it also emits its own radiation. Problems in the transmittance and the emittance are closely related, because a lower transmittance means a higher emittance and vice versa. Because of the impact of effect of atmospheric scattering, the 8-12 μm military thermal cameras are preferred in long distance conditions, as the effect of Solar radiation scattered into a line of sight of 3-5 μm thermal cameras can sometimes be devastating [10]. However, the civilian measuring thermal cameras, scanners and pyrometers usually are used in over short paths, when the distance spans a dozen or so meters long. Such a situation enables us to consider both the effects of atmospheric emittance and scattering as negligible; only the influence from absorptance must be analyzed.

As it was mentioned in Chapt.3 the calculation methods of output temperature used by most non-contact thermometers assume a case of a perfect atmosphere when the effective atmospheric transmittance $\tau_{a(a)}$ equals one. Because infrared radiation is always absorbed and scattered in the atmosphere the influence limited transmittance of the atmosphere always decreases the output temperature what causes a certain measurement error. This error caused by limited transmittance of the atmosphere was calculated using a following procedure.

First, the atmospheric transmittance function $\tau_a(\lambda)$ was calculated using the well-known LOWTRAN model for a typical atmosphere. Next, the real effective atmospheric transmittance $\tau_{a(r)}$ was calculated using Eq.3.7. Finally, the relative error of temperature measurement of the analyzed systems due to the influence limited transmittance of the atmosphere was calculated using Eq.(4.16). The results of the calculations are shown in Fig. 4.16.

As we can see in Fig. 4.16 the errors caused by the influence of the limited transmittance of the atmosphere are small. For case of VNIR, NIR and FIR systems we can even treat these errors as negligible. Only for MIR system of 3-5 μm spectral band the errors become rather significant for the distance about 10m. These results show that it is particularly important for the MIR thermal cameras to be equipped with software enabling calculation of the effective atmospheric transmittance and correcting the influence of the analyzed effect on measurement results.

The calculation results from the Fig. 4.16 suggest that the atmosphere do not cause significant errors of temperature measurement with the analyzed systems. The only exception is the MIR system. However, we must remember that results from Fig. 4.16 were calculated for a case of short-distance testing carried out in a typical clear atmosphere.

Non-contact thermometers are usually used in indoor conditions over short paths, when the distance spans a dozen or so meters long and in clear atmosphere. For such conditions the errors from the atmosphere are usually negligible even when the user do not even to try to correct the influence of the analyzed effect on measurement results. However, there occur also drastically different situations of long-distance measurements or measurements in dust, smoke etc. If not properly corrected, the errors caused by the atmosphere can be then significant.

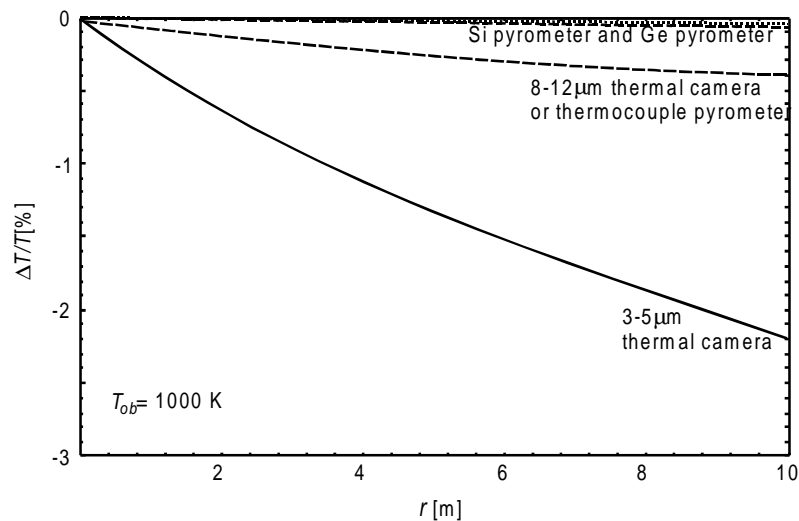


Fig. 4.16. Errors of temperature measurement due to limited transmittance of the atmosphere

4.2.2.4 Errors of estimation of the temperature of the optical components

The optics emits radiation in both laboratory and real working conditions. The errors of temperature measurement from the optics radiation are caused by difference between the assumed optics temperature $T_{op(a)}$ and the true optics temperature $T_{op(r)}$. The value of the $T_{op(a)}$ is assumed by the user or, in case of modern MIR or FIR thermal cameras, is automatically measured by contact temperature measurement method. In both cases the difference between values of $T_{op(a)}$ and $T_{op(r)}$ of 10 K can be considered as really high.

As we can see in Fig. 4.17 even for such a high difference the errors generated by improperly corrected radiation of the optical elements are small for MIR and FIR systems; for VNIR and NIR systems they are completely negligible. However, we must remember that sometimes objects of lower temperatures than the lowest temperature in the analyzed temperature range must be measured and for such cases these errors can be significant.

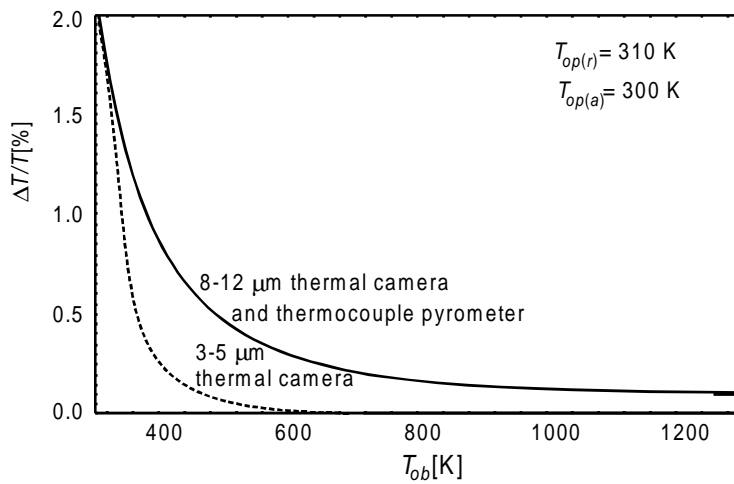


Fig. 4.17. Errors due to non-accuracy of estimation of temperature of optical components

4.2.3 Calibration errors

Nowadays, there are available blackbodies that enable setting temperature at some points within their temperature range with limit error below 0.1K or better. However, generally the limit error of a typical commercially available blackbody is not better than 0.25% of the blackbody temperature. Therefore, let us assume that the signal caused by radiation emitted by a blackbody S_{bb} can be determined experimentally at calibration condition with the randomly distributed errors ΔT_{cal} within the range equal to ± 0.025 of blackbody temperature. Next, let us calculate the dispersion of the signal S_{bb} values due to randomly distributed errors ΔT_{cal} using the Eq. (4.3). The results of the calculations shows that the errors of temperature measurement caused by non-accuracy of such a blackbody are within the range

± 0.025 of object temperature. Therefore, the temperature measurement errors due to non-accuracy of blackbody used for calibration can be considered as negligible in comparison to errors generated by the previously analyzed sources.

4.3 Conclusions

The accuracy of temperature measurement is an important figure of merit in comparison with different non-contact thermometers. It is difficult to formulate one general conclusion about superiority of one type of the analyzed pyrometers over others or to choose the best thermal camera on the basis of the presented earlier results.

The thermocouple pyrometer has an advantage of a wide temperature measurement range and can be used for measurement of both low and high temperature objects. It is almost not sensitive to influence of atmosphere and the errors due to limited digital resolution of the thermometer are low. However, this type of non-contact thermometer is very sensitive to non-accuracy of estimation of the effective object emissivity, the effective background temperature and variations of gain of electronic channel and detector responsivity.

In case of the Si pyrometer and the Ge pyrometer we have an inverse situation. They have relatively low sensitivity to non-accuracy of estimation of the effective object emissivity, the effective background temperature and the variations of the gain of electronic channel and the detector responsivity. However, their lower limit of temperature measurement range is located over about 600-700K and cannot be used to measure low temperature objects.

Differences between the analyzed thermal cameras are smaller than in the case of the pyrometers. The lower limit of the temperature measurement range of the 3-5 μm thermal camera is only a bit higher than the lower limit of the temperature measurement range of the 8-12 μm thermal camera. The 8-12 μm thermal cameras are more sensitive to non-accuracy of estimation of the effective object emissivity, the effective background temperature and variations of the gain of electronic channel and the detector responsivity, and non-accuracy of estimation of the temperature of the optical components. However, the 3-5 μm thermal cameras are more vulnerable to influence of the atmosphere.

On the basis of the calculation results presented earlier we can formulate a general conclusion that in order to improve measurement accuracy, spectral band of the thermometer should be located in as short wavelength as it is possible due to required measurement range. However, we must remember that the presented above study is limited to thermometers working in indoor conditions and short distance measurements. Therefore, the conclusion, formulated above, is valid only for this group of non-contact thermometers.

4.4 References

1. Chrzanowski K., Problem of determination of effective emissivity of some materials, *Infrared Physics and Technology*, 36, 679-684 (1995).
2. Chrzanowski K., Szulim M., A measure of influence of detector noise on temperature measurement accuracy with IR systems, *Applied Optics*, 37, 5051-5057 (1998).
3. Chrzanowski K., Z. Bielecki, Szulim M., Comparison of Temperature Resolution of Singleband, Dualband and Multiband Infrared Systems, *Applied Optics*, 38 (10), 2820-2823 (1999).
4. Sala A., *Radiant Properties of materials*, PWN-Polish Scientific Publishers Warsaw&Elsevier Amsterdam-Oxford (1986).
5. Temperature measurement in industry: Radiation Thermometry, VDI/VDE 3511 Part 4, Verein Deutscher Ingenieure, Dusseldorf, 1995.
6. Michael C. Dudzik ed., *The Infrared & Electro-Optical Systems Handbook*, Vol.4: Electro-Optical Systems Design, Analysis and Testing, Chapt. 4 Infrared Imaging System Testing, p.199, SPIE (1993).
7. US Military Standard MIL-STD-1859: *Thermal Imaging Devices, Performance Parameters Of*, Department of Defence, Washington, DC 20301, 1981.
8. Chrzanowski K., Matyszek R., Update on a model of noise equivalent temperature difference *NETD* of infrared systems for finite distance between sensor-object, *Optica Applicata*, 27, 49-54(1997).
9. Michael C. Dudzik ed., *The Infrared & Electro-Optical Systems Handbook*, Vol.4: Electro-Optical Systems Design, Analysis and Testing, Chapt. 1 Fundamentals of Electro-Optical Imaging System Analysis, p.24, SPIE (1993).
10. J.R. Schott, Methods for Estimation of and Correction for Atmospheric Effects on Remotely Sensed Data, SPIE, Vol. 1968, 448-482 (1993).
11. Radiance PM User Manual, Amber-A Ratheon Company, p.6 (1997).
12. Chrzanowski K., Experimental verification of theory of influence from measurement conditions and system parameters on temperature measurement accuracy with IR systems, *Applied Optics*, 35, 3540-3547 (1996).

5. Errors of passive dualband thermometers

In spite of a quite wide range of applications of dualband thermometers [1-8] the problem of accuracy of these systems has received rather small attention. Only the influence of a few factors such as emissivity [9], limited temperature resolution [10], location and width of the spectral bands [11,12] on the measurement accuracy have been separately analyzed. In addition, the analyses in Refs.[9,10] were made for the visible and the VNIR systems. Therefore, their results do not need to be valid for the MIR and FIR systems.

Let us now develop a model that would enable determination of influence of any source of errors on measurement accuracy with dualband systems.

5.1 Mathematical model

Dualband systems typically determine temperature of the tested objects on the basis of the ratio between two radiometric signals measured in two spectral bands using this 4 step measurement procedure described in detail in Chapt 3:

1. Determination of the calibration characteristic $R_{bb}=f(T_{bb})$
2. Measurement of the real output signals S_{r1} and S_{r2} in two spectral bands and calculation of the ratio of the two measured signals $R_r = S_{r1} / S_{r2}$
3. *Correction of the ratio R_r is to the new value R_{cor} on the basis of the assumed ratio of the object emissivity in the two spectral bands $r\varepsilon = \varepsilon(\lambda_1) / \varepsilon(\lambda_2)$.*
4. Calculation of the output temperature T_{out} on the basis of the value of the corrected ratio R_{cor} .

Although the step 3 is conditional and used only by a small minority of dualband thermometers let us assume that the corrected ratio is always determined and we will develop formulas for the output temperature T_{out} connected to the corrected ratio R_{cor} . If we later want to make calculations for the case when the step 3 is not carried out we will simply assume that the corrected ratio R_{cor} equals the real ratio R_r .

Assuming that the difference between the corrected ratio R_{cor} for object temperature T_{ob} and the ratio R_{bb} for the same temperature is not high then the relationship between the T_{ob} and T_{out} can be presented in the following form [Fig. 5.1]

$$T_{out} = T_{ob} + \frac{(R_{cor}(T_{ob}) - R_{bb}(T_{ob}))}{\left. \frac{dR_{bb}}{dT} \right|_{T=T_{ob}}}. \quad (5.1)$$

Using formula (5.1) the error of the temperature measurement ΔT that equals to the difference between the output temperature T_{out} and the true object temperature T_{ob} can be presented as

$$\Delta T = T_{out} - T_{ob} = \frac{(R_{cor}(T_{ob}) - R_{bb}(T_{ob}))}{\left. \frac{dR_{bb}}{dT} \right|_{T=T_{ob}}}. \quad (5.2)$$

As can we see in formula (5.2) when the corrected ratio $R_{cor}(T_{ob})$ equals the calibration ratio $R_{bb}(T_{ob})$ then the output temperature T_{out} equals T_{ob} and the measurement error ΔT is zero. When the equality $R_{cor}(T_{ob}) = R_{bb}(T_{ob})$ is not fulfilled then a difference between T_{out} and T_{ob} exists. This means that difference between the ratios $R_{cor}(T_{ob})$ and $R_{bb}(T_{ob})$ generates errors of temperature measurement with dualband systems.

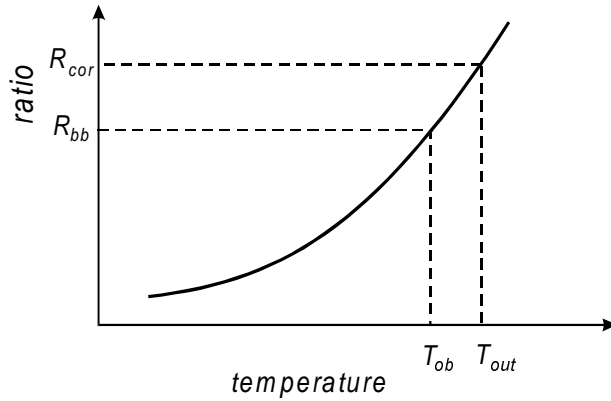


Fig. 5.1. Relationship between the output temperature T_{out} , true object temperature T_{ob} , the corrected ratio R_{cor} and the calibration ratio R_{bb}

The difference between the corrected ratio R_{cor} and the calibration ratio R_{bb} can be treated as the error of ratio measurement ΔR . Therefore, using the formula (5.2) we can present the relationship between the ratio measurement error ΔR and the error of temperature measurement ΔT in the following form

$$\Delta T = T_{out} - T_{ob} = \frac{R_{cor} - R_{bb}}{ADRF} = \frac{\Delta R}{ADRF}, \quad (5.3)$$

where

$$ADRF = \left. \frac{dR_{bb}}{dT} \right|_{T=T_{ob}}.$$

The new function $ADRF$ can called the absolute disturbance resistance function, because it represents the system resistance to the absolute errors of ratio measurement that can be treated as disturbances of the measured signal. The $ADRF$ gives us information about how many times the absolute error of the temperature measurement ΔT is smaller than the absolute error in the ratio measurement ΔR .

It is possible also to develop a relationship between the relative error of temperature measurement $\Delta T/T$ and the relative error of ratio measurement by transforming formula (5.2) to this form

$$\frac{\Delta T}{T_{ob}} = \frac{\Delta R / R}{RDRF}, \quad (5.4)$$

where

$$RDRF = \frac{\left. \frac{dR_{bb}(T)}{dT} \right|_{T=T_{ob}} T_{ob}}{R_{bb}(T_{ob})}, \quad (5.5)$$

and where the $RDRF$ was termed the relative disturbance resistance function for similar reasons as the $ADRF$.

If we analyze the presented above measurement procedure then we can conclude that the error ΔT is caused by limited accuracy of determination of the calibration characteristic $R_{bb}=f(T_{bb})$ and limited accuracy of determination of the corrected ratio R_{cor} . Let us develop mathematical models of the R_{bb} , the R_{cor} and the $RDRF$ to enable us calculation of the measurement errors using the formula (5.4).

The calibration characteristic $R_{bb}=f(T_{bb})$ is determined with some errors mostly due to limited accuracy of the blackbody used during calibration. We can present the ratio R_{bb} as

$$R_{bb}(T_{bb}) = \frac{S_{bb1}(T_{ob})}{S_{bb1}(T_{ob})}, \quad (5.6)$$

where

$$S_{bb1}(T_{ob}) = \frac{R_1^* g_1 A_{d1}}{4F_1^2 + 1} \left[\tau_{o1} \int_{\Delta\lambda_1} M(T_{bb} \pm \Delta T_{bb}, \lambda) \tau_{F1}(\lambda) s_1(\lambda) d\lambda \right. \\ \left. + \varepsilon_{opt1} \int_{\Delta\lambda_{d1}} M(T_{op(c)}, \lambda) s_1(\lambda) d\lambda \right],$$

$$S_{bb2}(T_{bb}) = \frac{R_2^* g_2 A_{d2}}{4F_2^2 + 1} \left[\tau_{o2} \int_{\Delta\lambda_2} M(T_{bb} \pm \Delta T_{bb}, \lambda) \tau_{F2}(\lambda) s_2(\lambda) d\lambda \right. \\ \left. + \varepsilon_{opt2} \int_{\Delta\lambda_{d2}} M(T_{op(c)}, \lambda) s_2(\lambda) d\lambda \right],$$

and where ΔT_{bb} is the limit error of indicated blackbody temperature.

The corrected ratio R_{cor} is

$$R_{cor}(T_{ob}) = \frac{R_r(T_{ob})}{r\epsilon_a}, \quad (5.7)$$

where the R_r is the ratio of the two real signals S_{r1}/S_{r2} that equals

$$R_r(T_{ob}) = \frac{S_{r1}(T_{ob})}{S_{r2}(T_{ob})}, \quad (5.8)$$

and the $r\epsilon_a$ is the assumed ratio of the object emissivity in the two spectral bands of the system:

$$r\epsilon_a = \frac{\epsilon_1}{\epsilon_2}. \quad (5.9)$$

The signals measured in both two spectral bands during real measurements can be presented on the basis of the analysis shown in subchapter 4.1 as

$$S_{r1} = \left\{ \left[\begin{aligned} &\epsilon_{ob1}\tau_{a1} \int_{\Delta\lambda_1} M(T_{ob}, \lambda)\tau_{o1}(\lambda)\tau_{F1}(\lambda)s_1(\lambda)d\lambda \\ &+ (1 - \epsilon_{ob1})\tau_{a1} \int_{\Delta\lambda_1} M(T_{ba(r)}, \lambda)\tau_{o1}(\lambda)\tau_{F1}(\lambda)s_1(\lambda)d\lambda \\ &+ \int_{\Delta\lambda_{d1}} M(T_{op(r)}, \lambda)\epsilon_{opt1}(\lambda)s_1(\lambda)d\lambda \end{aligned} \right] \times \frac{(R_1^* \pm \sigma R_1^*)A_{d1}}{4F^2 + 1} (g_1 \pm \sigma g_1) \right\} \pm V_{a1} \pm V_{d1}$$

$$S_{r2} = \left\{ \left[\begin{aligned} &\epsilon_{ob2}\tau_{a2} \int_{\Delta\lambda_1} M(T_{ob}, \lambda)\tau_{o2}(\lambda)\tau_{F2}(\lambda)s_2(\lambda)d\lambda \\ &+ (1 - \epsilon_{ob2})\tau_{a2} \int_{\Delta\lambda_2} M(T_{ba(r)}, \lambda)\tau_{o2}(\lambda)\tau_{F2}(\lambda)s_2(\lambda)d\lambda \\ &+ \int_{\Delta\lambda_{d2}} M(T_{op(r)}, \lambda)\epsilon_{opt2}(\lambda)s_2(\lambda)d\lambda \end{aligned} \right] \times \frac{(R_2^* \pm \sigma R_2^*)A_{d1}}{4F^2 + 1} (g_2 \pm \sigma g_2) \right\} \pm V_{a2} \pm V_{d2}$$

If we differentiate Eq.(5.6) then we obtain

$$ADRF = \frac{dR_{bb}(T_{bb})}{dT_{bb}} = \frac{S_{bb2}(T_{ob}) \frac{dS_{bb1}(T_{bb})}{dT_{bb}} - S_{bb1}(T_{bb}) \frac{dS_{bb2}(T_{bb})}{dT_{bb}}}{S_{bb2}^2(T_{bb})}. \quad (5.10)$$

Next, the relative disturbance function $RDRF$ can be presented as

$$RDRF = \frac{\left[S_{bb2}(T_{ob}) \frac{dS_{bb1}(T_{bb})}{dT_{bb}} - S_{bb1}(T_{bb}) \frac{dS_{bb2}(T_{bb})}{dT_{bb}} \right] T_{bb}}{S_{bb2}^2(T_{bb}) R_{bb}(T_{bb})}. \quad (5.11)$$

Now we have all necessary formulas to calculate errors of temperature measurement with dualband systems using Eq.(5.4).

5.2 Calculations

Dualband systems are usually built using non-cooled Si, Ge or InAsGa photoelectric detectors of spectral bands located within VNIR and NIR ranges. However, let us make calculations for 4 types of thermoelectrically cooled detectors: Si, Ge, HgCdTe optimized for 3-5 μm and HgCdTe optimized for 8-12 μm in order to estimate full capabilities of the dualband systems. Parameters of the assumed systems shown in Tab. 5.1 and in Fig. 5.2 are based on data from Ref.[13].

Tab. 5.1. Parameters of the assumed four systems

Detector spectral band	Si 0.4-1.1 μm	Ge 1-1.8 μm	HgCdTe 3-5 μm	HgCdTe 8-12 μm
D^* [cm Hz ^{1/2} /W]	58×10^{12}	2×10^{12}	3×10^{10}	6×10^8
bands location	$\lambda_1=0.81\mu\text{m}$ $\lambda_2=0.96\mu\text{m}$ $\Delta\lambda=0.02\mu\text{m}$	$\lambda_1=1.325\mu\text{m}$ $\lambda_2=1.625\mu\text{m}$ $\Delta\lambda=0.05 \mu\text{m}$	$\lambda_1=3.95\mu\text{m}$ $\lambda_2=4.95\mu\text{m}$ $\Delta\lambda=0.1\mu\text{m}$	$\lambda_1=8.1\mu\text{m}$ $\lambda_2=10.1\mu\text{m}$ $\Delta\lambda=0.2\mu\text{m}$
τ_F	0.7			
τ_o	0.9			
F	2			
A_d	0.01 cm ²			
Δf	2 kHz			

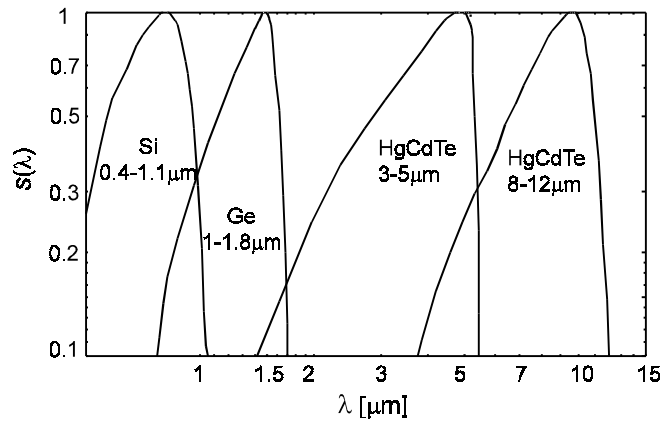


Fig. 5.2. The relative sensitivity functions $s(\lambda)$ of the assumed four detectors

5.2.1 Relative disturbance resistance function

The relative disturbance function $RDRF$ gives us information on how much the temperature-measurement error is smaller than the ratio-measurement error and is a good figure of merit for comparison of different dualband systems. As shown in Fig. 5.3 the $RDRF$ clearly prefers the shortwave dualband systems. The values of the $RDRF$ are always higher for the shortwave systems than for the longwave systems. Consequently, the same errors of the ratio measurement cause smaller temperature measurement errors for shortwave systems. Next, we can conclude from Fig. 5.4 that the systems of narrow spectral bands located far from each other are more resistible to the disturbances than the systems of wide spectral bands located close to each other.

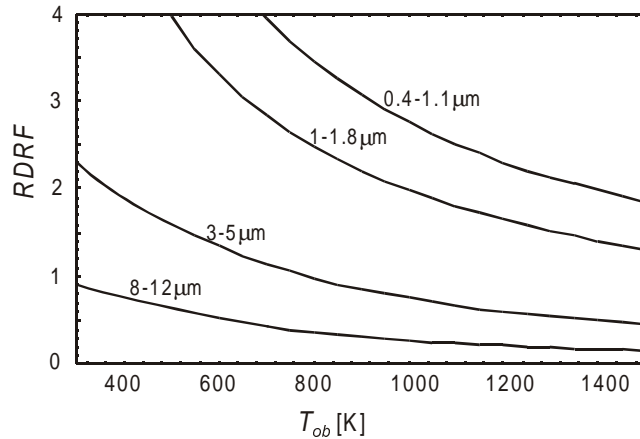


Fig. 5.3. The relative disturbance resistance function $RDRF$ for four systems of parameters as presented in Tab.1 and in Fig. 5.2.

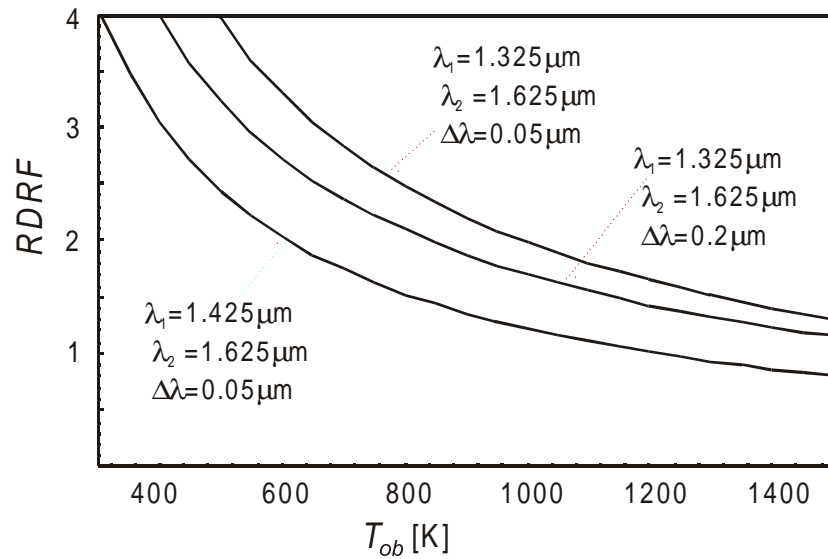


Fig. 5.4. The relative disturbance resistance function $RDRF$ for the three 1-1.8 μm systems of different spectral bands

The results of the presented above calculations clearly show that the short-wave shortwave dualband are more resistant on the errors of ratio measurement received by the detector than the longwave ones. However, accuracy in the temperature measurement depends not only on the system resistance on the errors of ratio measurement but also on the level of the errors. The $RDRF$ can be used as a useful figure of merit for comparison of dualband systems but the most important figure of merit for comparing these systems is their accuracy.

When we analyze the measurement procedure we can distinguish following sources of errors of temperature measurement with passive dualband systems:

1. difference between the assumed by the user ratio re_a and the true ratio $re_a = \varepsilon_{ob1} / \varepsilon_{ob2}$ (for most dualband systems is assumed that $re_a = 1$),
2. non-negligible radiation reflected by the object,
3. non-equal atmospheric transmittance in the two spectral bands,
4. non-negligible influence of radiation emitted by the optical elements,
5. noise generated in detector (detectors) or other analog electronic blocks,
6. variation of the detector peak responsivity R^* and variation of the preamplifier gain g ,
7. limited resolution of analogue/digital converter,
8. limited accuracy of the blackbody used during calibration.

The first 4 sources can be grouped as sources of radiometric errors, the next 3 sources are sources of electronic errors and the last source is a source of the calibration errors.

We pointed above 8 sources of errors with dualband systems. However, we will limit calculations to the 4 most important sources:

1. difference between the assumed by the user the ratio re_a and the true ratio $\varepsilon_{ob1}/\varepsilon_{ob2}$,
2. non-negligible radiation reflected by the object,
3. non-equal atmospheric transmittance in both spectral bands,
4. noise generated in detector (detectors) or other analog electronic blocks.

At first let us calculate the errors of the temperature measurement caused by the system noise, because these errors determine the lower limit of the temperature measurement range with the four analyzed systems.

5.2.2 Detector noise

Analysis of the influence of the detector noise is usually done for case of blackbody type objects. However, in order to better simulate real measurements, we will make calculations of the standard deviation of the random variations of the output temperature due to the detector noise for a case of an object of low emissivity equals 0.3. As demonstrated in Fig. 5.5, the temperature measurement errors caused by the system noise decrease with the object temperature, particularly strongly for the NIR systems. We can determine the temperature measurement range for the four analyzed systems on the basis of these errors. Let us assume that the measurement errors from the system noise must be below the level of 1%. According to this condition the 0.4-1.1 μm systems can be used for the measurements of temperature over the level of 800 K, the 1-1.8 μm systems for temperature over the level of 600K, and the 3-5 μm systems for temperature over the level of 410 K. However, the 8-12 μm systems do not fulfil the condition in the entire analyzed temperature range 300-1500K. These high temperature measurement errors resulting from the system noise for the 8-12 μm system are caused by two factors. First, by low values of the *RDRF* of these systems. Second, by low value of the peak normalized detectivity of the assumed thermoelectrically cooled 8-12 μm detector. Currently, the detectivity of the thermoelectrically cooled detectors for the 8-12 μm spectral range is almost a hundred times lower than the detectivity of the same detector for the 3-5 μm spectral range and this results in high temperature measurement errors of the assumed 8-12 μm system. However, the technology of the thermoelectrically cooled detectors for the 8-12 μm range is developed rapidly, and in near future their detectivity can be significantly improved. This improvement could significantly reduce the errors caused by the system noise. In addition, the detectivity of the 8-12 μm detectors can also be significantly improved by using other, more effective, cooling systems (liquid nitrogen, Joule-Thomson cooler, Stirling cooler). Now, let us calculate the errors caused by the other disturbances.

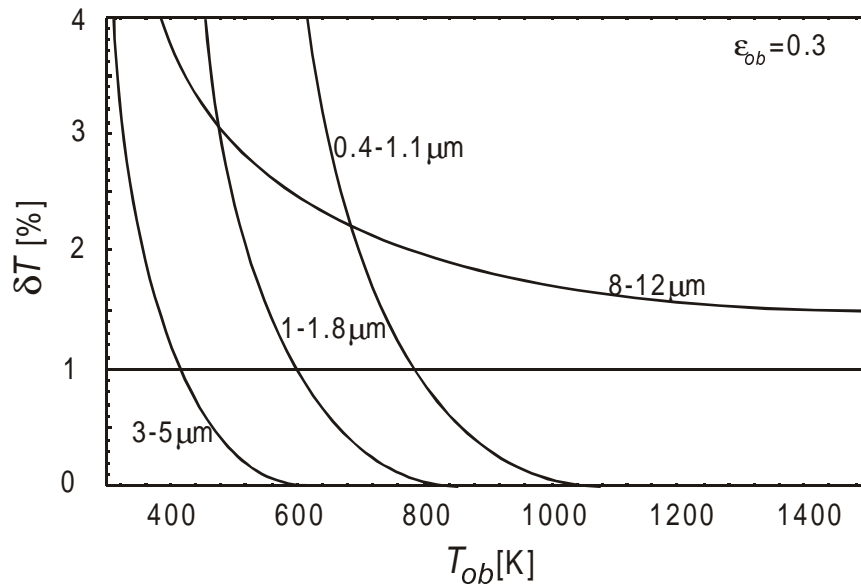


Fig. 5.5. The relative standard deviation of the random errors of temperature measurement $\sigma T/T$ due to detector noise

5.2.3 Emissivity

There are dualband systems that use fully the presented earlier measurement procedure are capable of producing accurate results even when object emissivity is different in the two spectral bands. However, the user is then required to determine the ratio of object emissivity in the two spectral bands $r\epsilon$ to enable correction of the difference of the object emissivity in these two bands. This is inconvenient for users of dualband systems and for most systems it is assumed that the ratio of the object emissivity in the two spectral bands is equal one. Let us limit our analysis to just this case.

The difference between emissivity values in the two spectral bands depends on the type of the tested object, and on the location and the width of the system spectral bands. However, on the basis of some experience it seems reasonable to say that the emissivity differences over the level of about 0.03 occur for many materials. The errors of the temperature measurement caused by this level of the emissivity differences are plotted in Fig. 5.6. As we can see the errors increase with the object temperature and, in general, they are high for the 8-12 μm systems, significantly smaller for the 3-5 μm systems, and relatively small for the 0.4-1.1 μm systems, and the 1-1.8 μm systems.

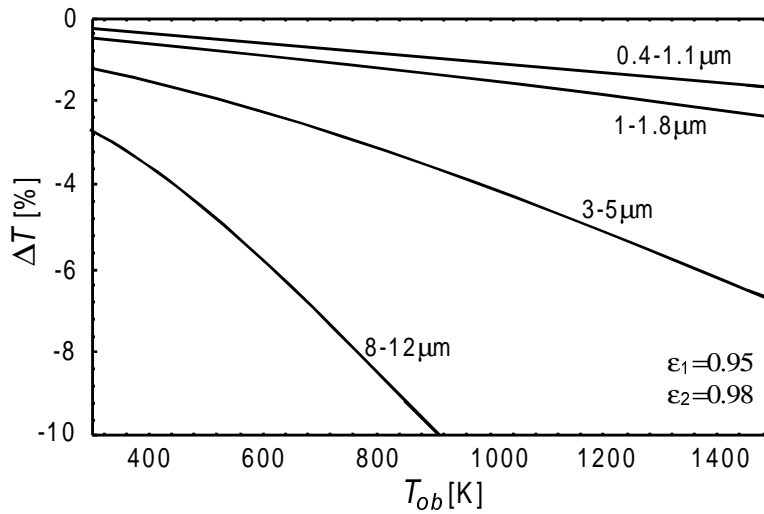


Fig. 5.6. Errors of temperature measurement due to difference of object emissivity in two different spectral bands

5.2.4 Reflected radiation

Many measurements under industrial conditions are made in hot environments when background temperature sometimes reaches a level of 320K, or more. As can be seen in Fig. 5.7, the background radiation reflected by the objects significantly reduce accuracy of the MIR and FIR systems during measurements of low emissivity objects. The errors can be treated as relatively small for the 3-5 μm systems over the level of 600K but they are significant in the almost entire analyzed temperature range for the 8-12 μm systems.

The results of the calculations presented in Fig. 5.7 refer to the situation when the background temperature, although high for humans, is relatively low comparing to the object temperature. However, the measured objects are sometimes put to a furnace, and then the background temperature can be close to the object temperature. As demonstrated in Fig. 5.8, the errors under such conditions are the lowest for the 0.4-1.1 μm systems, and the highest for the 8-12 μm systems.

It should be also noticed that the temperature measurement errors caused by the background radiation are small when the difference between the background temperature and the object temperature is small. This feature can be treated as an important advantage of the dualband systems comparing to the singleband systems.

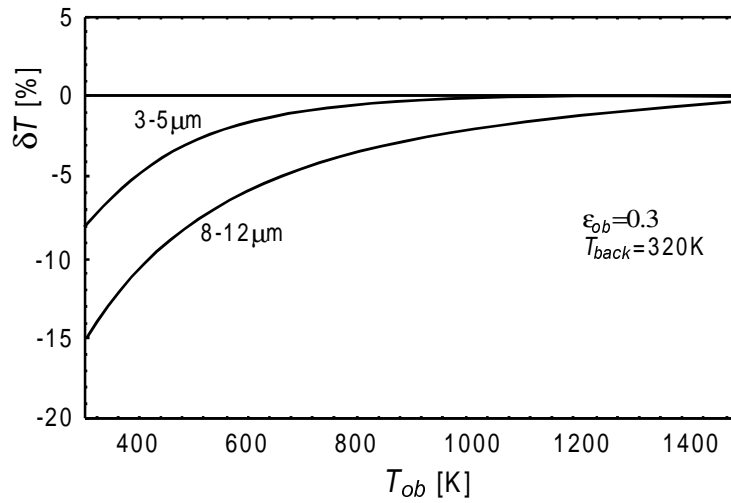


Fig. 5.7. Errors of temperature measurement caused by radiation emitted by low temperature background

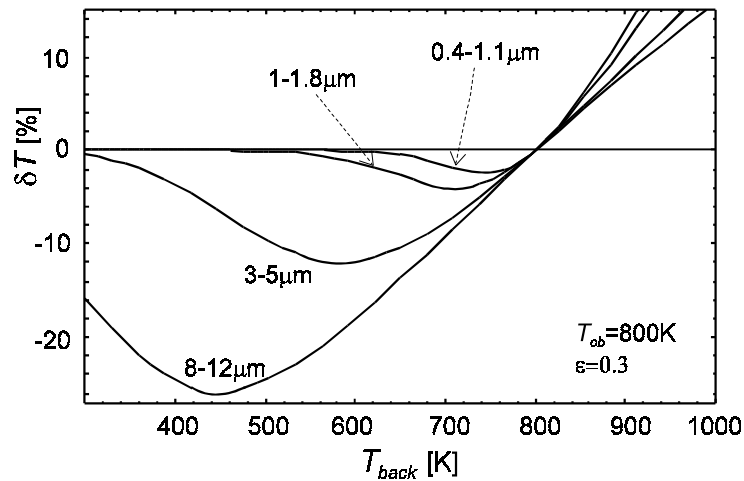


Fig. 5.8. The temperature measurement errors caused by the background radiation reflected by the object for the four assumed systems. The case of variable-temperature background.

5.2.5 Atmosphere

Infrared radiation is always absorbed by the atmosphere. The dualband systems usually operate in atmospheric windows where atmospheric transmittance is relatively good. However, independently of the spectral band, the atmosphere always suppresses the emitted and the reflected radiation. The atmospheric trans-

mission depends on many parameters. The results of many studies dealing with the problem of determination of this parameter have been presented; sometimes with contrary results. For an analysis of the influence of the atmosphere, the transmittance was calculated with the popular *LOWTRAN* model for the conditions that can be considered as typical (midlatitude, summer, visibility equal to 5km, height equal to 2m, horizontal path). Next, the ratio-measurement errors and the temperature-measurement errors from the influence of the limited transmittance of the atmosphere were calculated and they are presented in Fig.10.

The ratio-measurement errors are significant for the 8-12 μm systems and the 1-1.8 μm systems. It can be treated as a surprise because the spectral bands of all the systems have been located in the so called "atmospheric windows". However, the results show that even within the "windows" some transmission variation occur and it can cause significant ratio measurement errors for the two above mentioned systems. However, due to the differences in the *RDRF*, the errors of the temperature measurement from the influence of the limited transmittance are significant only for the 8-12 μm systems.

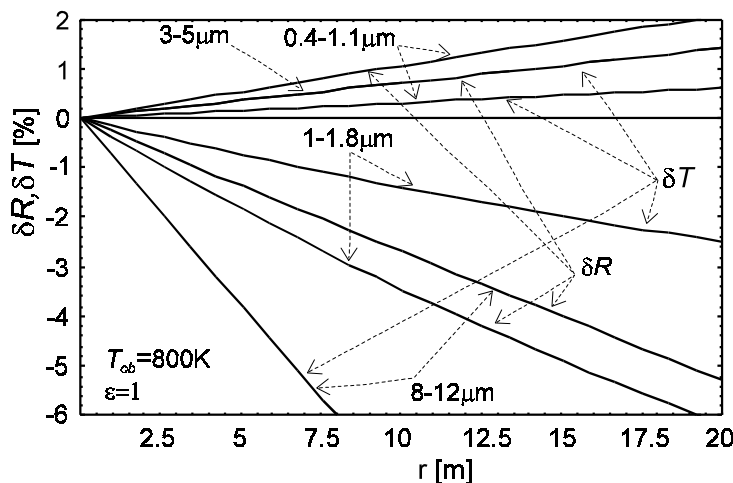


Fig. 5.9. The ratio measurement errors, and the temperature measurement errors caused by the limited transmittance of the atmosphere.

5.3 Conclusions

The accuracy of the temperature measurement is the most important factor that should be used in comparison between different dualband IR systems for temperature measurements. The results presented above definitively show that the errors of the temperature measurements resulting from the analyzed disturbances are generally smaller for the NIR and VNIR systems. These systems behave generally better than the MIR and FIR systems do, particularly for the low-emissivity

objects. Therefore, if it is possible due to the required temperature measurement range we should use the NIR or VNIR thermometers. If it is not possible due to the required temperature range then we should prefer the MIR systems as the measurement errors with these systems are always lower than they are FIR systems.

5.4 References

1. Maldague X., Dufour M., Dual imager and its applications to active vision robot welding, surface inspection, and two color pyrometry, *Opt. Eng.* 28, 872-880 (1989).
2. Spjut R. E., Transient response of one and two- color optical pyrometry, *Opt. Eng.*, 26, 467-472 (1987).
3. Brownson J., Gronokowski K., Meade E., Two-color imaging radiometry for pyrotechnic diagnostics, *Proc. SPIE* 780, 194-201 (1987).
4. Jorgensen F. R. A., Zuyderwyk M., Two-color pyrometer measurement of temperature of individual combusting particles, *J. Phys. E*, 18, 486-491 (1985).
5. Levendis Y.A., Estrada K.R., Hottel H.C., Development of multicolor pyrometers to monitor transient response of burning carbonaceous particles, *Rev. Sci. Instrum.* 63, 3608-3621 (1992).
6. Beckwith P.J., Crane K.C., Two wavelength infrared pyrometer for rapid and large temperature changes, *Rev. Sci. Instrum.* 53, 871-875 (1982).
7. Chrzanowski K., Madura H., Polakowski H, Pawłowski M., Fast dualspectral pyrometer, in *Quantitative Infrared Thermography Conference QIRT-94*, Sorrento, Italy, 1994.
8. Jiang H., Qian Y., Rhee K.T., High-speed dual-spectral infrared imaging, *Opt. Eng.* 32, 1281-1289 (1993).
9. Foley G. M., Modification of emissivity response of two-color pyrometers, *High. Temp.-High Press.* 10, 391-398 (1978).
10. Bedford R.E., Keung M.C., Effect of uncertainties in detector responsivity on thermodynamic temperatures measured with an optical pyrometer, *High. Temp.-High Press.* 15, 119-130 (1983).
11. Fehribah J.D., Johnson R.B., Temperature measurement validity for dual spectral-band radiometrics techniques, *Opt. Eng.* 28, 1255-1259 (1989).
12. Lao K. Q., Temperature measurement using video cameras, in *Proc. SPIE* 819, 311-317 (1987).
13. EG&G Optoelectronics - Data Sheet 1996.

Third, the radiometric signals coming to the detector or detectors can differ significantly from the assumed signals and this difference generates errors that we will call radiometric errors. The reasons for this difference are following.

In some cases object emissivity at system spectral bands $\lambda_1, \dots, \lambda_n$ cannot be exactly interpolated by the assumed function $f(a_0, \dots, a_m, \lambda)$. Next, atmosphere due to its limited transmittance apparently changes object emissivity. Further, the signal coming to IR detector consists not only of the signal emitted by the object and the signal caused by radiation from optical elements as during calibration but also of the signal reflected by the object. Additionally, the signal emitted by the system optical elements during measurement conditions can differ from the signal received during calibration because of change of temperature of the optical elements.

To summarize our discussion we can say that the errors of temperature measurement with multiband IR systems, according to their source, can be generally divided into three groups: radiometric errors, electronic errors and calibration errors. Radiometric errors are caused by differences between the assumed measurement conditions (object emissivity can be exactly interpolated using the assumed function, influence of reflected radiation is negligible, radiation emitted by optical elements is negligible or is known, atmospheric transmittance is equal to one at all system spectral bands) and the real measurement ones. Electronic errors are the errors of the transformation of the radiometric signal into output electrical signal during real measurements. Calibration errors are caused by errors of determination of signal generated by a non-accuracy of the blackbody at laboratory conditions.

6.2 Model of errors

It is necessary to make a few assumptions about the measurement method and the thermometer used in measurement in order to formulate a model of errors of temperature measurement with passive multiband thermometers.

First, let us estimate the number of system spectral bands. As we can see from the set of equations (6.1) the object temperature T_{ob} and parameters a_0, \dots, a_m can be determined by solving this set only if the number of spectral bands n is higher than number of unknowns m . From analysis of analytical functions for approximation of object emissivity presented in work [1] we can conclude that a function of 1-2 parameters can well approximate emissivity functions of most objects. As emissivity function used in multiband thermometry must very well interpolate object emissivity at system spectral bands then we will assume a function of at least 3 parameters is needed. This means that to solve the set of equations (6.1), system of number of spectral bands higher or equal to 4 is needed.

Second, let us choose a mathematical function to interpolate values of object emissivity in system bands. From a few possible functions we will choose a $m-2$ -th degree polynomial in form

$$\varepsilon_{ob}(\lambda) = a_0 + a_1\lambda + \dots + a_{m-2}\lambda^{m-2}. \quad (6.2)$$

where $m \geq 4$.

Third, let us assume uniform distribution of true blackbody temperature within the range $[T_{out} - \Delta T_{cal}; T_{out} + \Delta T_{cal}]$ where ΔT_{cal} is the parameter describing blackbody accuracy. Next, we will additionally assume that limited accuracy of the blackbody is the only source of calibration errors and the signal S_{bb} can be predicted theoretically in form

$$S_{bbn}(T_{out}) = g_n \frac{R_n^* A_{dn}}{4F^2 + 1} \int_{\Delta\lambda_n} M(T_{out} \pm \Delta T_{cal}, \lambda) \tau_o(\lambda) \tau_{F_n}(\lambda) s_n(\lambda) d\lambda \quad (6.3)$$

where g_n is the electronic systems amplification in n spectral channel, $M(T, \lambda)$ is the spectral exitance at the temperature T and the wavelength λ , R_n^* is the detector peak spectral responsivity at n spectral channel, A_{dn} is the detector area, $s_n(\lambda)$ is the detector relative spectral responsivity, $\tau_o(\lambda)$ is the transmittance of optics, F is optics F-number and $\tau_F(\lambda)$ is the filter transmittance in n spectral channel.

Fourth, let us assume that the signal caused by radiation emitted by the optics can be determined precisely at calibration condition and that can be expressed as

$$S_{optn} = \frac{g_n R_n^* A_{dn}}{4F^2 + 1} \int_{\Delta\lambda_{dn}} M(T_{opt}, \lambda) \epsilon_{opt}(\lambda) s_n(\lambda) d\lambda \quad (6.4)$$

where T_{opt} and ϵ_{opt} are the temperature and emissivity of optical blocks and $\Delta\lambda_{dn}$ is the n detector spectral sensitivity range.

Now, we can present the set of equations (6.1) in a new form

$$\left\{ \begin{array}{l} S_1 = g_1 \frac{R_1^* A_{d1}}{4F^2 + 1} \left[\left(a_0 + a_1 \lambda_1 + \dots + a_{m-2} \lambda_1^{m-2} \right) \int_{\Delta\lambda_1} M(T_{out} \pm \Delta T_{cal}, \lambda) \tau_o(\lambda) \tau_{F_1}(\lambda) s_1(\lambda) d\lambda \right. \\ \left. + \int_{\Delta\lambda_{d1}} M(T_{opt}, \lambda) \epsilon_{opt}(\lambda) s_1(\lambda) d\lambda \right] \\ \dots \\ S_n = g_n \frac{R_n^* A_{dn}}{4F^2 + 1} \left[\left(a_0 + a_1 \lambda_n + \dots + a_{m-2} \lambda_n^{m-2} \right) \int_{\Delta\lambda_n} M(T_{out} \pm \Delta T_{cal}, \lambda) \tau_o(\lambda) \tau_{F_n}(\lambda) s_n(\lambda) d\lambda \right. \\ \left. + \int_{\Delta\lambda_{dn}} M(T_{opt}, \lambda) \epsilon_{opt}(\lambda) s_n(\lambda) d\lambda \right] \end{array} \right. \quad (6.5)$$

It is necessary to define the left part of the set of equations (6.5) -signals measured at real measurement S_1, \dots, S_n in order to solve that set of equations

and calculate the object temperature T_{ob} . The signal S_n at the output of electronic channel can be presented as

$$\begin{aligned}
 S_n = & \left\{ \left[\varepsilon_{ob}(\lambda) \int_{\Delta\lambda_n} M(T_{ob}, \lambda) \tau_a(\lambda) \tau_o(\lambda) \tau_{Fn}(\lambda) s_n(\lambda) d\lambda \right. \right. \\
 & + (1 - \varepsilon_{ob}(\lambda)) \int_{\Delta\lambda_n} \varepsilon_{back}(\lambda) M(T_{back}, \lambda) \tau_a(\lambda) \tau_o(\lambda) \tau_{Fn}(\lambda) s_n(\lambda) d\lambda \\
 & \left. \left. + \int_{\Delta\lambda_{dn}} M(T_{opt}^r, \lambda) \varepsilon_{opt}(\lambda) s_n(\lambda) d\lambda \right] \right. \\
 & \left. \times \frac{(R_n^* \pm \sigma R_n^*) A_{dn}}{4F^2 + 1} (g_n \pm \sigma g_n) \right\} \pm V_{an} \pm V_{dn}
 \end{aligned} \tag{6.6}$$

where $\varepsilon_{ob}(\lambda_n)$ is the real object emissivity at n -spectral band of the wavelength λ_n , $\tau_a(\lambda)$ is the atmospheric transmittance, T_{back} is the background temperature, T_{opt}^r is the temperature of the optics at real measurement conditions, V_{an} is the standard deviation of the noise at the output of the analog n channel, V_{dn} is the standard deviation of the rectangular probability distribution within range determined by least significant bit LSB of the A/D converter used in *the* channel n , σg is the standard deviation of the gain g treated as a random variable, σR^* is *the* standard deviation of the detector peak responsivity R^* treated as a random variable.

As we can see there are significant differences between the assumed signal shown in the set of equations (6.5) and the real signal shown in equation (6.6). First, instead of the assumed emissivity function in form of a polynomial we have the real emissivity function $\varepsilon(\lambda)$ that can differ from the assumed function. Second, signal generated by the radiation reflected by the object is included into formula (6.6). Third, both the signals generated by the radiation emitted and the reflected by the object are suppressed because of limited transmittance of atmosphere. Fourth, to the signal at the output of the detector during measurement condition the detector noise of the standard deviation V_a is added. Fifth, because of possible variations of the detector the responsivity R^* caused by limited stability of the detector temperature the responsivity R^* is treated as a random variable of the standard deviation σR^* . Sixth, the gain g is treated as a random variable of the standard deviation σg .

The standard deviation V_{an} represents rms value of the noise at output of analog electronic channel. This output noise consists of two components: the noise generated by the detector and amplified by electronic blocks and additional noise generated by these blocks. For a well designed electronics the noise caused by preamplifier and other electronic blocks should not be greater than noise

generated by the detector. Therefore, let us assume that V_{an} equals two rms value of the noise caused by the detector and can be calculated as

$$V_{an} = 2g_n \frac{R_n^* \sqrt{A_{dn} \Delta f_n}}{D_n^*} \quad (6.7).$$

where D_n^* is the peak normalized spectral detectivity of detector used in the channel n and Δf is the noise equivalent bandwidth to the output of the analog channel n .

The V_{dn} that represents errors generated by limited resolution of the digitization system used in channel n can be calculated as standard deviation of rectangular probability distribution within range determined by least significant bit LSB of the converter

$$V_{dn} = \frac{LSB_n}{\sqrt{12}} \quad (6.8).$$

LSB_n can be determined as

$$LSB_n = \frac{S_{\max n} - S_{\min n}}{2^k}, \quad (6.9)$$

where $S_{\max n}$ and $S_{\min n}$ are maximal and minimal values of the analog signal to be digitized at electronic channel n , and k is bit number of the A/D converter.

The σ_g and σR^* cannot be modeled mathematically similarly to V_a or V_d . However, for a well-defined system they can be usually estimated.

Now, the quantities presented in the set of equations (6.5) are defined and it is possible to determine object temperature. The set of equations (6.5) cannot be solved analytically. It can be solved numerically using a few numerical methods; the least squared method was chosen by authors to calculate unknown parameters T_{ob} , a_o , a_1, \dots, a_{m-2} . All these numerical methods differ according to their calculation speed and calculation accuracy. However, the calculation errors are negligible in comparison to the radiometric, electronics and calibration errors and we can say that all these methods produce the same results. Therefore the calculations methods will not be discussed here in detail.

6.3 Calculations

Multiband systems can be designed in many different ways. However, to precise our discussion let us make a few assumptions about parameters of a system that could potentially fulfill requirements of present day market and make some calculations for these example systems.

Multiband systems, as they are more sophisticated and expensive, can find applications only in areas where simple, low-cost single- and dualband systems failed. Objects of emissivity whose strongly depends on wavelength and temperature are such an area. As examples we can treat: non-contact temperature measure-

ment of thin films, some optical material or semiconductor material, metals during heating or welding processes. For these applications it seems reasonable to assume that the required temperature measurement range could be from about 400K up to about 1400K.

For temperature measurement range mentioned above systems built using such detectors as Si, Ge, InAsGa, PbS, PbSe, HgCdTe, pyroelectric and others can be used. All these detectors are available in non-cooled, thermoelectrically cooled or cryogenically versions. However, to limit our discussion let us analyze only systems built with thermoelectrically cooled PbSe, PbS and non-cooled Si detectors. thermoelectrically cooled PbSe and PbS detectors were chosen because of they cover spectral range of 1-5 μm that seems to be optimal for the required temperature range and because of their relatively low cost in comparison to HgCdTe detectors. Si detectors were assumed in non-cooled version as cooled such detectors are not commonly available. Spectral characteristics of the assumed detectors are presented in Fig. 6.1 and other system parameters in Tab. 6.1.

It was shown in Ref. [2] that increasing number of unknowns m in the set of equations means increasing errors of temperature measurement caused by the detector noise and other internal disturbances. Therefore we will keep m low and assume that $m=4$. It means that 2-degree polynomial is used to interpolate object emissivity at system spectral bands.

It was also shown in the Ref.[2] that the same errors decreases when difference between the number of system spectral bands n and the number of measured unknowns m rise. Therefore we will assume systems of 6 spectral bands to have condition $n > m$ fulfilled but not to make the system sophisticated too much.

We will start calculations from the analysis of electronic errors. One of sources of such errors - detector noise - determine theoretical limit of system accuracy and others can reduce it significantly even when there is no radiometric or calibration errors.

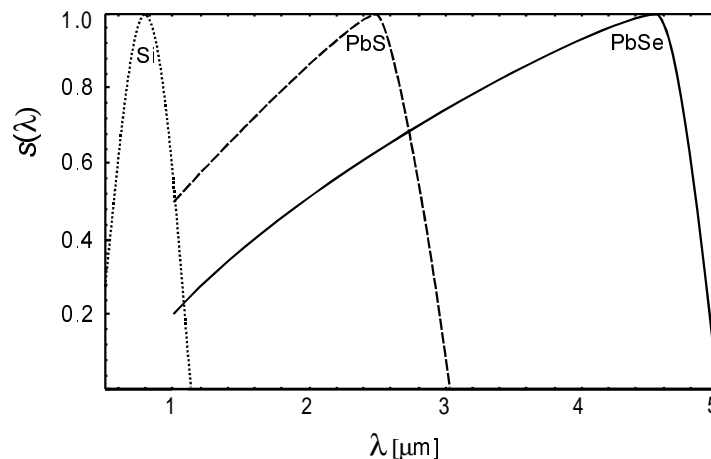


Fig. 6.1. Relative sensitivity $s(\lambda)$ of the assumed detectors

Tab. 6.1. The system parameters used in the calculations

Detector spectral band	Si 0.4-1.1 μm	PbS 1-2.5 μm	PbSe 2-5 μm
D^* [cm Hz ^{1/2} /W]	2×10^{12}	4×10^{11}	3×10^{10}
R^* [V/W]	20000	600 000	100000
bands location	$\lambda_1=0.75 \mu\text{m}$ $\lambda_2=0.8 \mu\text{m}$ $\lambda_3=0.85 \mu\text{m}$ $\lambda_4=0.9 \mu\text{m}$ $\lambda_5=0.95 \mu\text{m}$ $\lambda_6=1 \mu\text{m}$ $\Delta\lambda=0.02\mu\text{m}$	$\lambda_1=1.47 \mu\text{m}$ $\lambda_2=1.6 \mu\text{m}$ $\lambda_3=1.75 \mu\text{m}$ $\lambda_4=2 \mu\text{m}$ $\lambda_5=2.2 \mu\text{m}$ $\lambda_6=2.35 \mu\text{m}$ $\Delta\lambda=0.05\mu\text{m}$	$\lambda_1=3.15 \mu\text{m}$ $\lambda_2=3.5 \mu\text{m}$ $\lambda_3=3.8 \mu\text{m}$ $\lambda_4=4.1 \mu\text{m}$ $\lambda_5=4.5 \mu\text{m}$ $\lambda_6=4.7 \mu\text{m}$ $\Delta\lambda=0.1\mu\text{m}$
g	10		
τ_F	0.5		
τ_o	0.8		
F	2		
Δf	20 kHz		
ϵ_{opt}	0.3		

6.3.1 Electronic errors

6.3.1.1 Noise in the analog electronic channel

The errors caused by noise in the analog electronic channel are represented by the standard deviation of the output temperature dispersion σT . For the purpose of the calculations noise in the analog electronic channel of normal distribution of the standard deviation V_{an} was assumed. Calculations were repeated about 100 times to determine parameters of output temperature distribution with satisfactory accuracy. A blackbody was used as a simulated measurement object.

As demonstrated in Fig. 6.2, the errors caused by noise in the analog electronic channel decrease with the object temperature. We can determine lower limit of the temperature measurement range for the three analyzed systems on the basis of these errors. Let us assume that they must be below the level 1 K as it occurs for most singleband systems within their measurement range.

As we can see in Fig. 6.2, only the system using PbS detector fulfills the mentioned above condition for temperatures higher than 800K; the systems built with PbSe and Si detectors do not fulfill it within whole analyzed temperature range. This means that lower limits of usable temperature measurement ranges of multiband systems are significantly higher than those of single- and dualband systems built using the same or similar detectors. Additionally, by comparing PbS system and PbSe system we can conclude that location of system spectral bands into longer wavelengths does not guarantee lowering this limit.

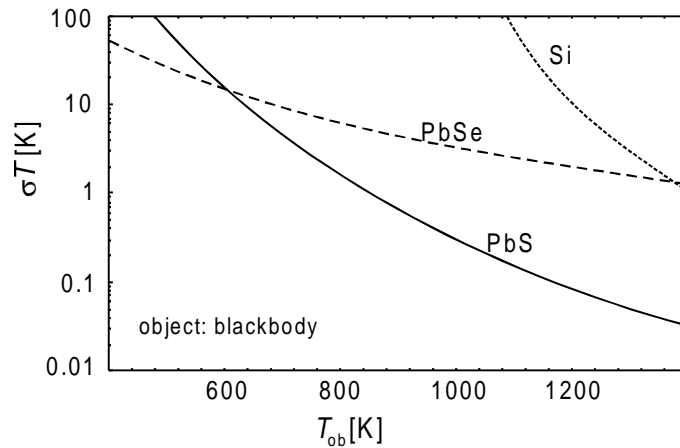


Fig. 6.2. Standard deviation of output temperature dispersion σT due to the detector noise

As temperature resolution of only PbS system is acceptable within most of the analyzed temperature range; other systems will be omitted in next calculations.

6.3.1.2 Limited digital resolution

The analyzed temperature measurement range 400K-1400K is wider than ranges of many commercially available singleband pyrometers. Therefore, we will divide it into two sub-ranges 400K-900K and 900-1400K. Next, let us assume that output analog signals are converted into digital signals using 14-bit converters of the fixed voltage conversion ranges set up to cover whole range of signals in analyzed two sub-ranges.

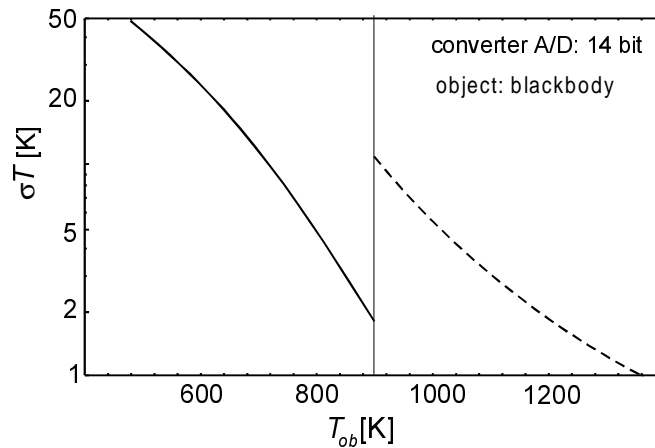


Fig. 6.3. Standard deviation of the output temperature dispersion σT due to the limited resolution of the digitization system

As can we see in Fig. 6.3 the errors caused by the limited resolution of the A/D converters for a system built with PbS detector are significant in both two sub-ranges in spite of the fact that we assumed the converters of a very good resolution for the present day. It is possible to lower these errors by optimizing a conversion range of the A/D converter for only maximum signal difference during a single measurement cycle. However, such solution require more sophisticated electronics blocks and can increase errors generated by other disturbances in the analog channel.

6.3.1.3 Variations of gain of electronic channel and detector responsivity

From electronic designer point of view, the multiband systems can be generally divided into two basic groups. The first group contains the systems using linear and matrix detectors and n separate electronic channels which continuously measure n different radiometric signals. The second one contains the systems with a single detector and single electronic channel that alternatively measure radiometric signals in n different spectral bands. The measurement process of a few radiometric signals for the single channel pyrometer can be achieved using, for example, a rotary wheel with n optical filters[3].

For the systems using a single detector and single electronic channel the quantities $R_n^*, g_n, s_n(\lambda), A_{dn}, V_{an}, V_{dn}$ used in formulas (6.5-6.9) are the same in all system spectral bands. Additionally, for such systems there exist a significant difference between the quantities $\Delta g, \Delta R^*$ and the quantities V_a, V_d although they all represent a standard deviation of a certain random variable. Variations of quantities g, R^* are low frequency variations and for systems using the single detector channel the gain g and the responsivity R^* have the same value for all system spectral bands during a single measurement cycle. V_a and V_d represent high frequency variations and they have different values in different system spectral band even during a single measurement cycle. In case of systems with n separate electronic channel all the quantities g, R^*, V_a and V_d can have different values in different system spectral band even during a single measurement cycle.

Variations of the detector responsivity R^* and the gain g both generate variations of the output electronic signals. Therefore we will analyze these factors together and calculate results of variations of the random variable $R^* g$ of standard deviation equals $0.0015R^* g$ on output temperature. Calculations carried out for a single electronic channel system showed that such variations do not generate any errors of temperature measurement. The reason for such a behavior is that these variations change the output signals proportionally in all systems spectral bands. However, as demonstrated in Fig. 6.4 they can cause very significant errors of temperature measurement in case of system using n separated electronic channels. As the assumed standard deviation of the product $R^* g$ treated as random variable can be considered as very low, it means that it is very difficult, almost impossible, to design multiband systems using linear matrix of detectors and separate electronic

channels of negligible errors caused by variations of gain of electronic channels and responsivity of the detectors.

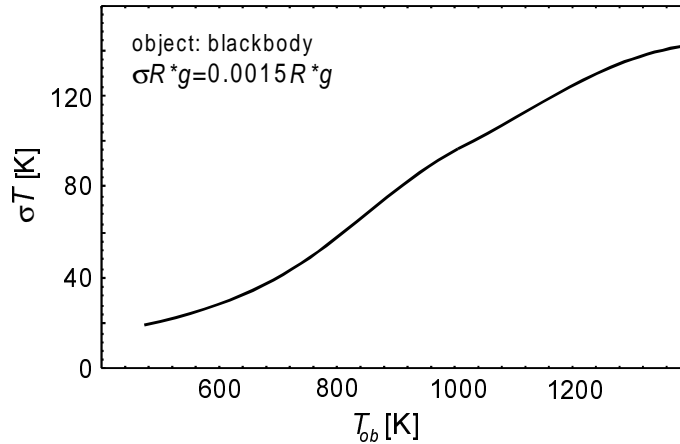


Fig. 6.4. Standard deviation of the output temperature dispersion σT due to the variations of detector responsivity and electronic gain

6.3.2 Radiometric errors

6.3.2.1 Emissivity and atmospheric transmittance

Results of emissivity measurements of the same objects presented in literature differ often quite significantly from one source to another [4]. Authors of this paper found out during experiments with emissivity measurements of different metals heated during measurement process that standard deviation of the dispersion of the measurement results was about 2-5% of measured value. Therefore authors cannot answer question what is the accuracy of approximation of emissivity curve of typical objects by the assumed type of function. However, it seems almost certain to assume that for most objects the standard deviation of the difference between the real curve and its approximation curve will be not lower than 0.3 % of the value of real object emissivity at system spectral band.

Emissivity of objects made from N-155ASTM steel of surface oxidized can be well approximated by polynomial $\epsilon_{ob}(\lambda) = 0.57 - 0.001 \lambda - 0.036 \lambda^2$ in spectral range 1-2.5 μm [4]. Errors of temperature measurement due to assumed random difference of the mentioned above level between the this emissivity curve and the real one for an the system built with PbS detector are shown in Fig. 6.5. As can we see these errors are significant in whole temperature measurement range, particularly for higher temperatures, although we assumed quite good accuracy of approximation.

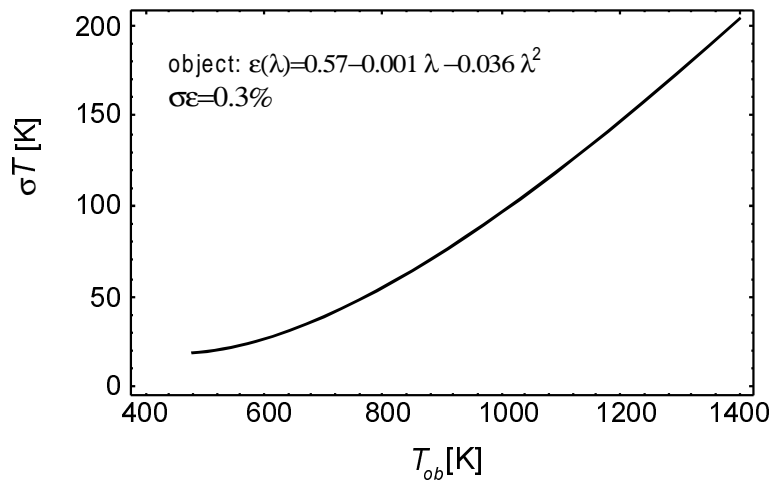


Fig. 6.5. Standard deviation of the output temperature dispersion σT due to assumed random difference between the assumed type of the emissivity curve and the real one

As we do not know what is the accuracy of approximation of emissivity curves of typical objects by the assumed 2-nd degree polynomial we cannot prove that errors of temperature measurement due to differences between the assumed type of emissivity curve and the real one will be significant in real measurement conditions. However, on the basis of analysis of emissivity curves presented in literature it seems reasonable to expect accuracy of approximation to be no better than the assumed value for most practical objects. Therefore, errors of temperature measurement of real object with multiband systems due to differences between the assumed type of emissivity curve and the real one should be not smaller, probably much higher, than those presented in Fig. 6.5.

It can be argued that by increasing degree of polynomial used for approximation we can increase approximation accuracy below the assumed level. However, as shown in Ref. [2], increasing number of unknowns m in the set of equations will increase system sensitivity to detector noise and other disturbances generated in the electronic channel. Therefore, it may bring no accuracy gain at all.

Atmosphere due to its limited transmittance apparently makes change of object emissivity. For an analysis of the influence of the atmosphere on measurement results, the transmittance was calculated with the popular *LOWTRAN* model for the conditions that can be considered as typical (midlatitude, summer, visibility equal to 5km, height equal to 2m, horizontal path). Errors of temperature measurement with PbS system of previously assumed object due to apparent change of its emissivity curve are shown in Fig. 6.6. As can we see for the distance below 1m these errors can be considered as almost negligible. However, for a distance of about 10 m they become quite significant in spite of the fact that system spectral bands were located in so called atmospheric windows and transmittance was over

98% in whole analyzed distance range. It can be expected much worse atmospheric transmittance in many industrial conditions. Therefore we can come to the conclusion that accuracy of multiband systems depends strongly on atmospheric transmittance and we can expect significant temperature measurement errors due to limited atmospheric transmittance in many industrial conditions.

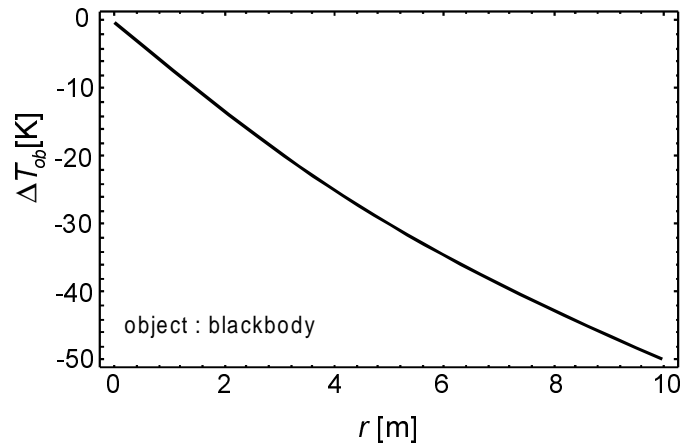


Fig. 6.6. Errors of temperature measurement due to limited transmission of the atmosphere

6.3.2.2 Radiation reflected by object and radiation emitted by optical elements

Theoretically, additional unknowns such as background temperature, optics temperature, function of background emissivity, function of emissivity of optical elements describing radiation reflected by the object and radiation emitted by system optical elements can be added as unknowns to the set of equations used for determination of object temperature. This could lead theoretically to elimination of influence of radiation reflected by object and radiation emitted by optical elements on temperature measurement results on condition that the assumed type of functions can perfectly interpolate real emissivity curves of the background and the optics.

Because of the reasons similar to those presented in the previous section there exist serious doubts about validity of this condition. Additionally, inclusion of the parameters mentioned above describing radiation reflected by the object and radiation emitted by system optical elements in the set of equations would lead to significant increase of number of unknowns m what would cause increase of sensitivity of measurement results to any disturbances of measurement process. Next, sophisticated systems of high number of spectral bands would be needed. Therefore, such a solution can be treated as only a theoretical possibility.

Influence of radiation reflected by object on measurement results depends on the background temperature T_{back} , its emissivity ϵ_{back} , and the object reflectivity

$\rho_{ob}(\lambda)=1-\varepsilon_{ob}(\lambda)$. As typical can be considered situation when the background emissivity ε_{back} is high, near one, and the object reflectivity $\rho_{ob}(\lambda)$ is around 0.5. For some industrial applications the background temperature T_{back} is not higher than 350K, for others it can be close, or even higher than object temperature. Calculations carried out showed that for PbS system influence of low temperature background of temperature below 350K is almost negligible in the whole analyzed temperature range 400-1400K. Errors of temperature measurement of object of temperature equal to 1000K caused by high temperature background are shown in Fig. 6.7. As demonstrated in this figure, these errors cannot be relatively small when the difference between object temperature and background temperature is over 100-200K or more. They become really significant only when background temperature is higher than object temperature. This low sensitivity of accuracy of temperature measurement with multiband systems can be treated as significant advantage of these systems.

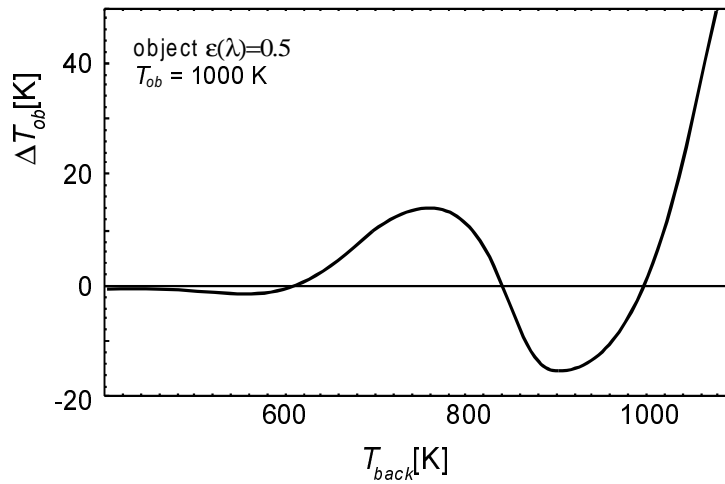


Fig. 6.7. Errors of temperature measurement caused by radiation emitted by background radiation

Changes of temperature of optical elements cause first changes of radiation emitted by these elements, next -changes of signals measured in systems spectral bands, and finally they generate changes of measurement results. However, using contact temperature measurement sensors located on the optical elements such temperature changes can be detected and output signals corrected. Calculations carried out for situations when temperature of optical elements is measured with accuracy ± 1 K showed that errors generated by changes of radiation emitted by optical elements are completely negligible in the whole analyzed temperature range 400-1400K for both PbS and Si systems and small, almost negligible for PbSe systems.

6.3.3 Calibration errors

Absolute accuracy of typical commercially available blackbodies is not better than 0.25% of blackbody temperature. Therefore, let us assume that the signal caused by radiation emitted by a blackbody S_{bb} can be determined experimentally at calibration condition with the randomly distributed errors ΔT_{cal} within range equal to ± 0.025 of blackbody temperature. Calculation results showed that errors of temperature measurement caused by non-accuracy of such a blackbody are within range ± 0.025 of object temperature. Therefore, the temperature measurement errors due to non-accuracy of blackbody used for calibration can be considered as negligible in comparison to errors generated by previously analyzed sources.

6.4 Conclusions

Method of temperature measurement with multiband systems is, similarly to single- and dualband systems, based on validity of some following assumptions about measurement conditions, system design and calibration process. First, the product of object emissivity and atmospheric transmittance can be exactly interpolated by an assumed type of mathematical function. Second, the radiation reflected by the object and the radiation emitted by the optical elements is negligible, or it is known and its influence on measured signals can be corrected. This assumption can be theoretically eliminated for systems of high number of spectral bands using a set of equations with additional unknowns describing also radiation reflected by the object and by radiation emitted by system optical elements. Third, errors of signals measurement generated by sources within electronics blocks are negligible. Fourth, errors due to use of non-accurate blackbodies used during calibration are negligible, too.

Errors of temperature measurement with multiband systems are strongly dependent on validity of all of the mentioned above assumptions. However, they are critically dependent on validity of the first and the third of the assumptions mentioned above.

Differences below the level of 0.1% between the assumed type of mathematical function and the product of real emissivity curve and atmospheric transmittance can cause very significant errors of temperature measurement even over the level of 100%. Electronic errors generated by noise in the analog channels and limited resolution of analog/digital converter can be also quite significant (a few percents) even for situation when the signal- to-noise relationship is high ($SNR > 100$) in all system spectral bands and high resolution A/D converters are used. This is a sharp contrast to singleband systems where difference of the level of 1% between the assumed value of object effective emissivity and the real value of this parameter and noise in analog channel for such a SNR generate errors of temperature measurement of the level of tenths of per-cent [5,6].

Non-negligible or not corrected radiation reflected by the object and the radiation emitted by the optical elements can cause significant errors of temperature meas-

urement, too. However, for low temperature background and system spectral bands located below about $3\ \mu\text{m}$ we can expect these errors to be significantly smaller than the previously discussed errors.

The calibration errors are of the order of the accuracy of the blackbody used during calibration. Even for typical commercially available blackbodies these errors are usually much smaller than radiometric and electronic errors.

Indications of multiband systems with a single electronic channel do not depend on variation of detector responsivity and channel gain in time. However, in case of multiband systems with separated electronic channels such variations can cause very significant errors of temperature measurement.

Errors of temperature measurement with multiband systems caused by most sources of electronic errors significantly increase with number of unknowns m in the set of equations used for determination of object temperature, and decrease when difference between number of system spectral bands n and number of unknowns m rise. This means that to design a multiband system of negligible electronic errors number of unknowns m should be kept low and difference $n - m$ as high as possible.

As the number of spectral bands n cannot be too high because of system costs, it also limits the number of unknowns of the assumed type of function used for approximation of object emissivity curve. Further, it means that to have multiband systems of negligible electronics errors it is necessary to assume that object emissivity can be interpolated by functions of low number of variables that can be fulfilled only for some objects.

Finally, we can conclude that the multiband systems are capable of producing accurate results of non-contact temperature measurement only in limited number of applications when the real measurement conditions are almost equal to the assumed ones. Additionally, multiband systems must be designed and built with much greater care than in case of typical single- and dual band systems in order to have low errors of temperature measurement caused by sources of electronic errors. It means that accuracy gains by using multiband systems are limited but the costs of such multiband systems will be much higher than costs of singleband system. Therefore we can come to final conclusion that multiband systems will not probably become a real rival for single band systems and will not improve significantly temperature measurement accuracy in most industrial and scientific applications.

6.5 References

1. Duvaut T., Georgeault D., Beaudoin J., Multiwavelength infrared pyrometry: optimization and computer simulations, *Infrared Phys. & Technology*, 36, 1089-1103 (1995).
2. Chrzanowski K., Szulim M., A measure of the influence of detector noise on temperature-measurement accuracy for multiband IR systems, *Applied Optics*, 37, 5051-5057(1998).
3. Z. Bielecki, K. Chrzanowski, T. Piatkowski, M. Szulim, Multiband Infrared Pyrometer, National Congress of Metrology, Gdansk, Poland, Vol.4, p.121-1128 (1998).

4. Sala A., *Radiant Properties of materials*, PWN-Polish Scientific Publishers Warsaw & Elsevier Amsterdam-Oxford (1986).
5. Chrzanowski K. Comparison of shortwave and longwave measuring thermal imaging systems, *Applied Optics*, 34, 2888-2897(1995).
6. Chrzanowski K., Experimental verification of theory of influence from measurement conditions and system parameters on temperature measurement accuracy with IR systems, *Applied Optics*, 35, 3540-3547 (1996).
7. Chrzanowski K., Szulim M., Errors of temperature measurement with multiband IR systems, *Applied Optics*, 38 (10), 1998-2006, 1999.

7. Errors of active singleband thermometers

An active singleband thermometer can be treated as a typical passive singleband thermometer co-operating with an emitter of radiation of known power. Such a system should theoretically determine accurately object effective emissivity and eliminate the most important source of errors of passive singleband thermometers.

We will analyze only errors of determination of object emissivity in active thermometry as other sources of errors works in the same way as described in Chapt.4. Let us carry out analysis for the active singleband pyrometer Pyrolaser[®] described in subchapter 4.2.1. Its manufactures does not states it clearly but it seems that the device determines automatically object emissivity using a following formula

$$\varepsilon_{ob} = 1 - a \frac{P_r}{P_e}, \quad (7.1)$$

where S_r is the output signal caused by the radiant flux reflected by the object and measured by the receiver, S_e is the output signal due to the radiant flux emitted by the emitter, and a the coefficient that depends on design parameter of the pyrometer that can be determined experimentally.

In case of an ideal diffusive object the reflected signal S_r does not depend on angular position of the active pyrometer; but in case of typical reflective-diffusive objects the reflected signal S_r usually depends on angular position of the active pyrometer [Fig. 7.1].

In a case of typical reflective-diffusive objects their emissivity calculated using the formula (7.1) will depend significantly on angular position of the active pyrometer although the true object emissivity can be non-dependent on angular direction.

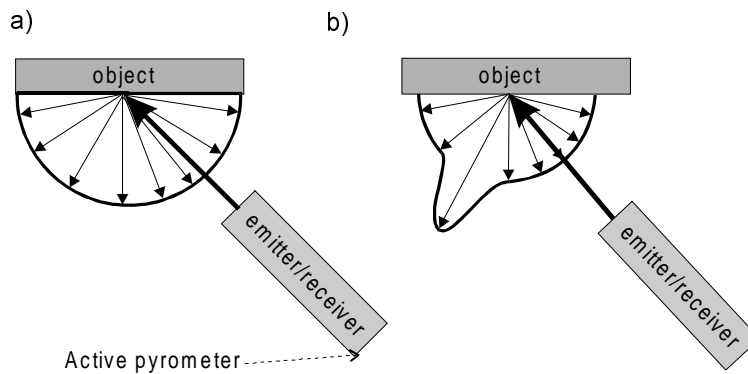


Fig. 7.1. Angular distribution of the radiation emitted by the emitter of the active pyrometer and reflected by a) a diffusive object b) reflective-diffusive object

Errors of determination of the object emissivity can be particularly high in a case of highly reflective objects. Emissivity of such objects is very low. However, for most angular positions of the pyrometer the reflected signal S_r , measured by the receiver is very low. Consequently the object emissivity calculated using the formula (7.1) will be almost 1. This means that errors of determination of object emissivity with active singleband pyrometer can be even a few hundredths per cents in case of highly reflective objects. These errors are a few times smaller in case of typical reflective-diffusive objects but still they can be significant. Therefore, practical applications of active singleband pyrometers designed like the Pyrolaser[®] is limited to a narrow group of nearly ideal diffusive objects.

Appendix: Relative Disturbance Resistance Function *RDRF*

In case of passive singleband thermometers the Relative Disturbance Resistance Function is a ratio of the relative error of signal measurement of the output signal $\Delta S/S$ to the relative error of the temperature measurement $\Delta T/T$.

$$RDRF = \frac{\Delta S / S}{\Delta T / T} , \quad (1)$$

Values of the relative disturbance resistance function *RDRF* can be useful for a quick determination of errors of instrument indications when the error of the signal measurement $\Delta S/S$ can be estimated.

Example: Calculate relative error of temperature measurement due to non-accuracy of estimation of the object effective emissivity. System *RDRF* for estimated object temperature equals 5. True object effective emissivity equals 0.5 but it was improperly estimated by the user as equal to 0.55.

Solution: Relative error of signal measurement is equal to relative error of emissivity determination

$$\frac{\Delta S}{S} = \frac{\varepsilon_a - \varepsilon_r}{\varepsilon_r} = 0.1 \quad (2)$$

where ε_a is the object estimated effective emissivity, and ε_r is the object true effective emissivity.

Next, using formula (1) we can calculate the relative error of temperature measurement $\Delta T/T$ as equal to 0.02 or 2%.

Using the same method as shown in the example above we can estimate relative error of temperature measurement $\Delta T/T$ when the relative error of the signal measurement due to non-accuracy of estimation of effective atmospheric transmittance, effective background temperature or any other source is known.

RDRF depends on object temperature and the relative spectral sensitivity $sys(\lambda)$ of the non-contact thermometer. As there are many non-contact thermometers of different relative spectral sensitivity $sys(\lambda)$, therefore there are also many possible *RDRFs*. However, let us limit analysis to the four broadband thermometers (the thermometer built using HgCdTe detector optimized for the 8-12 μ m spectral band, the thermometer built using HgCdTe detector optimized for the 3-5 μ m spectral band, the thermometer built using Ge detector, and the thermometer built using Si detector) and 9 narrow-band thermometers of following centers of their spectral bands: 7.9 μ m, 5.0 μ m, 3.9 μ m, 3.43 μ m, 2 μ m, 1.65 μ m, 1 μ m, 0.9 μ m, 0.65 μ m.

Values of the *RDRF* of the broad-band thermometers are shown in Tab. 1, and the *RDRF* of the narrow-band thermometers are shown in Tab. 2.

Tab. 1. *RDRFs* of the broadband thermometers

<i>T</i> [K]	HgCdTe 8-12 μm thermometers	HgCdTe 3-5 μm thermometers	Ge 1-1.8 μm thermometers	Si 0.4-1.1 μm thermometers
200	7.64	14.59	42.76	67.62
300	5.57	10.18	29.39	45.97
400	4.53	7.996	22.56	35.20
500	3.90	6.698	18.39	28.72
600	3.47	5.846	15.58	24.39
700	3.15	5.246	13.55	21.26
800	2.90	4.804	12.02	18.90
900	2.70	4.464	10.83	17.05
1000	2.54	4.194	9.87	15.55
1100	2.40	3.975	9.08	14.32
1200	2.29	3.791	8.42	13.28
1300	2.19	3.636	7.86	12.40
1400	2.10	3.502	7.38	11.64
1500	2.02	3.385	6.96	10.98
1600	1.96	3.281	6.59	10.39
2000	1.76	2.952	5.48	8.62

Tab. 2. *RDRFs* of the narrow-band thermometers

<i>T</i> [K]	7.9 μm	5.0 μm	3.9 μm	3.43 μm	2 μm	1.65 μm	1 μm	0.9 μm	0.65 μm
200	9.1	14.4	18.4	21.	35.9	43.5	71.9	79.9	110.4
300	6.1	9.6	12.3	13.9	23.9	29.0	47.9	53.3	73.7
400	4.6	7.2	9.2	10.5	17.9	21.8	35.9	39.9	55.3
500	3.7	5.8	7.4	8.4	14.3	17.4	28.7	31.9	44.2
600	3.2	4.8	6.2	6.9	11.9	14.5	23.9	26.6	36.8
700	2.8	4.1	5.2	6.0	10.2	12.4	20.5	22.8	31.6
800	2.5	3.6	4.6	5.2	8.9	10.8	17.9	19.9	27.6
900	2.3	3.3	4.7	4.7	7.9	9.6	15.9	17.7	24.5
1000	2.1	3.0	3.7	4.2	7.1	8.7	14.3	15.9	22.1
1100	2.0	2.8	3.4	3.8	6.5	7.9	13.0	14.5	20.1
1200	1.9	2.6	3.2	3.6	6.0	7.2	11.9	13.3	18.4
1300	1.8	2.4	3.0	3.3	5.5	6.7	11.0	12.2	17.0
1400	1.7	2.3	2.8	3.1	5.1	6.2	10.2	11.4	15.8
1600	1.6	2.1	2.5	2.8	4.5	5.4	8.9	9.9	13.8
2000	1.5	1.8	2.1	2.3	3.6	4.4	7.1	7.9	11.0

SUBJECT INDEX

absorptance	32, 33, 35, 36, 40, 99
absorption.....	9, 16, 31, 39
ADC	86, 92, 93
atmospheric transmittance.....	12, 16, 39, 40, 41, 65, 77, 79, 80, 99, 100, 110, 120, 126, 128, 130, 135
blackbody....	5, 22, 23, 25, 26, 29, 31, 56, 57, 58, 59, 61, 78, 79, 80, 83, 111, 117, 119, 123, 130, 131
broadband pyrometer	52, 58
calibration chart.....	5, 6, 56, 58, 59, 66, 67, 68, 69, 77
calibration errors	13, 79, 83, 86, 110, 117, 118, 119, 121, 122, 131
calibration process.....	13, 56, 58, 67, 130
CIE.....	17, 18, 19, 20, 31, 49
cooling system.....	13, 81, 86, 111, 117
detectivity.....	57, 82, 88, 90, 111, 121
digital resolution	92, 102, 124
dualband method	6, 15, 54, 64, 66
effective atmospheric transmittance	16, 56, 60, 61, 62, 77, 79, 80, 83, 99, 100, 135
effective background temperature	16, 56, 59, 61, 62, 79, 80, 83, 86, 94, 97, 98, 102, 135
effective emissivity	12, 13, 16, 56, 57, 59, 60, 61, 62, 63, 80, 81, 83, 95, 96, 97, 103, 130, 133, 135
electrical channel.....	88, 90
electronic errors.....	13, 83, 86, 88, 110, 118, 122, 131
emission	29, 31, 32, 33, 35, 39, 40
error.....	5, 6, 10, 11, 12, 13, 16, 24, 25, 52, 78, 79, 82, 83, 90, 92, 96, 99, 104, 105, 106, 109, 135
fiber pyrometer.....	50, 51
F-number.....	46, 57, 67, 71, 79, 88, 119
focal length.....	46, 57, 79
graybody	5, 60, 64, 68, 80
humidity	56, 61
infrared range	4, 18, 19, 20, 35, 53, 64, 77
internal error.....	13, 78
internal errors	13, 78
International Lighting Vocabulary	17, 18, 19, 31, 49
irradiance.....	46, 47, 48
Lambert law	28
LART	2
lateral magnification.....	47, 48
limit error	10, 11, 12, 79, 101, 106
LOWTRAN.....	40, 41, 100, 115, 127
LSB	81, 82, 92, 120, 121
magnification factor	47, 48
MDTD.....	46
measurement procedure	7, 55, 58, 59, 63, 66, 68, 75, 77, 78, 80, 104, 106, 110, 112
MF.....	47, 48

MODTRAN.....	40, 41
NETD	46, 90, 103
Newton formula.....	46, 47
NGE.....	89, 90, 91, 92
noise	5, 13, 65, 80, 81, 82, 86, 88, 89, 90, 91, 93, 103, 117, 120, 121, 122, 123, 124, 127, 130, 131
optical filter	8, 57, 65, 67, 79, 85, 88, 125
optical radiation	3, 5, 14, 18, 19, 20, 31, 35, 38, 39, 40, 46
optical range	35
optical system.....	40, 45, 46, 47
passive method	15, 54
passive thermometer.....	5, 16
Planck law	6, 22, 23, 24, 25, 26, 28, 31
preamplifier	13, 65, 81, 86, 90, 110, 117, 120
pyrometer.....	3, 9, 16, 50, 51, 57, 58, 66, 67, 68, 75, 76, 77, 87, 91, 93, 97, 102, 116, 125, 133, 134
radiance	22, 27, 28, 33, 34, 39, 44, 45, 60, 80
radiant exitance.....	22, 23, 25, 26, 27, 28, 29, 30, 55
radiant intensity	28
radiant power.....	25, 28, 29, 30
radiometric channel	13, 94
radiometric errors	13, 83, 86, 110, 118
random.....	10, 40, 81, 89, 90, 91, 92, 93, 94, 111, 112, 120, 125, 126, 127
random error	10, 90, 92, 93, 94, 112
RDRF	84, 85, 106, 108, 109, 110, 111, 115, 135, 136
reflectance	31, 32, 33, 35, 36, 56, 73, 75
reflection.....	31
responsivity	71, 81, 86, 88, 90, 94, 102, 110, 116, 119, 120, 125, 126, 131
rms.....	81, 90, 93, 120
singleband method.....	7, 13, 15, 54, 73
sinus condition.....	45, 47
spectral sensitivity	57, 65, 67, 71, 79, 84, 85, 87, 88, 119, 135
Stefan-Boltzman law	25, 31
systematic error	10, 11
temperature resolution	49, 89, 91, 104, 124
thermal camera	7, 8, 14, 15, 19, 26, 37, 40, 46, 50, 53, 56, 57, 61, 62, 87, 88, 91, 99, 100, 101, 102
thermal imaging.....	14, 16, 76, 132, 138
thermal scanner.....	14, 15, 50, 51, 52, 53, 57, 79
thermometry	1, 16, 20, 118, 133, 137
transmission.....	2, 8, 9, 31, 32, 41, 50, 115, 128
transmittance	5, 16, 32, 39, 42, 45, 53, 60, 80, 81, 83, 86, 87, 88, 95, 99, 120, 126, 127, 130, 135
uncertainty	10, 11, 138
VIM	10, 11
visible range	3, 4
Wien law.....	24, 25

Research & Development Treaties

Maksymilian Pluta, RDT Series Editor

Number	Author	Title
Vol. 1	Romuald Jóźwicki	Distorter Approach to Wave Optical Imaging
Vol. 2	Maksymilian Pluta	Variable-Wavelengths Interferometry
Vol. 3	Małgorzata Sochacka	Transmitted – Light Phase – Stepping Interferometry
Vol. 4	Tadeusz Kryszczyński	Analysis of four component zoom systems with mechanical compensations
Vol. 5	Zbigniew Jaroszewicz	Axicons – Design and propagation properties
Vol. 6	Artur Olczak	Computer Aided speckle pattern interferometer using diode laser and fiber optic
Vol.7*	Krzysztof Chrzanowski	Non-contact thermometry – Measurement errors

For further information on these and other SPIE PL titles, contact:

SPIE Polish Chapter
 c/o Institute of Applied Optics
 18 Kamionkowska Street
 03-805 Warsaw, Poland
 phone: (48-22) 8132051
 fax: (48-22) 8133265
 email: iosto@warman.com.pl
 web: <http://www.spie.org/poland>

* Vol. 7 is available in printed version, CD version or can be downloaded as Acrobat file

Author' biography

Krzysztof Chrzanowski Ph.D, D.Sc works as an Associate Professor in Institute of Optoelectronics of Military University of Technology. His primary research interests include analysis, design, testing of infrared systems, and accuracy analysis and design of non-contact thermometers. However, he also pursues work in basic metrology; particularly in the field of models of uncertainty of measurement of physical quantities. Computer simulation of imaging systems is another area of interest.

Krzysztof Chrzanowski received his PhD, and DSc both in Electronics, from Military University of Technology in Warsaw, Poland in 1991 and 1997. He was a guest scientist in Korean Advanced Institute of Technology (Korea, Taejon) in 1997, and in National Metrological Institute PTB (Berlin, Germany) in 1999 and 2000. He is a member of the Polish Chapter of SPIE.

He is an author or co-author of over 60 scientific papers and conference communications. Over 20 papers were published in peer-reviewed international journals like Applied Optics, Infrared Physics and Technology, Optical Engineering, and Optica Applicata. One of his papers was re-edited in SPIE Milestones Series. Accuracy analysis of different methods of non-contact temperature measurement is the subject of most of his papers.

A series of apparatuses and computer programs developed by his group received acclaim in many international scientific centers. The measuring sets for testing of thermal imaging systems, LLLTV cameras, TV cameras and night vision devices were awarded the silver medal at the 49th World Exhibition of Innovation, Research and New Technology, Brussels 2000. The viewer USC enabling visualization of surfaces covered with paints, sprays and plastics was awarded the golden medal at 49th World Exhibition of Innovation, Research and New Technology, and the silver medal at the III International Exhibition of Inventions - Innovations, Gdansk 2000. The software packages Assistant and Thermax that enable calculations of uncertainty of measurements of physical quantities are nowadays used in many scientific, educational and industrial centers.

More information about the author of this book can be found at the web sites:
<http://www.wat.waw.pl/ioe/pmup> or <http://www.kchrza.polbox.pl>

